

Towards Cooperative Organometallic and Enzymatic Catalysis to Develop New Value Chains from Organic Wastes

Ana Elisabete da Silva Fernandes

Supervisors: Prof. Ligia O. Martins and Beatriz Royo

Instituto de Tecnologia Química e Biológica António Xavier | Universidade Nova de Lisboa

Dissertation presented to obtain the Ph.D degree in Chemistry

Instituto de Tecnologia Química e Biológica António Xavier | Universidade Nova de Lisboa

Oeiras, September, 2019



Acknowledgments.....	V
Thesis Outline and objectives.....	VII
Abstract.....	XI
Resumo.....	XV
List of publications.....	XIX
List of abbreviations	XXI

Chapter 1

1. Introduction.....	1
1.1 Sustainable Chemistry.....	3
1.1.1 Biotechnology: a tool to improve sustainability.....	4
1.1.2 Organometallic catalysts to enhance biocatalytic processes.....	8
1.2 Wasteful Xenobiotic Compounds as Potential Alternative of Raw Materials.....	10
1.2.1 Biocatalysis for azo dye rich wastewater treatment.....	12
1.2.1.1 Laccases in dye degradation.....	15
1.2.1.2 Peroxidases in dye degradation.....	16
1.2.1.3 Azoreductases in azo dye degradation.....	17
1.3 Valorization of aromatic amines with chemo and biocatalysts.....	19
1.3.1 Enzymatic conversion of aromatic amines using laccases.....	20
1.3.2 N-alkylation of amines by organometallic complexes in an aqueous medium.....	22

1.4 Combining biocatalysis and organometallic catalysis: organometallic regeneration of NAD(P)H.....	25
1.5 References.....	28

Chapter 2

2. Dye-containing wastewaters as a source of biologically active building blocks: whole-cell catalysis by design.....	41
2.1 Abstract.....	43
2.2 Introduction.....	45
2.3 Results and discussion.....	48
2.3.1 Two-step bioconversion of dyes using purified enzymes.....	48
2.3.2 Set-up of free and immobilized whole-cells systems for the sequential degradation and valorization of MB9.....	60
2.4 Conclusion.....	71
2.5 Experimental Section.....	72
2.6 References.....	79

Chapter 3

3. Water-Soluble Iridium N-Heterocyclic Carbene Complexes for the Alkylation of Amines with Alcohols.....	85
3.1 Abstract.....	87
3.2 Introduction.....	89
3.3 Results and discussion.....	91
3.3.1 Synthesis and characterization.....	91

3.3.2 Catalytic studies.....	95
3.3.2.1 Conditions optimization.....	95
3.3.2.2 <i>Substrate scope with monosubstituted aromatic amines, aliphatic amines, and primary and secondary alcohol....</i>	97
3.3.2.3 <i>Substrate scope of sulfonated aromatic amines.....</i>	101
3.3.2.4 <i>Sequential reaction of enzymatic azo reduction and organometallic N-alkylation of amines.....</i>	102
3.4 Conclusion.....	104
3.5 Experimental Section.....	105
3.6 References.....	111
3.7 Supporting Information.....	119

Chapter 4

4. Half-sandwich Iridium(III) complexes for the regeneration of NADH in the enzymatic reduction of MB9.....	147
4.1 Abstract.....	149
4.2 Introduction.....	151
4.3 Results and discussion.....	154
4.3.1 Synthesis and characterization.....	154
4.3.2 Catalytic NADH regeneration.....	155
4.3.3 Chemoenzymatic reduction of Mordant black 9.....	159
4.4 Conclusion.....	163
4.5 Experimental Section.....	164
4.6 References.....	168

Chapter 5

5. Conclusion and Future Remarks.....	171
---------------------------------------	-----

Acknowledgments

The development of this thesis was only possible due to my supervisors Beatriz Royo and Ligia O. Martins, which I thank for accepting me as a PhD student, supporting and guiding me in the development of this multidisciplinary project. I also thank M. Paula Robalo for all her support in the development of this thesis. I would like to thank the Sustainable Chemistry PhD program for my PhD grant PD/BD/109637/2015. I am grateful to the ITQB technicians of the research facilities, Conceição Almeida, João Carita, Isabel Pacheco, Teresa Baptista, Helena Matias and especially Cristina Leitão who was always available.

I would like to thank all my lab partners and friends at ITQB, Mara, Rita, Sofia, Naiara, Inês, Arturo, Diana, Diogo, Francisco, Vera, André, Magdalena, Vânia and Sónia for helping me scientifically but also for the breaks and conversations.

A special thanks to my newly acquired friends in Lisbon Carla, Pedro, Priscilla and David that were simply awesome. Your support was crucial in the final stretch and the gatherings were full of fun moments. Never thought I would make such good friends.

A great thanks to my biochemical family Samy, Mika, Jé, Joana, Joantina, Cat, Ponto, Xavi, Raquel, and Nuno. Although we were all

separated it was like we were sharing the same experiences. You are the perfect support group, the scientific conversations and the venting out were fundamental. All the fun moments are forever with me.

A big thank you to my parents for everything throughout all my life and to my brother Gil for the small conversations. Also, I would like mention Sara and Matilde although they didn't do our weekends was what made me through the week.

And of course, a special thanks to Davide, that was always there enduring all my bad mood and lack of patience, but helping me every day. I wouldn't do any of this without you. And in the end, I was gifted with a small reward that had to endure the stress of a final year of thesis. I hope you don't hold it against me Helena.

Thesis outline and objectives

Green chemistry is nowadays the pillar for the development of new sustainable technologies that aim to prevent waste instead of remediating it. The use of (bio- or chemo-) catalysts is a powerful tool for the implementation of sustainable technologies. Moreover, the tandem use of different catalysts potentiates processes sustainability since they can mutually complement catalytic reactions, reducing synthetic and purification steps, increasing yields and selectivity of reactions.

Therefore, the main aim of this thesis was to develop new processes for the reintroduction of toxic wasteful materials, such as azo dyes, into product life cycles, helping in the cleaning-up of the environment from waste and simultaneously producing valuable end products, creating a circular economy. To achieve this goal the specific objectives were:

- a) Develop and optimize enzymatic systems for the azo reduction of azo dyes and conversion to aromatic amines through the action of the azoreductase PpAzoR from *P. putida* followed by their oxidation to relevant end products by CotA-laccase from *B. subtilis*
- b) Develop new water-soluble iridium catalysts for the valorization of aromatic amines through their *N*-alkylation with alcohols

- c) Investigate the activity of water-soluble iridium catalysts in the reaction of NADH regeneration, and its cooperative use with the azo reduction using the azoreductase PpAzoR.

This thesis is divided in five chapters. Chapter 1 depicts the importance of the implementation of green chemistry principals through biotechnological tools with the cooperative use of bio- and chemo catalysts.

In Chapter 2 sustainable methodologies for the conversion of toxic azo dyes into valuable end products are disclosed. Herein, the azoreductase PpAzoR and CotA-laccase were sequentially used in the reduction of azo dyes into aromatic amines, catalyzed by PpAzoR, followed by their oxidation into phenazines, phenoxazinones or quinones, catalyzed by CotA-laccase. This chapter highlights the complementary use of two biocatalysts for the production of relevant end products.

Chapter 3 describes the synthesis and characterization of new water-soluble iridium N-heterocyclic carbene complexes and their application in the green catalysis of *N*-alkylation of amines with alcohols. This chapter highlights the potential cooperative use of chemo and biocatalysis for the development of new molecules.

In Chapter 4 an iridium organometallic catalyst is used in the regeneration reaction of the co-factor NADH. Furthermore, it was demonstrated that the azo reduction of the model azo dye mordant black 9 catalyzed by PpAzoR can be performed with the simultaneous iridium catalyzed regeneration of the co-factor NADH. This chapter highlights the potential of organometallic regenerating system to aid in the application of reductive enzymes in industrial processes.

Finally, in Chapter 5 is summarized and discussed the major conclusions of this doctoral thesis and final remarks are made.

Abstract

The procurement of sustainable technologies is the major driving force for current industrial development. The 12 principles of Green Chemistry are important guidelines for their development and the first one directs towards waste reduction instead of remediation. To achieve this goal the circular economy concept was created, that emphasizes on the development of processes in a closed loop where waste is integrated as part of the product life cycle. In this thesis different strategies were applied for the development of sustainable methodologies that apply the circular economy concept, converting waste into valuable end products.

First, an environmental-friendly enzymatic strategy was developed for the valorization of azo dye-containing wastewaters. We set-up a 2-step biocatalytic process using purified preparations of enzymes as proof of concept and then free and immobilized whole-cells were used to increase the process eco-friendliness and sustainability. We show that *Pseudomonas putida* PpAzoR azoreductase efficiently reduces a set of azo dyes into aromatic amines and CotA-laccase from *Bacillus subtilis* efficiently oxidize these into phenoxazinones, phenazines and naphthoquinones. Free and alginate-immobilized whole-cells of recombinant *Escherichia coli* containing the overproduced enzymes, in

a two-step enzymatic process, were shown to successfully catalyze the conversion of the model azo dye mordant black 9 dye into sodium 2-amino-3-oxo-3H-phenoxazine-8-sulfonate. The use of whole cells reduces the process costs, increases the stability of the system, and we showed that their immobilization in sodium alginate further improve the downstream processing and allows recycling of the biocatalytic system. A one-pot process in water was implemented using immobilized cells co-producing PpAzoR and CotA. When the first step was performed in a recycled manner, 90% product yields were obtained, showing enormous potential for dye-containing wastewaters sustainable and eco-friendly valorization.

Secondly, a sustainable method for the valorization of aromatic amines using water-soluble organometallic catalysts was developed. A new series of water-soluble $\text{Cp}^*\text{Ir}(\text{NHC})\text{Cl}_2$ complexes with N-heterocyclic carbene (NHC) ligands were obtained and fully characterized. The new complexes showed high reactivity and selectivity for the sustainable formation of secondary amines through the alkylation of amines with alcohols. This catalysis was conducted with equimolar quantities of substrates (1:1 ratio), in water and in the absence of a base or other additives, highlighting its sustainability since large amounts of toxic reagents are avoided and it is performed in a green solvent in an atom economy reaction. The catalytic system was active towards a broad

substrate scope, allowing the synthesis of a variety of secondary amines in excellent yields.

Finally, the cooperative action of bio- and chemo catalysts was studied for the development of a sustainable NAD(P)H regeneration system to enhance the sustainable use of pure azoreductase enzymes, such as PpAzoR. A series of half-sandwich iridium(III) catalyst complexes were shown to be active in the regeneration of NADH using formate anions as the source of hydrogen. Furthermore, the enzymatic reduction of the model azo dye mordant black 9 was performed using the iridium(III) NADH regeneration system as the sole proton donor. Although with some loss in activity, it was demonstrated that iridium(III) complexes can be used in a cooperative manner under enzymatic conditions.

Resumo

A procura por tecnologias sustentáveis é um grande potenciador de desenvolvimento industrial. Os 12 princípios da Química Verde são diretrizes importantes para o desenvolvimento de tecnologias sustentáveis, sendo que o primeiro princípio afirma que deve haver uma redução do lixo produzido em vez da sua remediação. Para alcançar esse objetivo, foi criado o conceito de economia circular, focando-se no desenvolvimento de processos em loop fechado onde o lixo é integrado como parte do ciclo de vida do produto. Nesta tese de doutoramento, diferentes estratégias foram aplicadas para o desenvolvimento de metodologias sustentáveis que usam o conceito de economia circular, conversão de lixo em produtos de valor industrial.

Primeiro, foi desenvolvida uma estratégia enzimática amiga do ambiente para a valorização de águas residuais ricas em corantes azo. Para provar o conceito, foi estabelecido um sistema em one-pot usando preparações de enzimas puras, seguindo-se da utilização de células inteiras de forma a aumentar a sustentabilidade do processo. Foi demonstrado que a azoreductase PpAzoR de *Pseudomonas putida* reduz de forma eficiente um conjunto de corantes azo em aminas aromáticas e que a CotA-laccase de *Bacillus subtilis* oxida

estas de forma eficiente em fenoxazinonas, fenazinas e naftoquinonas. Células inteiras de *Escherichia coli* recombinante com estas enzimas superproduzidas catalisaram, em dois passos enzimáticos, a conversão do modelo de corante azo mordant black 9 na molécula 2-amino-3-oxo-3H-fenoxazine-8- sódio sulfato. O uso de células inteiras reduz o custo associado ao processo e aumenta a estabilidade do sistema. Foi demonstrado que a sua imobilização em alginato de sódio melhora o processamento final e permite que o sistema biocatalítico seja reciclado. Foi implementado um processo em one-pot em água usando células imobilizadas co-produzindo PpAzoR e CotA. A reciclagem das células no primeiro passo levou a um rendimento de 90%, demonstrando grande potencial para a valorização de águas residuais contendo corantes de uma forma sustentável e amiga do ambiente.

Em segundo lugar, foi desenvolvido um método sustentável para a valorização de aminas aromáticas usando catalisadores organometálicos solúveis em água. Foram obtidos e caracterizados novos complexos solúveis em água de Cp*Ir(NHC)Cl₂ com ligandos de carbeno N-heterocíclicos. Estes novos complexos apresentaram uma elevada reatividade e seletividade para a formação de aminas secundárias de forma sustentável através da alquilação de aminas com álcoois. Esta catalise foi realizada com quantidades equimolares

de substratos (ratio 1:1), em água e na ausência de base ou outros aditivos, destacando a sustentabilidade da reação pois são evitadas grandes quantidades de reagentes tóxicos, num processo com economia de átomos eficiente realizado num solvente verde. Este sistema catalítico manteve uma boa atividade para vários substratos, permitindo a síntese de várias aminas secundárias com rendimentos excelentes.

Finalmente, foi estudado o uso cooperativo de catalisadores químicos e biológicos para o desenvolvimento de um sistema sustentável para a regeneração de NAD(P)H de forma a aumentar a sustentabilidade associada ao uso de azoreductases, como a PpAzoR. Foi demonstrado que um conjunto de complexos em half-sandwich de irídio(III) eram ativos na regeneração de NADH usando aniões de formato como fonte de hidrogénio. Para além disso, a redução enzimática do modelo de corante azo mordant black 9 foi realizada usando o sistema de irídio(III) para a regeneração de NADH como única fonte de prótons. Apesar de alguma perda de atividade, foi demonstrada a potencialidade de complexos de irídio(III) para serem usados de forma cooperativa em condições enzimáticas.

List of Publications

Ana Fernandes, Beatriz Royo, 'Water-Soluble Iridium N-Heterocyclic Carbene Complexes for the Alkylation of Amines with Alcohols', *ChemCatChem*, 2017, 9, 3912-3917, DOI: 10.1002/cctc.201700678

Ana Fernandes, Bruna Pinto, Lorenzo Bonardo, Beatriz Royo, M. Paula Robalo, Lígia O. Martins, 'Dye-containing wastewaters as a source of biologically active building blocks: whole-cell catalysis by design', submitted manuscript

List of abbreviations

NHC – N-heterocyclic carbene

E. coli – *Escherichia coli*

CotA-laccase – Laccase from *Bacillus subtilis*

DyP – dye decolorizing peroxidase

E. C. – enzyme commission number

NADH - Nicotinamide adenine dinucleotide

NADPH – Nicotinamide adenine dinucleotide phosphate

FAD - Flavin adenine dinucleotide

FMN - Flavin mononucleotide

FMNH₂ – Reduced flavin mononucleotide

PpAzoR – Azoreductase from *Pseudomonas putida* MET94

PDB – Protein Data Bank

TvL – Laccase from *Trametes villosa*

Cp* - Pentamethylcyclopentadienyl

bpy – bipyridine

HPLC – High pressure liquid chromatography

NMR – Nuclear magnetic resonance

MB3 – Mordant black 3

MB9 – Mordant black 9

AR266 – Acid red 266

RY145 – Reactive yellow 145

DR80 - Direct red 80

UV-Vis – Ultraviolet visible spectroscopy

λ_{\max} – maximum wavelength

NAD⁺ Oxidized Nicotinamide adenine dinucleotide

SAHBS – sodium 3-amino-4-hydroxybenzene

SAHNS – sodium 4-amino-3-hydroxynaphthalene-1-sulfonate

SDAHNS – sodium 5,6-diamino-4-hydroxynaphthalene-2-sulfonate

SANTS – sodium 7-aminonaphtalene-1,3,6-trisulfonate

SABS – sodium 4-aminobenzene sulfonate

SDBS – sodium 2,5-diaminobenzene sulfonate

RB5 – Reactive black 5

DCW – dry cell weight

pLOM10 – plasmid coding for CotA-laccase from *Bacillus subtilis*

pVB-8 – plasmid coding for the evolved variant 2A1-Y179H of *Pseudomonas putida* MET94 PpAzoR azoreductase

pAIF-2 – plasmid coding for both wild-type PpAzoR azoreductase and CotA-laccase genes

LB – Luria-Bertani media

ϵ_{420} – extinction coefficient at 420 nm

ϵ_{340} – extinction coefficient at 340 nm

AQS - anthraquinone-2-sulfonate

OD₆₀₀ – optical density at 600 nm

HRMS-ESI – High resolution mass spectroscopy – electrospray ionization

RT – Room temperature

TOF – turnover frequency

$t_{1/2}$ – half-life

TON – Turnover number

Chapter 1

1. Introduction

1.1. Sustainable Chemistry

The demands of modern society required a rapid growth of the chemical industry resulting in an increased production, distribution, use, and discharge of chemicals rising huge environmental and health concerns ^[1,2]. In order to promote the establishment of green and sustainable chemical manufacturing processes, the 12 principles of green chemistry were formulated in the early 1990s ^[3] and they are summarized in Figure 1.1.

1. Prevent wastes
2. Renewable materials
3. Omit derivatization steps
4. Degradable chemical products
5. Use safe synthetic methods
6. Catalytic reagents
7. Temperature and pressure ambient
8. In-Process monitoring
9. Very few auxiliary substances
10. E-factor, maximize feed in product
11. Low toxicity in chemical products
12. Yes it's safe

Figure 1.1 The condensed 12 principles of green chemistry, that include the mnemonic PRODUCTIVELY ^[4]

A definition of sustainable chemistry is that *'resources should be used in a rate in which they can be replaced naturally and waste generation should not be faster than its remediation'* ^[1]. Therefore one major problem that is raised by modern society in order to accomplish sustainable development is the one related to waste management, which in fact is the first principle of green chemistry, *waste prevention*

instead of remediation ^[3]. Indeed, waste generation goes hand to hand with social awareness and economic development. The established XX-century economical notion of take-make-use is no longer suitable in a society with environmental awareness concerns. An urgent need emerged for the development of sustainable technologies that are at the same time economically competitive. Therefore, the concept of circular economy was developed emphasizing the need to reuse, recycle, redesign, remanufacture, reduce and recover wastes ^[2,5,6]. Through the implementation of the circular economy concept, waste can be reintroduced in the product chain production acting as raw material ^[7-9]. Thus, sustainable development can be achieved through the conversion of wasteful materials into valuable end products. This concept has gathered enlarged interest in academic research but also in companies from different industrial fields, since it allows to take economic advantages of a closed loop of materials in the product life cycle ^[5,6].

1.1.1. Biotechnology, a tool to improve sustainability

Biotechnology is considered a technological strength for a competitive and sustainable implementation of circular economy. It enables the creation of sustainable products and processes based on renewable raw materials and carbon recycling providing the tool to turn waste into a resource, which is a key pillar for the European Commission circular

economy ^[10,11]. Biotechnology, considered a white technology, is environmentally safer offering benefits over more conventional chemical-based alternatives.

Biotechnology applied to environmental issues has many applications: pollutant monitoring and biodegradation, groundwater clean-up, site and air bioremediation, among others ^[12]. The main tool behind biotechnology is biocatalysis, that comprises 6 of the green chemical principals since its reactions are performed in mild conditions, and reduces the number of synthetic steps, of toxic reagents, of by-products, and wastes ^[2,13]. Table 1.1 summarizes the advantages and disadvantages of biocatalysts. Biocatalysts catalyze reactions otherwise performed by chemical methods in a more sustainable manner with high yields and excellent chemo-, regio-, and stereoselectivities. Even the few disadvantages reported (see Table 1.1) can be overcome with protein engineering, producing enzyme variants with higher stability and activity in different solvents, temperatures, pH or pressure, or with a lower propensity to inhibition ^[14].

Table 1.1 Advantages and disadvantages of different biocatalysts: isolated enzymes, resting whole cells, and growing whole cells ^[15]

Advantages	Disadvantages
Environmentally friendly	Unstable in extreme conditions of temperature, pH or pressure
Higher efficiency, faster 10^8 - 10^{10} times than noncatalytic reactions	Highest catalytic activity in water
Performance in mild conditions	Enantioselectivity cannot be fine-tuned
Allows multi-enzymatic cascade reactions in a single flask	Require natural co-factors
High substrate tolerance, substrate promiscuity	Prone to inhibition by substrate or product
Broad-spectrum of reactions	
Can be used in nonnatural conditions	
High chemo-, regio-, diastereo-, and enantioselectivity	

Different types of biocatalysts can be used to catalyze the bioconversion of a substrate into a product, (i) isolated enzymes, (ii) resting whole cells or (iii) growing whole cells, commonly known as fermentation. The selection of the appropriated system is affected by different factors that are summarized in Table 1.2. The correct selection of biocatalyst can have effects on the cost, time and scale used in the biotransformation of interest. Immobilization of biocatalysts can be accomplished allowing its reuse leading to decreased reaction costs e.g. by increasing the enzymatic system robustness.

Table 1.2 Characteristics of different biocatalysts: isolated enzymes, resting whole cells and growing whole cells [15].

	Isolated Enzymes	Resting Whole Cells	Growing Whole Cells
Catalyst amount	Catalytic	Biomass	Large biomass
Purification	Yes	No	No
External co-factor	Yes	No	No
Reaction time	Short	Medium	Long
Starting material	Substrate	Substrate	Growth medium
Apparatus	Simple	Complex and expensive	Complex and expensive
Scale	Small	Large	Large
Enzyme stability	Low	High	High
Activity	High	Low	Medium
Concentration tolerance	High	High	Low
Organic solvents tolerance	Medium	Low	Low
Active enzymes	Target one(s)	Few	Many
Substrate	Natural or non-natural	Natural or non-natural	Natural
Workup	Simple	Moderate	Tedious
By-products	Few to none	Few	Many

The development of molecular biology tools allowed the application of protein engineering methodologies targeted at the production of more stable and active enzymes, but also to the use of recombinant cells holding increased amounts of the desired enzyme. Thus, whole cells are currently not limited to the use of wild-type microorganism and recombinant cells overproducing a target enzyme can be used in biotransformation reactions. This results in systems showing increased

catalytic rates and making side reactions, and consequently by-products, a minor problem [15,16].

1.1.2. Organometallic catalysts to enhance biocatalytic processes

The substitution of conventional stoichiometric chemical reactions for catalytic reagents is one of the 12 principles of Green Chemistry [3]. Catalytic reactions lead to more energy-efficient and selective chemical processes eliminating undesirable by-products and waste, with fewer reaction steps and milder conditions. Catalytic synthesis is based on three pillars: organocatalysis, organometallic catalysis, and biocatalysis.

Organometallic complexes have an important role in the implementation of catalytic processes since it comprises very active metal centers and organic ligands that can be tailored to improve different parameters. Simultaneously, biocatalysis has also been demonstrated to bring several advantages in the combination with catalytic processes (Table 1.1). The cooperative use of chemo- and biocatalysts can help overcome hindrances that they possess individually leading to the production of a wider range of interesting molecules through more sustainable synthetic paths. This combination can reduce the number of purification steps and enhance reactivity, selectivity, stereochemical control, substrate scope, and diminish side

reactions [17,18]. The application of these two systems together is frequently hampered by incompatibilities issues, due to the different and sometimes incompatible reaction conditions that each requires, leading to mutual inactivation. As a consequence, only a few examples are found in the literature reporting the successful cooperative application of chemo- and biocatalysts [19]. The coupling of chemo- and biocatalysts requires the biocatalysts to maintain activity *e.g.* in organic solvents and other harsh conditions and/or the organometallic compounds to maintain good activity in an aqueous medium and other mild conditions. Lipases and serine proteases are the only reported enzymes that are able to maintain activity in organic solvents and at high temperatures [20].

On the other hand, only some examples can be found in the literature of the cooperative use of organometallic complexes and biocatalysts in aqueous mediums [21–24]. The development of organometallic complexes that are stable and catalytic active in water is of great interest in different research fields due to increased concern on sustainability [25]. In addition to increasing the compatibility to biocatalysts, it also allows the use of a more inexpensive, non-toxic and non-flammable solvent. The increased water solubility of organometallic complexes is usually accomplished by the functionalization of ligands with hydrophilic substituents. N-

heterocyclic carbene (NHC) ligands are largely used ligands in organometallic since they confer great stability to the complexes and are easily tailored to obtain the desired proprieties. Although solubility in water of organometallic complexes can be achieved, their stability is not always optimal. Therefore, it is also imperative to choose an adequate metal environment capable to stabilize the complexes in water.

1.2. Wasteful xenobiotic compounds as potential alternative raw materials

Synthetic dyes are the most consumed chemicals in a large array of industries, like textile, pharmaceutical, food, and cosmetics. Annually, more than 7×10^5 tons of dyes and/or pigments are produced being comprised of almost 10,000 different molecules ^[26]. In the annual production of dyes, more than 70% are azo dyes which are aromatic compounds with one or more azo groups (-N=N-) (Fig. 1.2). The industry preference for this class of dyes is due to their simple synthetic process, easy application, high photolytic stability, their myriad of brilliant shades, structural diversity, strong covalent adherence to textile fibers and minimal energy requirement ^[27]. These favorable features also make them resistant to treatments which leads to a release of almost 50% of azo dyes annually produced into the environment ^[26,28-30]. Their xenobiotic proprieties are due to sulfonated

groups present in most of their structures that cause electron deficiency making them recalcitrant to biodegradation [31,32]. This represents a major environmental threat that directly affects almost 50% of the world's population [30].

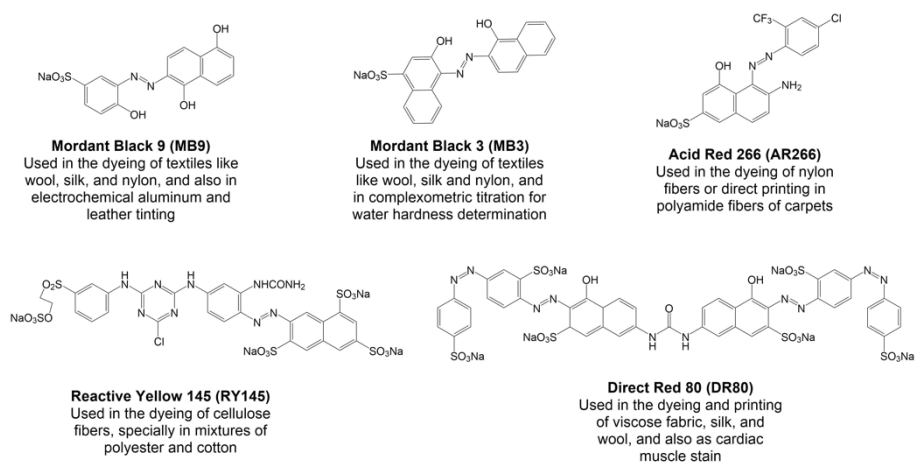


Figure 1.2 Chemical structures of representative azo dyes from different classes selected for this work.

The bioaccumulation of these compounds leads to aesthetic problems but more importantly, by reducing light penetration into aquatic environments they reduce oxygen production leading to a deficient growth and development of aquatic life. Furthermore, azo dyes and their breakdown products, mostly aromatic amines, have toxic and carcinogenic properties that put at risk human health [33–36]. The selection of an adequate method for degrading azo dyes can potentiate the transformation of these toxic wasteful materials into valuable end products which is the aim of this thesis.

Azo dyes are conventionally treated by physicochemical methods. The main ones employed are oxidative remediation, reverse osmosis, ozonation, Fenton process, adsorption, coagulation, membrane separation, and ion exchange. These methodologies although efficient in decolorizing azo dyes, don't efficiently detoxify the wastewaters. Furthermore, these methodologies have high cost and energy requirements, generate large amounts of toxic sludge and produce damaging by-products [34,37,38].

Hence, it is imperative the development of more cost-effective and sustainable methods for the removal of azo dyes from the hydrosphere. Biological methodologies are attracting the attention of researchers and industries as alternatives to physicochemical treatments. They are cost-effective, produce less sludge, and have a selective action without perturbing the surrounding ecosystems, reinforcing its eco-compatibility [34,39,40]. Furthermore, their implementation may allow the development of a circular economy methodology, converting wasteful azo dyes into valuable end products.

1.2.1. Biocatalysis for azo dye rich wastewater treatment

As previously mentioned, conventional physicochemical methods used to treat dye rich wastewaters do not represent sustainable solutions due to their economic and technical hindrances. Biological methodologies are considered more efficient economical alternatives.

The bioremediation of dyes can be achieved resorting to two methodologies: (i) adsorption of dyes onto microorganism's biomass; or (ii) enzymatic action, either isolated or in whole cells. The first methodology is not suitable for long term treatments since the biomass becomes saturated and has to be disposed of ^[41].

Bioremediation of azo dyes can be performed with different microorganisms, like bacteria, fungi, algae, and yeasts, that can decolorize and completely mineralize azo dyes in the adequate conditions. Algae have great potential in dye degradation since it was demonstrated that it can grow in effluents from paper and pharmaceutical industries ^[42,43]. Furthermore, their cultivation is almost inexpensive since they can obtain their carbon source from the air. White-rot fungi have been shown to efficiently degrade azo dyes, due to their unspecific extracellular enzymatic systems ^[44,45]. These microorganisms have a rapid adaptation to the surrounding environments, but their relatively long growth cycles impair their wide application. The utilization of yeasts in dye degradation is still very little studied, but their high tolerance to dyes and heavy metals makes them quite promising microorganisms ^[41,46].

Amongst the microorganisms used for dye degradation, bacteria are the most frequently used ones. Their appeal is due to their easy cultivation, rapid growth under either anaerobic or aerobic conditions

and resistance to extreme conditions of pH, salinity, and temperature [39,47]. Different groups of bacteria are capable of degrading azo dyes under different conditions: anaerobic, facultative anaerobic, and aerobic.

The first step in bacterial anaerobic or aerobic degradation of azo dyes is mainly the reduction of the azo bond, which leads to the production of toxic aromatic amines. The complete mineralization of dyes may require a second step of reaction usually in aerobic conditions, to achieve the complete mineralization of aromatic amines. Although this methodology simultaneously decolorizes and detoxifies dye rich wastewater, it also completely destroys relevant chemicals that could be further transformed into valuable end products. The degradation of azo dyes by bacteria is due to enzymatic activity mainly from the oxidoreductase family. These enzymes perform redox catalysis being able to degrade a wide range of structurally diverse azo dyes. The most important enzymes in dye degradation are laccases, peroxidases, and azoreductases [48].

The pioneer work of Mendes *et al* (2011) reported the used of recombinant *Escherichia coli* cells overproducing simultaneously two enzymes for the degradation and detoxification of an array of azo dyes and model wastewaters [49]. A heterologous *E. coli* strain co-expressing an azoreductase and a laccase was used in a sequential manner. This

system successfully decolorized and detoxified different azo dyes and model wastewaters demonstrating the potential of recombinant cells and opening doors to the set-up of a system targeted at the production of relevant products.

1.2.1.1. *Laccases in dye degradation*

Laccases are multicopper oxidoreductases that have low substrate specificity being able to oxidize a wide range of different molecules, including azo dyes in the presence of oxygen ^[50–52]. They catalyze the four-electron reduction of oxygen to water by a sequential one electron uptake from the substrates. Their biotechnological importance comes mainly from its distinct features such as non-specific oxidation capacity, no requirement for co-factors and the ability to use oxygen as electron acceptor ^[32,50].

The majority of laccases used in biotechnological processes have fungal or plant origin. The first bacterial laccase used in dye degradation was CotA-laccase from *Bacillus subtilis* ^[52,53]. Pereira *et al* demonstrated the versatility of CotA-laccase towards the degradation of a wide range of dyes without redox mediators. In their work they also disclosed the complex radical mechanism behind the action of this enzyme in the degradation of anthraquinone dyes or azo dyes. They studied in detail the oxidation of Sudan Orange G demonstrating that the degradation of the dye chromophore was accompanied by the

formation of unstable radicals. These radicals can further react between them and generate an unpredictable and complex mixture of oligomeric products ^[52].

1.2.1.2. *Peroxidases in dye degradation*

Peroxidases are haemoproteins that efficiently degrade a wide range of small molecules. A family of microbial peroxidases, known as dye decolorizing peroxidases (DyP), were shown to degrade, among other molecules, a range of azo or non-azo dyes in the presence of hydrogen peroxide ^[50,54]. The azo dye degradation usually occurs through a multiple-step path that starts with a simultaneous symmetric and asymmetric azo bond cleavage leading to a complex mixture of compounds ^[32,50]. This allows a complete degradation of dyes and their products which leads to a complete detoxification of wastewaters. This feature makes them interesting for treating dye rich wastewaters but hampers the exploitation of the formed molecules.

Their efficiency in dye degradation has been widely demonstrated, but their further industrial application has been hampered by constraints in genetic manipulation and high costs in protein production ^[50]. DyP's were initially discovered in fungi but they have already been isolated from bacterial strains. This brings them a step closer of industrial application since the production in bacterial systems can improve their

production yields and simplify their engineering towards improved proprieties ^[54].

1.2.1.3. *Azoreductases in azo dyes degradation*

The main class of enzyme being expressed during biodegradation processes of azo dyes are azoreductases (E. C. 1.7.16). Azoreductases are a diverse group of enzymes with variations on structure and function. The correct classification of the different enzymes in this superclass of enzymes is still under debate. Their low level of sequence homology makes it necessary to take into account their oxygen tolerance, co-factor dependence or preference (NADH or NADPH), presence or absence of flavin molecules (FAD or FMN) and substrate specificity, azo, nitro, or quinone molecules ^[55].

Their different co-factor dependence leads to different reaction mechanisms. Flavin-dependent azoreductase promotes the azo reduction through a Ping-Pong bi-bi mechanism ^[56,57], illustrated in Figure 1.3, while in flavin-free this mechanism is not viable ^[58]. In the Ping-Pong bi-bi mechanism, it's required two reducing cycles that are dependent on NAD(P)H this leads to the sequential reduction of the azo compound into a hydrazine intermediate and then to the final amine compounds.

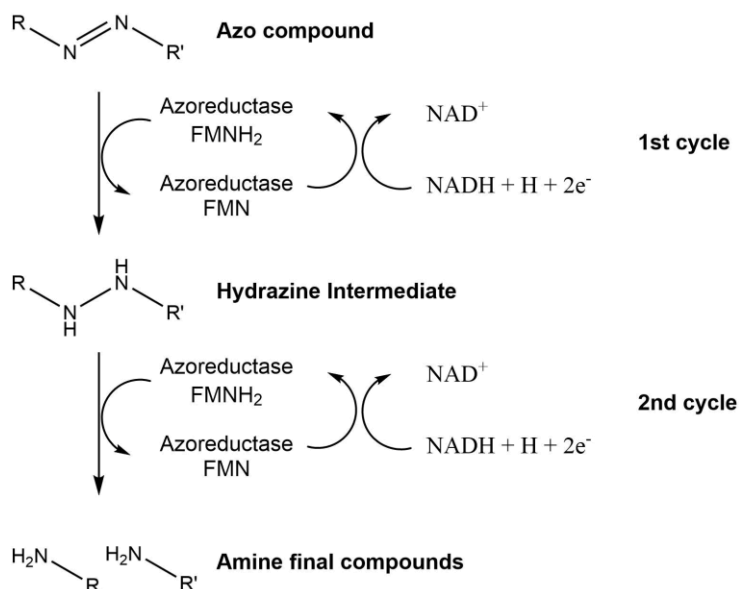


Figure 1.3 Mechanism of flavin-dependent azoreductases for the reduction of azo substrates.

Different azoreductases have been isolated and characterized from aerobic and anaerobic microorganisms [56,58–62]. Mendes *et al* (2011) isolated and characterized the PpAzoR azoreductase from *Pseudomonas putida* MET94, a bacteria particularly efficient in the degradation of structurally different azo dyes [62]. The crystal structure of this enzyme (Protein Data Bank (PDB) code 4C0W) indicated an FMN-dependent homodimer (Fig 1.4) [63]. This azoreductase is very active in the degradation of structurally diverse azo dyes through the Ping-Pong bi-bi mechanism, in the absence of oxygen, at the optimal conditions of pH 7 and 32°C [62]. PpAzoR can be classified as an oxygen-sensitive, flavin-containing NAD(P)H azoreductase. On the other hand, in the presence of oxygen, it has a clear preference for

quinones, so it can also be classified as a flavin-containing NAD(P)H-dependent quinone oxidoreductase.

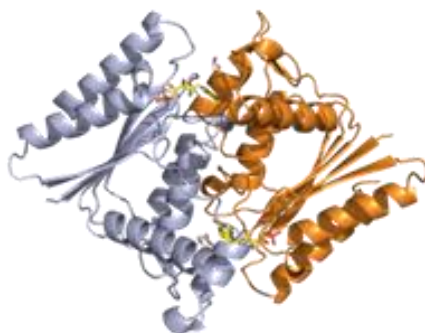


Figure 1.4 Representation of PpAzoR dimer: the two subunits are in grey and orange, and the prosthetic group, FMN, is represented in stick model ^[63].

In order to improve this enzyme, PpAzoR was subjected to rounds of directed evolution ^[64]. Brissos *et al* (2014) disclosed variants of this enzyme with increased kinetic and thermostability that could be more interesting for further application on dye rich wastewater treatments.

1.3. Valorization of aromatic amines with chemo- and biocatalysts

Aromatic amines have a myriad of chemical structures, from simple to complex ones, and all these molecules have high impact in the environment and the industry. They represent the second most abundant family of organic compounds present in the biosphere and are widely used in different industries as precursors for cosmetics, pharmaceuticals, dyes, rubbers, textiles, agrochemicals, pesticides

and explosives ^[65]. On the other hand, they are problematic pollutants since it was demonstrated that aromatic amines are toxic, carcinogenic and mutagenic ^[33,36,65].

The sustainable procurement of these amines raises environmental concern since they are usually obtained from harsh chemical processes, that use large amounts of hazardous reagents and produce large amounts of waste ^[66]. Through the introduction of a circular economy, aromatic amines can be obtained from problematic industrial wastes, such as dye rich wastewaters. In this way, a more sustainable source of raw material can be introduced in the industrial utilization of aromatic amines.

Furthermore, the conventional methodologies used for the chemical conversion of aromatic amines into other molecules often require harsh conditions, have poor yields and selectivity ^[66–68]. So, through the use of sustainable enzymatic or organometallic catalysis, aromatic amines can be converted into an array of relevant molecules in a sustainable manner.

1.3.1. Enzymatic conversion of aromatic amines using laccases

As already addressed in this thesis, the use of biocatalysts such as enzymes has several advantages (see section 1.1.1, Table 1.1). Laccases (E. C: 1.10.3.2) are multicopper oxidases with high oxidative

selectivity, active in mild reaction conditions that use oxygen as electron donor, producing only water as by-product. These characteristics make them attractive alternatives for applications in organic synthesis for the implementation of green methodologies. This class of enzymes has already been successfully applied in the oxidation of an array of organic molecules such as benzenediols, aminophenol's, polyphenols, polyamines, and lignin-related molecules [69]. Furthermore, the one-electron oxidation can lead to reactions of crosslinking allowing the homo and hetero-coupling of organic molecules. Besides, it has already been demonstrated the industrial application of these enzymes in the food, pulp and paper, textile, cosmetics, and nanobiotechnology industries [69].

CotA-laccase is an interesting bacterial laccase from *Bacillus subtilis* that is thermoactive and thermostable being a robust enzyme for biotechnological applications [70]. Sousa and co-workers have demonstrated the potential of CotA-laccase in the production of chemical relevant molecules, such as dyes [71–73], benzocarbazole frameworks [74], phenazines and phenoxazinones [75,76] using aromatic amines as substrates. Their work showed the superior performance of CotA-laccase when compared to TvL, commercially available fungal laccase, in the homocoupling reactions of *p*-substituted aromatic amines. They have studied the applicability of this enzyme to a large

array of aromatic amines demonstrating the correlation between the substrate redox potential and CotA-laccase activity. Also, they showed the effect of the substitution of the aromatic ring in the formation of different compounds.

1.3.2. *N*-alkylation of amines by organometallic complexes in an aqueous medium

N-alkylation of amines with alcohols catalyzed by organometallic complexes is a modern methodology for the sustainable production of secondary amines. This synthetic path avoids toxicity issues associated with alkyl bromides and waste formation. It displays higher selectivity and reduces the number of synthetic steps when compared to traditional alkylation methodologies [77]. Furthermore, this reaction is atom efficient using cheap alcohols, and the only by-product is water. These characteristics enable this reaction to be conducted in an aqueous medium.

Organometallic complexes were first used in *N*-alkylation of amines by Grigg [78], Watanabe [79] and Murahashi [80], in independent projects, using transition metals such as iridium, rhodium, and ruthenium. This reaction follows a hydrogen borrowing methodology (or hydrogen auto-transfer) and is based on the hydrogen removal from the alcohol by the organometallic complex, generating an aldehyde that is readily attacked by the amine. The formed imine is then converted to the

corresponding amine with the hydrogen stored in the organometallic complex (Fig. 1.5) ^[81].

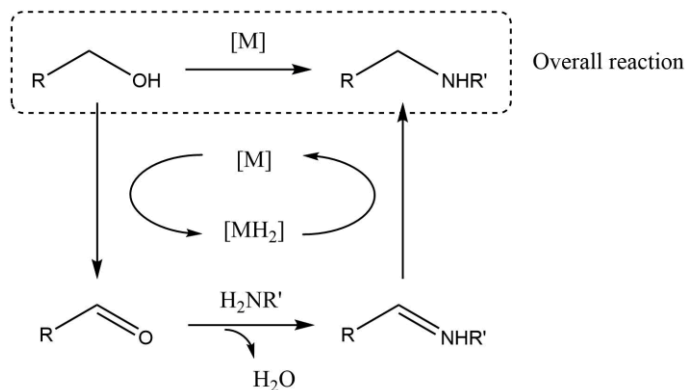


Figure 1.5 Reaction pathway for the N-alkylation of amines with alcohols through catalytic hydrogen borrowing.

After the disclosure of the transition metals potential, several researchers directed their attention towards this subject. Especially after the ACS Green Chemistry Institute and global pharmaceutical companies founded an ACS GCI Pharmaceutical Roundtable reinforcing the importance of a sustainable *N*-alkylation of amines ^[82,83].

Several metals have been shown to be active in *N*-alkylation of amines with alcohols, like ruthenium, rhodium, iridium, palladium, silver, gold, osmium, iron, and copper ^[84]. The use of more sustainable metals, like iron or copper, is sometimes impaired by their low substrate scope ^[84]. Among the metals applied to this reaction, the most studied ones are usually ruthenium- or iridium-based catalysts with the iridium ones being usually the most active ones ^[85,86]. Excellent results have been

obtained by different authors when applying iridium-based catalysts to this hydrogen borrowing reaction [86–92].

N-alkylation of amines is mostly performed in organic solvents with the addition of a base or other additives, and an excess of alcohol [93]. Williams and Yamaguchi's teams were pioneers in the performance of *N*-alkylation of amines catalyzed by organometallic complexes in water [94,95]. To do so, they developed stable water-soluble iridium complexes (Fig. 1.6). Yamaguchi described in 2010 the aqueous *N*-alkylation of ammonia with alcohols, and extended later the reaction to a broad variety of different aromatic amines [96]. Soon later, Wetzel reported one more example of *N*-alkylation of amines in water [97].

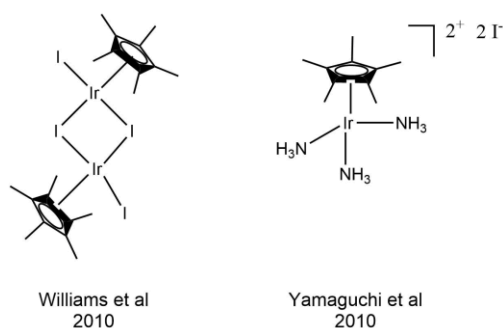


Figure 1.6 First iridium-based catalysts used in *N*-alkylation of amines in water [94,95].

To the best of our knowledge, although NHC-iridium catalysts have been shown to be active in *N*-alkylation of amines with alcohols [88,91,98,99], no example was yet reported in an aqueous medium.

1.4. Combining biocatalysis and organometallic catalysis: organometallic regeneration of NAD(P)H

The need for the addition of external co-factors is a major impairment in the industrial application of several oxidoreductases, for example, azoreductases, a class of enzymes very important in the pharmaceutical and chemical industry. As previously mentioned, their activity depends on co-factors like nicotinamide adenine dinucleotide (NADH) or its phosphorylated form (NADPH) to act as hydride donor. The industrial production of this co-factors is very expensive (in the US the bulk price is around \$ 3,000 and \$ 215,000 per mol) impairing their stoichiometric use in industrial processes limiting the application of relevant enzymatic systems^[100]. Synthetic chemists still have not found suitable synthetic replacements for these rather unstable molecules, so an effective co-factor regeneration system is required for the implementation of enzymatic reductions^[101]. This system should regenerate NAD(P)H simultaneously as the enzymatic reduction is occurring, in a second concurrent redox reaction. The selection of an adequate regeneration method has to ponder its activity, selectivity, sustainability, and compatibility with the main enzyme. Different methods have been studied for the regeneration of these co-factors: enzymatic, chemical, homogeneous catalysis, electrochemical, photocatalytic, and heterogeneous catalysis. Currently, only one

regenerating system is employed at industrial scale, an enzymatic methodology using formate dehydrogenase or glutamate dehydrogenase ^[101].

Organometallic complexes are interesting catalysts for the homogeneous regeneration of NAD(P)H. The application of organometallic catalysts in the regeneration of NAD(P)H it is still in its infancy, and the reports found are based on half-sandwich complexes of rhodium, ruthenium, and iridium. Table 1.3 summarizes a series of characteristics of selected examples of organometallic complexes studied in NAD(P)H regeneration reactions. By far, rhodium catalysts are the most studied, where $[\text{Cp}^*\text{Rh}(\text{bpy})\text{H}_2\text{O}]^+$ stands out due to its versatility and regioselectivity sparking the interest of different research groups ^[102–104]. Only for this catalyst and catalyst mentioned in Table 1.3, entry 3, reports on enzymatic compatibility can be found. It is described for both catalysts a mutual inactivation of organometallic complex and enzymatic system ^[103,105]. Although there is some interest in developing ruthenium catalysts, their activity is far from suitable for industrial application as it can be seen in Table 1.3, entry 8-10.

Iridium catalysts applied in the regeneration of NAD(P)H has a lot of potential due to its reported enhanced activity in hydrogen transfer reactions ^[106]. Furthermore, biological compatible temperatures can be used (Table 1.3, entry 11-13) ^[103,107,108].

Table 1.3 Selected examples of organometallic catalysts that were studied for the regeneration of NADH.

Entry	Metal	Cp ^x / Arene	Ligand	Catalyst:NAD ⁺ ratio	Temperature (°C)	TOF (h ⁻¹)	Reference
1	Rh	Cp [*]	bpy	1:17	38	81.5	Ruppert et al, 1988 ^[109]
2	Rh	Cp [*]	bpy	1:1000	60	875	Canivet et al, 2007 ^[103]
3	Rh	Cp [*]	phen	1:1000	60	560	Canivet et al, 2007 ^[103]
4	Rh	Cp [*]	5-NO ₂ -phen	1: 1000	60	2000	Canivet et al, 2007 ^[103]
5	Rh	Cp [*]	4,4'-CH ₂ OH-bpy	1:1000	60	710	Sivanesan et al, 2013 ^[110]
6	Rh	Cp ^{xPh}	en	1: 2-9	36	35.5	Soldevila-Barreda et al, 2015 ^[111]
7	Rh	Cp [*]	5,5'-CH ₂ OH-bpy	1:1000	60	1100	Ganesan et al, 2017 ^[112]
8	Ru	(CH ₃) ₆ bn	en	1:2	37	1.46	Yan et al, 2006 ^[113]
9	Ru	Cp [*]	5-NO ₂ -phen	1:100	38	10	Canivet et al, 2007 ^[103]
10	Ru	bn	TfEn	1: 2	36	10.39	Soldevila-Barreda et al, 2012 ^[114]
11	Ir	Cp [*]	5-NO ₂ -phen	1:100	38	58	Canivet et al, 2007 ^[103]
12	Ir	Cp [*]	pyraz	1:100	25	54	Maenaka et al, 2012 ^[115]
13	Ir	Cp [*]	pica	1:100	25	143	Bucci et al, 2017 ^[108]

1.5. References

- [1] I. T. Horváth, *Chem. Rev.* **2018**, *118*, 369–371.
- [2] R. A. Sheldon, J. M. Woodley, *Chem. Rev.* **2018**, *118*, 801–838.
- [3] P. T. Anastas, M. M. Kirchhoff, *Acc. Chem. Res.* **2002**, *35*, 686–694.
- [4] S. L. Y. Tang, R. L. Smith, M. Poliakoff, *Green Chem.* **2005**, *7*, 761.
- [5] M. Geissdoerfer, P. Savaget, N. M. P. Bocken, E. J. Hultink, *J. Clean. Prod.* **2017**, *143*, 757–768.
- [6] S. Ritzén, G. Ö. Sandström, *Procedia CIRP* **2017**, *64*, 7–12.
- [7] H. C. Erythropel, J. B. Zimmerman, T. M. De Winter, L. Petitjean, F. Melnikov, C. H. Lam, A. W. Lounsbury, K. E. Mellor, N. Z. Janković, Q. Tu, et al., *Green Chem.* **2018**, *20*, 1929–1961.
- [8] R. A. D. Arancon, C. S. K. Lin, K. M. Chan, T. H. Kwan, R. Luque, *Energy Sci. Eng.* **2013**, *1*, 53–71.
- [9] P. Marion, B. Bernela, A. Piccirilli, B. Estrine, N. Patouillard, J. Guilbot, F. Jerome, *Green Chem.* **2017**, DOI 10.1039/C7GC02006F.

- [10] European Commission, *A Sustainable Bioeconomy for Europe: Strengthening the Connection between Economy, Society and the Environment*, **2018**.
- [11] J. Dupont-Inglis, A. Borg, *N. Biotechnol.* **2018**, *40*, 140–143.
- [12] F. Fava, H. Ohtake, P. Pesaresi, *J. Biotechnol.* **2012**, *157*, 443–445.
- [13] H. Sun, H. Zhang, E. L. Ang, H. Zhao, *Bioorganic Med. Chem.* **2018**, *26*, 1275–1284.
- [14] M. Wang, T. Si, H. Zhao, *Bioresour. Technol.* **2012**, *115*, 117–125.
- [15] K. Faber, in *Biotransformations Org. Chem.*, Springer Berlin Heidelberg, Berlin, Heidelberg, **2011**, pp. 1–27.
- [16] C. C. C. R. De Carvalho, *Biotechnol. Adv.* **2011**, *29*, 75–83.
- [17] T. J. Schwartz, B. J. O'Neill, B. H. Shanks, J. A. Dumesic, *ACS Catal.* **2014**, *4*, 2060–2069.
- [18] C. A. Denard, J. F. Hartwig, H. Zhao, *ACS Catal.* **2013**, *3*, 2856–2864.
- [19] Y. Wang, H. Ren, H. Zhao, *Crit. Rev. Biochem. Mol. Biol.* **2018**, *53*, 115–129.
- [20] O. Verho, J. E. Bäckvall, *J. Am. Chem. Soc.* **2015**, *137*, 3996–

4009.

- [21] C. A. Denard, H. Huang, M. J. Bartlett, L. Lu, Y. Tan, H. Zhao, J. F. Hartwig, *Angew. Chemie - Int. Ed.* **2014**, *53*, 465–469.
- [22] C. A. Denard, M. J. Bartlett, Y. Wang, L. Lu, J. F. Hartwig, H. Zhao, *ACS Catal.* **2015**, *5*, 3817–3822.
- [23] Z. J. Wang, K. N. Clary, R. G. Bergman, K. N. Raymond, F. D. Toste, *Nat. Chem.* **2013**, *5*, 100–3.
- [24] M. Fuchs, M. Schober, J. Pfeffer, W. Kroutil, R. Birner-Gruenberger, K. Faber, *Adv. Synth. Catal.* **2011**, *353*, 2354–2358.
- [25] P. H. Dixneuf, V. Cadierno, *Metal-Catalyzed Reactions in Water*, Wiley-VCH Verlag GmbH & Co. KGaA, Weinheim, Germany, **2013**.
- [26] K. Vikrant, B. S. Giri, N. Raza, K. Roy, K. H. Kim, B. N. Rai, R. S. Singh, *Bioresour. Technol.* **2018**, *253*, 355–367.
- [27] B. J. Brüsweiler, C. Merlot, *Regul. Toxicol. Pharmacol.* **2017**, *88*, 214–226.
- [28] X. C. Jin, G. Q. Liu, Z. H. Xu, W. Y. Tao, *Appl. Microbiol. Biotechnol.* **2007**, *74*, 239–243.
- [29] H. S. Rai, M. S. Bhattacharyya, J. Singh, T. K. Bansal, P. Vats,

- U. C. Banerjee, *Crit. Rev. Environ. Sci. Technol.* **2005**, *35*, 219–238.
- [30] D. Rawat, V. Mishra, R. S. Sharma, *Chemosphere* **2016**, *155*, 591–605.
- [31] A. Pandey, P. Singh, L. Iyengar, *Int. Biodeterior. Biodegrad.* **2007**, *59*, 73–84.
- [32] R. L. Singh, P. K. Singh, R. P. Singh, *Int. Biodeterior. Biodegradation* **2015**, *104*, 21–31.
- [33] J. Feng, C. E. Cerniglia, H. Chen, *Front. Biosci.* **2012**, *4*, 568–586.
- [34] H. Chen, *Curr. Protein Pept. Sci.* **2006**, *7*, 101–111.
- [35] T. Ito, Y. Adachi, Y. Yamanashi, Y. Shimada, *Water Res.* **2016**, *100*, 458–465.
- [36] K. T. Chung, *J. Environ. Sci. Heal. - Part C Environ. Carcinog. Ecotoxicol. Rev.* **2016**, *34*, 233–261.
- [37] T. Robinson, G. McMullan, R. Marchant, P. Nigam, *Bioresour. Technol.* **2001**, *77*, 247–255.
- [38] E. Forgacs, T. Cserhádi, G. Oros, *Environ. Int.* **2004**, *30*, 953–971.
- [39] S. Sarkar, A. Banerjee, U. Halder, R. Biswas, R.

- Bandopadhyay, *Water Conserv. Sci. Eng.* **2017**, 121–131.
- [40] S. Rodriguez-Couto, *Curr. Drug Metab.* **2010**, *10*, 1048–1054.
- [41] R. Khan, P. Bhawana, M. H. Fulekar, *Rev. Environ. Sci. Biotechnol.* **2013**, *12*, 75–97.
- [42] S. K. Dubey, J. Dubey, A. J. Viswas, P. Tiwari, *Br. Biotechnol. J.* **2011**, *1*, 61–67.
- [43] D. Tischler, J. Qi, A. C. R. Ngo, M. Schlömann, in *Handb. Res. Microb. Tools Environ. Waste Manag.*, **2018**, pp. 341–371.
- [44] P. S., *Appl. Microbiol. Biotechnol.* **2001**, *57*, 20–33.
- [45] K. M. G. Machado, L. C. A. Compart, R. O. Morais, L. H. Rosa, M. H. Santos, *Brazilian J. Microbiol.* **2006**, *37*, 481–487.
- [46] S. Ertuğrul, M. Bakir, G. Dönmez, *Ecol. Eng.* **2008**, *32*, 244–248.
- [47] M. Solís, A. Solís, H. I. Pérez, N. Manjarrez, M. Flores, *Process Biochem.* **2012**, *47*, 1723–1748.
- [48] A. Kandelbauer, G. M. Guebitz, in *Environ. Chem. Green Chem. Pollut. Ecosyst.* (Eds.: E. Lichtfouse, J. Schwarzbauer, D. Robert), Springer Berlin Heidelberg, Berlin, Heidelberg, **2005**, pp. 269–288.
- [49] S. Mendes, A. Farinha, C. G. Ramos, J. H. Leitão, C. A.

- Viegas, L. O. Martins, *Bioresour. Technol.* **2011**, *102*, 9852–9859.
- [50] S. Mendes, M. P. Robalo, L. O. Martins, in *Microb. Degrad. Synth. Dye. Wastewaters* (Ed.: S.N. Singh), Springer, Switzerland, Cham, **2015**, pp. 27–55.
- [51] D. T. D'Souza, R. Tiwari, A. K. Sah, C. Raghukumar, *Enzyme Microb. Technol.* **2006**, *38*, 504–511.
- [52] L. Pereira, A. V. Coelho, C. A. Viegas, M. M. C. dos Santos, M. P. Robalo, L. O. Martins, *J. Biotechnol.* **2009**, *139*, 68–77.
- [53] L. Pereira, A. V. Coelho, C. A. Viegas, C. Ganachaud, G. Iacazio, T. Tron, M. P. Robalo, L. O. Martins, *Adv. Synth. Catal.* **2009**, *351*, 1857–1865.
- [54] A. Santos, S. Mendes, V. Brissos, L. O. Martins, *Appl. Microbiol. Biotechnol.* **2014**, *98*, 2053–2065.
- [55] S. A. Misal, K. R. Gawai, *Bioresour. Bioprocess.* **2018**, DOI 10.1186/s40643-018-0206-8.
- [56] M. Nakanishi, C. Yatome, N. Ishida, Y. Kitade, *J. Biol. Chem.* **2001**, *276*, 46394–46399.
- [57] S. A. Misal, D. P. Lingojar, R. M. Shinde, K. R. Gawai, *Process Biochem.* **2011**, *46*, 1264–1269.

- [58] S. Bürger, A. Stolz, **2010**, 2067–2076.
- [59] D. Cui, G. Li, D. Zhao, X. Gu, C. Wang, M. Zhao, *Process Biochem.* **2012**, *47*, 544–549.
- [60] J. M. Morrison, C. M. Wright, G. H. John, *Anaerobe* **2012**, *18*, 229–234.
- [61] S. A. Misal, D. P. Lingojar, K. R. Gawai, *Protein J.* **2013**, *32*, 601–608.
- [62] S. Mendes, L. Pereira, C. Batista, L. O. Martins, *Appl. Microbiol. Biotechnol.* **2011**, *92*, 393–405.
- [63] A. M. D. Gonçalves, S. Mendes, D. de Sanctis, L. O. Martins, I. Bento, *FEBS J.* **2013**, *280*, 6643–6657.
- [64] V. Brissos, N. Gonçalves, E. P. Melo, L. O. Martins, *PLoS One* **2014**, *9*, e87209.
- [65] L. Pereira, P. K. Mondal, M. Alves, in *Pollut. Build. Water Living Org.* (Eds.: E. Lichtfouse, J. Schwazbaeur, D. Robert), Springer International Publishing, **2015**, pp. 297–346.
- [66] R. N. Salvatore, C. H. Yoon, K. W. Jung, *Tetrahedron* **2001**, *57*, 7785–7811.
- [67] N. V. Borrero, F. Bai, C. Perez, B. Q. Duong, J. R. Rocca, S. Jin, R. W. Huigens III, *Org. Biomol. Chem.* **2014**, *12*, 881–886.

- [68] Shruti, J. Dwivedi, D. Kishore, S. Sain, *Synth. Commun.* **2018**, *48*, 1377–1402.
- [69] S. Witayakran, A. J. Ragauskas, *Adv. Synth. Catal.* **2009**, *351*, 1187–1209.
- [70] L. O. Martins, C. M. Soares, M. M. Pereira, M. Teixeira, T. Costa, G. H. Jones, A. O. Henriques, *J. Biol. Chem.* **2002**, *277*, 18849–18859.
- [71] A. C. Sousa, L. O. Martins, M. P. Robalo, *Adv. Synth. Catal.* **2013**, *355*, 2908–2917.
- [72] A. C. Sousa, M. F. M. M. Piedade, L. O. Martins, M. P. Robalo, *Green Chem.* **2016**, *18*, 6063–6070.
- [73] A. C. Sousa, S. R. Baptista, L. O. Martins, M. P. Robalo, *Chem. - An Asian J.* **2019**, *14*, 187–193.
- [74] A. C. Sousa, M. F. M. M. Piedade, L. O. Martins, M. P. Robalo, *Green Chem.* **2015**, *17*, 1429–1433.
- [75] A. C. Sousa, M. C. Oliveira, L. O. Martins, M. P. Robalo, *Green Chem.* **2014**, *16*, 4127–4136.
- [76] A. C. Sousa, M. Conceição Oliveira, L. O. Martins, M. P. Robalo, *Adv. Synth. Catal.* **2018**, *360*, 575–583.
- [77] R. H. Crabtree, *Organometallics* **2011**, *30*, 17–19.

- [78] R. Grigg, T. R. B. Mitchell, S. Sutthivaiyakit, N. Tongpenyai, *J C S chem comm* **1981**, 611–612.
- [79] Y. Watanabe, Y. Tsuji, Y. Ohsugi, *Tetrahedron Lett.* **1981**, 22, 2667–2670.
- [80] S. I. Murahashi, K. Kondo, T. Hakata, *Tetrahedron Lett.* **1982**, 23, 229–232.
- [81] G. E. Dobereiner, R. H. Crabtree, E. Nucleophiles, **2010**, 681–703.
- [82] D. J. C. Constable, P. J. Dunn, J. D. Hayler, G. R. Humphrey, J. L. Leazer, Jr., R. J. Linderman, K. Lorenz, J. Manley, B. a. Pearlman, A. Wells, et al., *Green Chem.* **2007**, 9, 411–420.
- [83] X. Ma, C. Su, Q. Xu, *Top. Curr. Chem.* **2016**, 374, 1–74.
- [84] S. Bähn, S. Imm, L. Neubert, M. Zhang, H. Neumann, M. Beller, *ChemCatChem* **2011**, 3, 1853–1864.
- [85] S. Agrawal, M. Lenormand, B. Martín-Matute, *Org. Lett.* **2012**, 14, 1456–1459.
- [86] J.-Q. Li, P. G. Andersson, *Chem. Commun.* **2013**, 49, 6131.
- [87] A. Bartoszewicz, R. Marcos, S. Sahoo, A. K. Inge, X. Zou, B. Martín-Matute, *Chem. - A Eur. J.* **2012**, 18, 14510–14519.
- [88] A. Prades, R. Corberán, M. Poyatos, E. Peris, *Chem. - A Eur.*

- J.* **2008**, *14*, 11474–11479.
- [89] Q. Zou, C. Wang, J. Smith, D. Xue, J. Xiao, *Chem. - A Eur. J.* **2015**, *21*, 9656–9661.
- [90] S. Ruch, T. Irrgang, R. Kempe, *Chem. - A Eur. J.* **2014**, *20*, 13279–13285.
- [91] D. Balcells, A. Nova, E. Clot, D. Gnanamgari, R. H. Crabtree, O. Eisenstein, *Organometallics* **2008**, *27*, 2529–2535.
- [92] S. Michlik, R. Kempe, *Chem. - A Eur. J.* **2010**, *16*, 13193–13198.
- [93] Q. Yang, Q. Wang, Z. Yu, *Chem. Soc. Rev.* **2015**, *44*, 2305–2329.
- [94] O. Saidi, A. J. Blacker, M. M. Farah, S. P. Marsden, J. M. J. Williams, *Chem. Commun. (Camb)*. **2010**, *46*, 1541–3.
- [95] R. Kawahara, K. Fujita, R. Yamaguchi, S. Kyoto, *J. Am. Chem. Soc.* **2010**, *3*, 15108–15111.
- [96] R. Kawahara, K. I. Fujita, R. Yamaguchi, *Adv. Synth. Catal.* **2011**, *353*, 1161–1168.
- [97] A. Wetzel, S. Wöckel, M. Schelwies, M. K. Brinks, F. Rominger, P. Hofmann, M. Limbach, *Org. Lett.* **2013**, *15*, 266–269.

- [98] A. P. Da Costa, M. Viciano, M. Sanaú, S. Merino, J. Tejada, E. Peris, B. Royo, *Organometallics* **2008**, *27*, 1305–1309.
- [99] A. Bartoszewicz, N. Ahlsten, B. Martín-Matute, *Chem. - A Eur. J.* **2013**, *19*, 7274–7302.
- [100] K. Faber, in *Biotransformations Org. Chem.*, **2011**, pp. 31–313.
- [101] X. Wang, T. Saba, H. H. P. Yiu, R. F. Howe, J. A. Anderson, J. Shi, *Chem* **2017**, *2*, 621–654.
- [102] E. Steckhan, S. Herrmann, R. Ruppert, E. Dietz, M. Frede, E. Spika, *Organometallics* **1991**, *10*, 1568–1577.
- [103] J. Canivet, G. Süß-Fink, P. Štěpnička, *Eur. J. Inorg. Chem.* **2007**, 4736–4742.
- [104] F. Hollmann, B. Witholt, A. Schmid, *J. Mol. Catal. B Enzym.* **2002**, *19–20*, 167–176.
- [105] M. Poizat, I. W. C. E. Arends, F. Hollmann, *J. Mol. Catal. B Enzym.* **2010**, *63*, 149–156.
- [106] D. Wang, D. Astruc, *Chem. Rev.* **2015**, *115*, 6621–6686.
- [107] Y. Maenaka, T. Suenobu, S. Fukuzumi, *J. Am. Chem. Soc.* **2012**, *134*, 9417–9427.
- [108] A. Bucci, S. Dunn, G. Bellachioma, M. Rodriguez, C. Zuccaccia, C. Nervi, A. Macchioni, *ACS Catal.* **2017**, DOI

10.1021/acscatal.7b02387.

- [109] R. Ruppert, S. Herrmann, E. Steckhan, **1988**, *1*, 1150–1151.
- [110] D. Sivanesan, S. Yoon, *Polyhedron* **2013**, *57*, 52–56.
- [111] J. J. Soldevila-Barreda, A. Habtemariam, I. Romero-Canelón, P. J. Sadler, *J. Inorg. Biochem.* **2015**, *153*, 322–333.
- [112] V. Ganesan, D. Sivanesan, S. Yoon, *Inorg. Chem.* **2017**, *56*, 1366–1374.
- [113] Y. K. Yan, M. Melchart, A. Habtemariam, A. F. A. Peacock, P. J. Sadler, *J. Biol. Inorg. Chem.* **2006**, *11*, 483–488.
- [114] J. J. Soldevila-Barreda, P. C. A. Bruijninx, A. Habtemariam, G. J. Clarkson, R. J. Deeth, P. J. Sadler, *Organometallics* **2012**, *31*, 5958–5967.
- [115] Y. Maenaka, T. Suenobu, S. Fukuzumi, *J. Am. Chem. Soc.* **2012**, *134*, 367–374.

Chapter 2

2. Dye-containing wastewaters as a source of biologically active building blocks: whole-cell catalysis by design

The work described in this chapter is part of a paper submitted for publication:

Ana Fernandes, Bruna Pinto, Lorenzo Bonnard, Beatriz Royo, M. Paula Robalo and Lúcia O. Martins (2019), Dye-containing wastewaters as a source of biologically active building blocks: whole-cell catalysis by design

Acknowledgements and contributions

Ana Fernandes performed most of the experiments described in this chapter and participated in the writing of the manuscript. Lúcia O. Martins directed the research and wrote the manuscript. Bruna Pinto developed the methodology for the two-step biotransformation and product characterization of MB3, RY145 and DR80 using purified enzymes. Lorenzo Bonnardò is acknowledged for his help in preliminary studies. M. Paula Robalo assisted in the correct analysis of NMR data and participated in discussion and in the writing of the manuscript. Beatriz Royo discussed the results and participated in the writing. João Carita, Isabel Pacheco and Cristina Leitão (Research Facilities, ITQB-NOVA) are acknowledged for technical assistance.

2.1. Abstract

In this work an environmental-friendly enzymatic strategy was developed for the valorization of dye-containing wastewaters. We set-up a one-pot system for the conversion of azo dyes (mordant, acid, reactive and direct), into valuable aromatic compounds. Firstly, using purified preparations of enzymes, we show that *Pseudomonas putida* PpAzoR azoreductase efficiently reduce these azo dyes into aromatic amines and CotA-laccase from *Bacillus subtilis* efficiently oxidize these into phenoxazinones, phenazines and naphthoquinones. Secondly, whole-cells of recombinant *Escherichia coli* containing the overproduced enzymes were successfully utilized in the two-step enzymatic conversion of the model mordant black 9 dye into sodium 2-amino-3-oxo-3H-phenoxazine-8-sulfonate, overcoming drawbacks associated with the use of expensive purified enzymes, co-factors (NAD(P)H) or exquisite reaction conditions. Thirdly cells were immobilized in sodium alginate, allowing to recycle the biocatalysts and to achieve very good yields (up to 80%). Finally, one-pot systems using recycled immobilized cells co-producing both enzymes resulted in higher phenoxazinone yields (90%) through the sequential use of static and shaking conditions, controlling the oxygenation of reaction mixtures and the successive activity of azoreductase (anaerobic) and laccase (aerobic), respectively.

2.2. Introduction

It is now widely accepted that the sustainability of life on earth is strictly dependent on the principles of circular economy emphasizing the urgency to design out waste and pollution, keep products and materials in use and regenerate natural systems ^[1,2]. In particular, the control of water pollution has become of increasing importance in recent years. Currently, more than 10,000 different recalcitrant synthetic dyes are used and it is estimated that 200 billion liters of wastewaters containing 10^5 tons of dyes, from which around 70% are azo dyes, are annually released from textile, food, paper, printing, leather and cosmetics industries ^[3,4]. The dye-containing wastewaters rise affects photosynthesis, decreasing dissolved oxygen levels and severely disturbs aquatic ecosystems and represent a liability since many azo dyes or their aromatic breakdown products, are toxic and potentially mutagenic to living organisms ^[5,6].

The vast majority of dye-containing wastewater treatments rely on the use of physical-chemical methods, including precipitation, coagulation, and filtration ^[7,8]. In spite of their recognized efficiency in decolorization processes, they are expensive, use hazardous chemical additives, produce large amounts of sludge and are frequently not skillful for full wastewaters detoxification. Biological treatment technologies are eco-friendly alternatives that allow overcoming in a cost-effective manner

the limitations of physical-chemical methods [9–11]. Enzymatic processes are particularly attractive considering that in contrast to the chemical variety of dyes present in wastewaters, the biological decolorization has been assigned to the action of a limited number of enzymes: azoreductases, laccases and peroxidases [12–14]. The enzymatic treatment of dye-containing wastewaters has been typically performed without concerns on the nature of products and their potential added-value. However, biological systems have proved useful in the conversion of a myriad of compounds offering opportunities for the smart implementation of bioprocess that couple dye degradation to their conversion into valuable chemicals.

The decolorization and detoxification of a large array of structurally diverse azo-dyes and model wastewaters has previously been reported through the synergistic action of *Pseudomonas putida* MET94 PpAzoR azoreductase and *Bacillus subtilis* CotA-laccase [15]. In this work, the coupled action of these enzymes was investigated in the valorization of wastewaters containing azo dyes. Azoreductases are highly effective in decolorizing azo dyes yielding aromatic amines [16] that are extensively used as building blocks in different industries, including agrochemical, fine chemical and pharmaceutical. CotA-laccase oxidize several aromatic amines through homo- and heteromolecular-coupling reactions into commercially interesting

products, including dyes, phenazines, phenoxazinones, benzocarbazoles, and quinones [17–22]. These compounds are important biological active motifs of antibiotics [23], antitumor agents [24–26], pesticides [27,28] and are useful precursors for the industrial manufacturing of pharmaceuticals [29], fine chemicals [30,31] biosensors [27,32] among others. Sustainable synthetic methodologies are highly sought considering that the traditional synthetic chemical approaches use stoichiometric amounts of chemicals, strong acids and high temperatures and result in low production yields [33,34].

In this study, we have assessed the degradation of five azo dyes (mordant black 9, mordant black 3, acid red 266, yellow reactive 145 and direct red 80) using enzyme preparations of PpAzoR and CotA-laccase. We have identified, using HPLC and NMR spectroscopy, the aromatic amines, PpAzoR products, and next, the heterocyclic products (phenazines, phenoxazinones and quinones), that resulted from the reaction of aromatic amines with CotA-laccase. After establishing the proof of concept, we have optimized the two-step bioprocess using free and alginate-immobilized *Escherichia coli* cells that have overproduced the enzymes of interest. A final one-pot bioprocess with immobilized cells, in water and at milder conditions of temperature, led to 90% product yields in the conversion of mordant black 9 in 2-amino-3-oxo-3H-phenoxazine-8-sulfonate.

2.3. Results and Discussion

2.3.1. Two-step bioconversion of dyes using purified enzymes

The dyes used in this study were chosen to represent the most common classes of azo dyes: mordant black 3 (MB3) and mordant black 9 (MB9), acid red 266 (AR266), reactive yellow 145 (RY145) and direct red 80 (DR80), commonly used in cotton and wool-dyeing processes and thus frequently present in textile industries wastewaters [3]. MB9 and MB3 are quite toxic dyes as assessed by the severe inhibitory effects on the reproduction of *Saccharomyces cerevisiae*, an important microbial eukaryotic model, and of the nematode *Caenorhabditis elegans*, a test organism with recognized relevance in soil and aquatic ecotoxicology [15]. Furthermore, AR266, DR80 and RY145 are dyes that upon degradation using azoreductases were shown to yield products that are more toxic than dyes themselves [15].

The reactions of the five azo dyes with PpAzoR azoreductase, under anaerobic conditions, yielded decolorization levels above 85% after 24 h of reaction as assessed by UV-Vis at the λ_{\max} of each dye (Table 2.1). The reaction mixtures were analyzed by ^1H NMR spectroscopy (in $\text{CD}_3\text{OD-d}_4$; Fig. 2.1-2.5), which indicated the complete disappearance of the dyes and the presence of aromatic amines as well as NAD^+ , the oxidation product of NADH , and other compounds derived from the

NADH/NAD⁺ degradation. The azo bond cleavage of MB9 promoted by the PpAzoR and responsible for the observed decolorization, is expected to yield two aromatic amines (Table 2.1), sodium 3-amino-4-hydroxybenzene and 2-aminonaphthalene-1,5-diol. The ¹H NMR spectrum of the reaction mixture showed the formation of sodium 3-amino-4-hydroxybenzene, which displayed three resonances, a singlet at 7.21 ppm and two doublets at 6.69 and 7.07 ppm (SAHBS, **1**) (Fig. 2.1C), in accordance with data reported in the literature ^[31]. The expected 2-aminonaphthalene-1,5-diol compound was not detected in the ¹H NMR spectrum of the reaction mixture. Probably, this amine is initially formed, but in the presence of oxygen it degrades forming insoluble oligomeric compounds ^[35–37]. Similar results were obtained for the other dyes tested, only one of the expected amines were identified, except in reactions with DR80, where two of the three possible amines (Table 2.1) were observed by ¹H NMR spectroscopy. The ¹H NMR spectrum of the MB3 reaction mixture showed four resonances for aromatic protons, two doublets at 8.71 and 7.93 ppm, a singlet at 7.83 ppm and one multiplet at 7.38 ppm, consistent with a substituted naphthalene structure and attributed to the sodium 4-amino-3-hydroxynaphthalene-1-sulfonate (SAHNS, **2**) (Fig. 2.2C), by comparison with a commercial sample. The spectra of the reaction mixtures obtained when AR266 and RY145 were used as substrates,

showed the presence of sodium 5,6-diamino-4-hydroxynaphthalene-2-sulfonate (SDAHNS, **3**) (Fig. 2.3C) and sodium 7-aminonaphthalene-1,3,6-trisulfonate (SANTS, **4**) products, respectively (Fig. 2.4C). Finally, the ^1H NMR spectrum of the reaction products obtained from DR80, displayed four doublets and one singlet in the range 6.5-7.2 ppm, indicating the presence of two aromatic amines out of the three expected: the commercially available sodium 4-aminobenzene sulfonate (SABS, **5**) and sodium 2,5-diaminobenzene sulfonate (SDBS, **6**) (Fig. 2.5C).

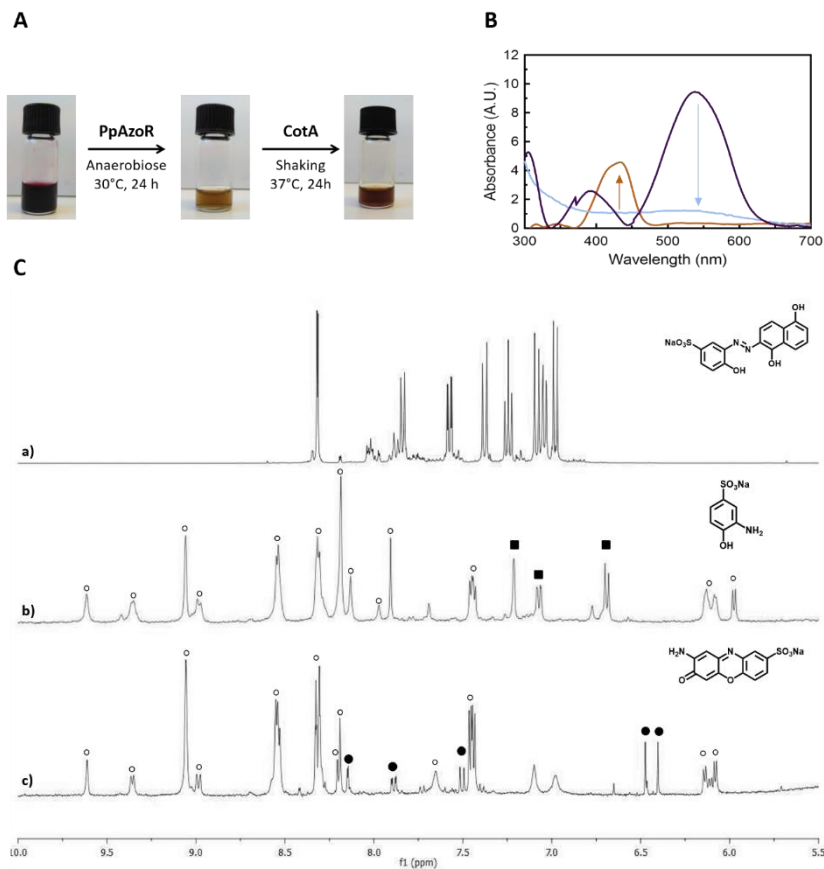


Figure 2.1 (A) Products of the MB9 bioconversion upon the sequential addition with purified PpAzoR azoreductase and CotA-laccase, under anaerobic and aerobic conditions, respectively. (B) UV-Vis spectra of the initial reaction mixture (purple) and after reaction with PpAzoR azoreductase (light blue) and CotA-laccase (light brown). (C) $^1\text{H-NMR}$ spectra (aromatic region) of MB9 (a), and of the products of reaction after addition of PpAzoR azoreductase (b) and CotA-laccase (c). Resonances due to NAD^+ and other intermediates resulting from NADH/NAD^+ degradation (open circles), SAHBS (filled squares) and compound **7** (filled circles) are labelled.

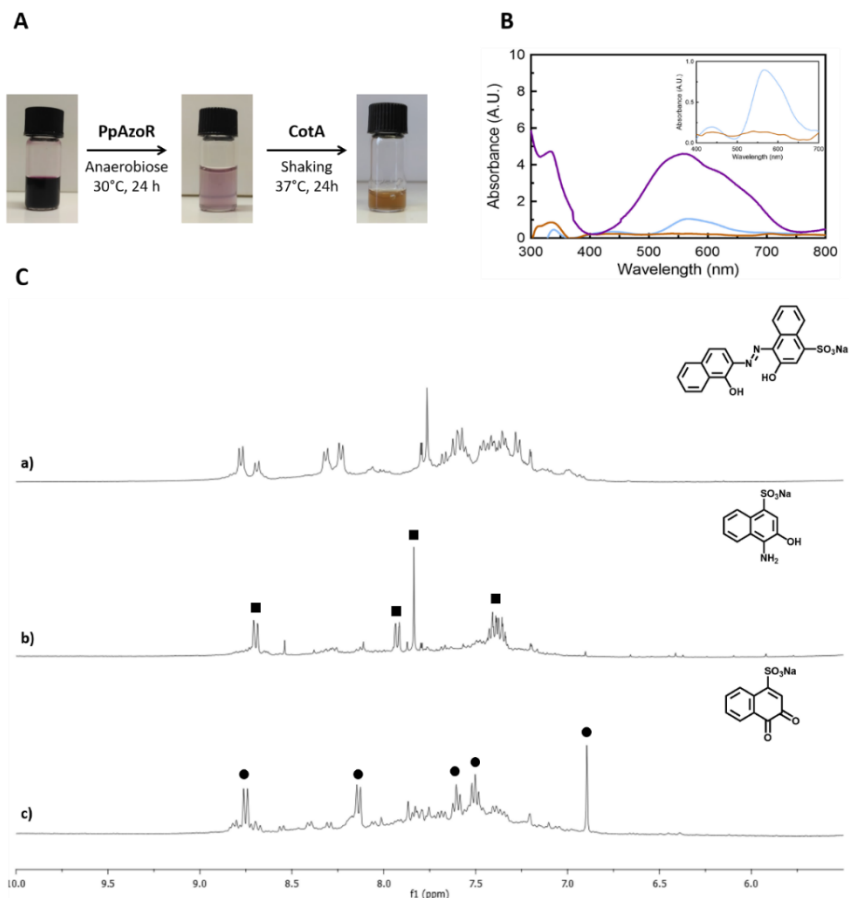


Figure 2.2 (A) Products of the MB3 bioconversion upon the sequential reaction with purified PpAzoR azoreductase and CotA-laccase, under anaerobic and aerobic conditions, respectively. (B) UV-Vis spectra of the initial reaction mixture (purple), after reaction with PpAzoR azoreductase (light blue) and CotA-laccase actions (light brown) (insert: zoom for lower absorbances). (C) $^1\text{H-NMR}$ spectra (aromatic region) of MB3 (a), and of the products of reaction after addition of PpAzoR azoreductase (b) and CotA-laccase (c). Resonances due to SAHNS (filled squares) and compound **8** (filled circles) are labelled.

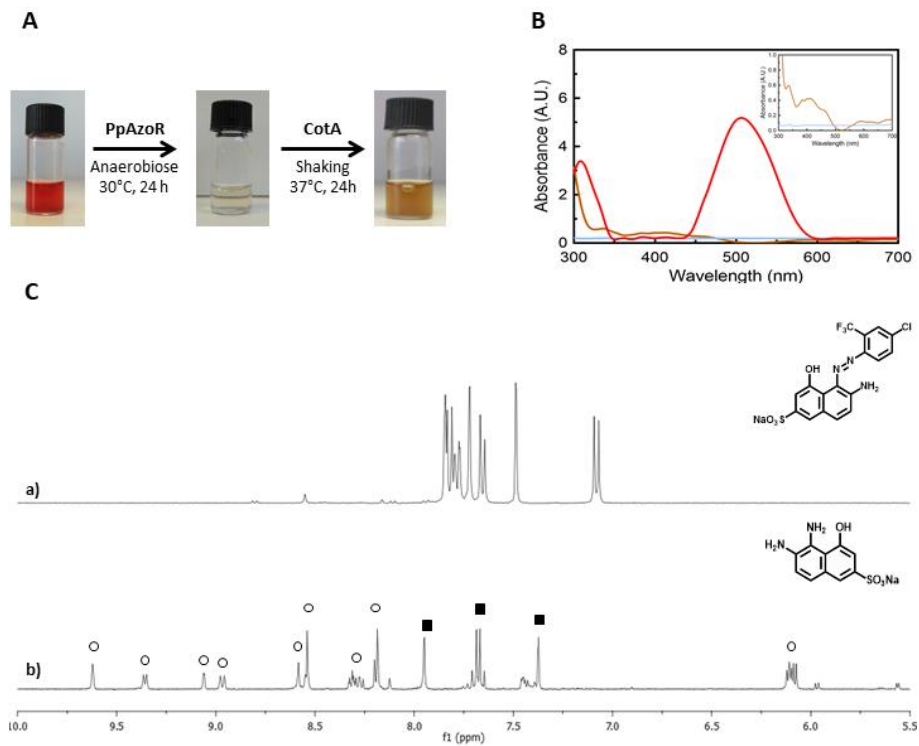


Figure 2.3 (A) Products of the AR266 bioconversion upon sequential reaction of purified PpAzoR azoreductase and CotA-laccase, under anaerobic and aerobic conditions, respectively. (B) UV-Vis spectra of the initial reaction mixture (dark orange), after reaction with PpAzoR azoreductase (light blue) and CotA-laccase (light brown) (insert: zoom for lower absorbances). (C) $^1\text{H-NMR}$ spectra (aromatic region) of AR266 (a), and of the products of reaction after addition of PpAzoR azoreductase (b). Resonances due to NAD^+ (open circles), and SDAHNS (filled squares).

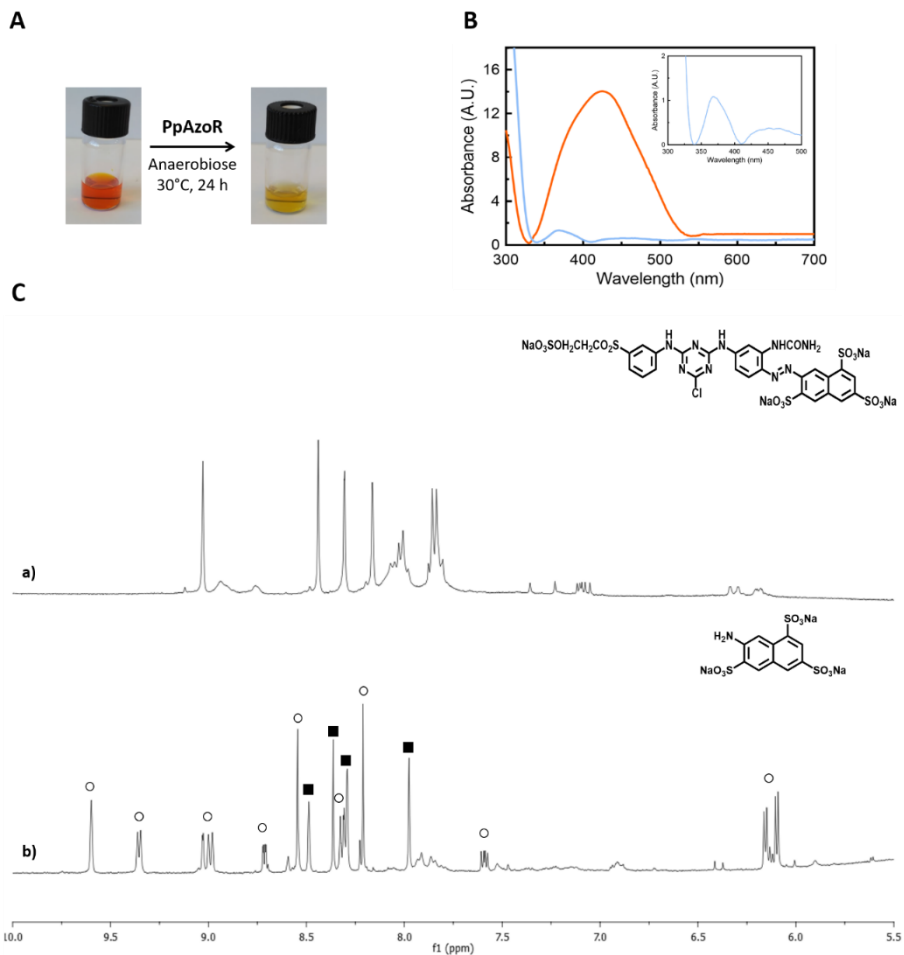


Figure 2.4 (A) Products of the RY145 upon reaction of purified PpAzoR azoreductase, under anaerobic conditions. (B) UV-Vis spectra of the initial reaction mixture (orange) and after reaction with PpAzoR azoreductase (light blue) (insert: zoom for lower absorbances). (C) $^1\text{H-NMR}$ spectra (aromatic region) of RY145 (a), and of the products of reaction after addition of PpAzoR azoreductase (b). Resonances due to SANT (filled squares) are labelled.

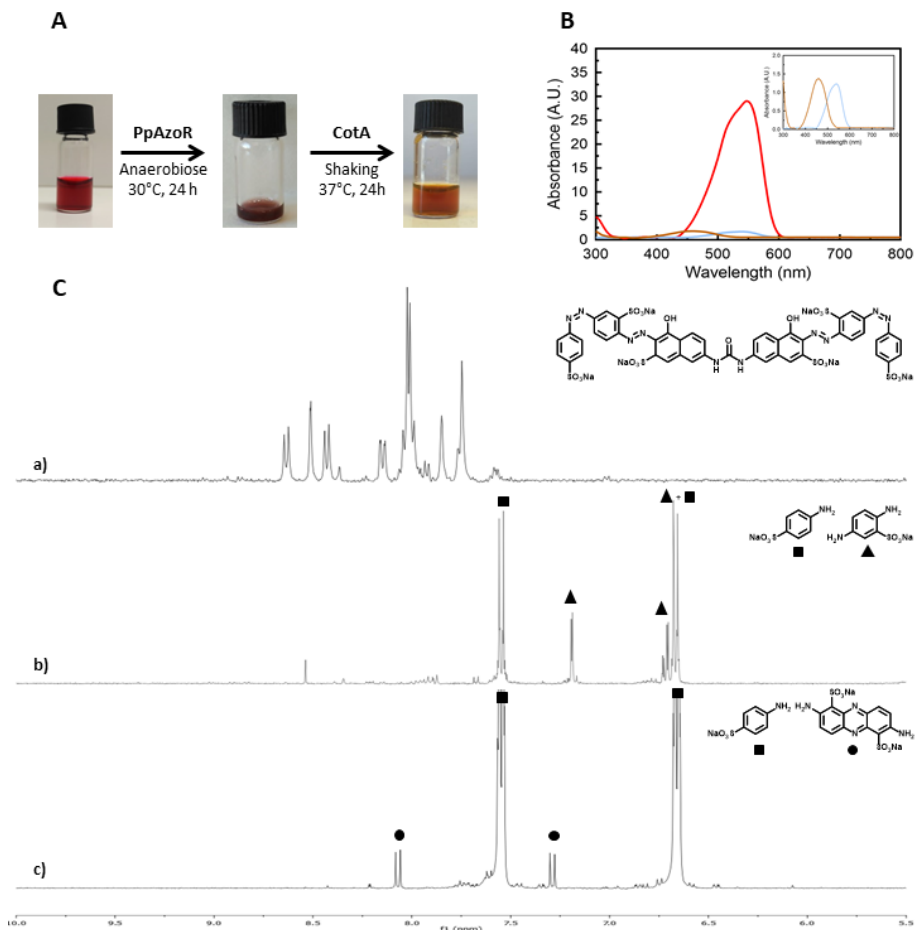


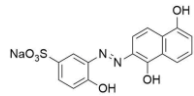
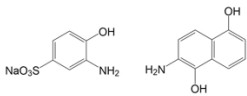
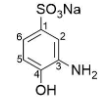
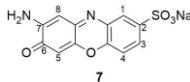
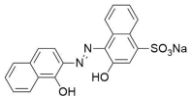
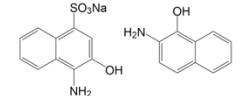
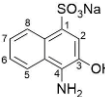
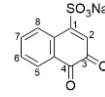
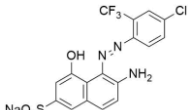
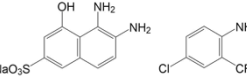
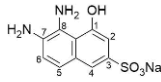
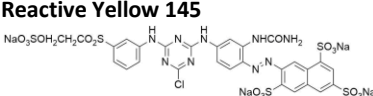
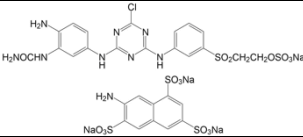
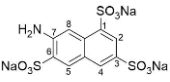
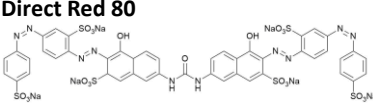
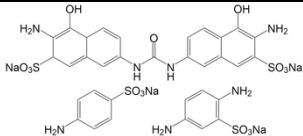
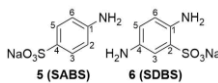
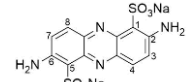
Figure 2.5 (A) Products of DR80 bioconversion upon the sequential reaction with purified PpAzoR azoreductase and CotA-laccase, under anaerobic and aerobic conditions, respectively. (B) UV-Vis spectra of the initial reaction mixture (dark orange), after reaction with PpAzoR azoreductase (light blue) and CotA-laccase (light brown). (C) $^1\text{H-NMR}$ spectra (aromatic region) of DR80 (a), and of the products of reaction with PpAzoR azoreductase (b) and CotA-laccase (c). Resonances due to SABS (solid squares), SDBS (solid triangles) and compound **9** (solid circles) are labelled.

CotA-laccase was added to the reaction mixtures containing the above-mentioned aromatic amines in order to set-up the second step of the biotransformation under aerobic conditions. The ability of CotA-laccase to mediate the oxidation of substituted aromatic amines was previously reported to be strongly dependent on the amines structural features, such as the electronic nature and the position of the substituents ^[17,18,20]. The oxidation of SAHBS (**1**), the PpAzoR product from the MB9 dye, resulted in the formation of a colored phenoxazinone with maximal absorbance at 430 nm (Fig. 2.1B). The ¹H NMR spectrum showed a downfield shielding of all proton signals relative to the parent aromatic amine and, in addition two new singlets at 6.48 and 6.43 ppm (Fig. 2.1C). These signals led to the identification of sodium 2-amino-3-oxo-3H-phenoxazine-8-sulfonate (**7**), in accordance with data reported in the literature ^[31]. The oxidation of compound **2**, the PpAzoR product when MB3 was used as a substrate, led to the formation of the ortho-naphthoquinone **8**, a product previously identified in the oxidation of SAHNS (**2**) by CotA-laccase ^[38]. The naphthalene scaffold is characterized by five signals in the aromatic region (6.9 – 8.8 ppm) and the ortho-quinone core is confirmed by the presence of the characteristic ¹³C NMR resonances at 183.5 and 180.1 ppm. Considering the enzymatic pathway proposed for the oxidation of ortho-aminophenol derivatives mediated by CotA-

laccase, the ortho-quinone core can be obtained through a hydrolysis process of the ortho-quinone imine intermediate formed during CotA-laccase oxidation ^[18]. Further coupling and cyclization are in this case, hampered by the substitution pattern of the aromatic rings. The CotA-laccase oxidation of the SDAHNS (**3**), obtained from the azo reduction of AR266, originates a complex mixture of products that prevented their full characterization without extensive purification. For the RY145 case, the analysis of the mixture obtained from the second enzymatic oxidative step showed the presence of the amine **4** resultant from the first step, revealing that this amine is not a substrate of CotA-laccase. This was attributed to the presence of the three electron-withdrawing sulfonate groups on the amine naphthalene structure, thereby decreasing the electron density in the rings making the amine group less favorable to oxidation ^[17]. The NMR analysis (Fig. 2.5C) of the resulting mixture obtained by CotA-laccase oxidation of amines SABS (**5**) and SDBS (**6**), the PpAzoR products when DR80 was the substrate, reveals the presence of a colored phenazine (**9**), with maximum absorbance at 450 nm, that resulted from the self-coupling reaction of SDBS ^[18]. Compound **5** due to the presence of the electron deficient sulfonate group in the para position was not a CotA-laccase substrate ^[17].

Overall, our results show that the decolorization of azo dyes through the sequential use of azoreductases and laccases, leads first to the formation of aromatic amines, which are then converted into quinones, phenoxazinones and phenazines, key cores for several relevant bioactive compounds, including antioxidants, antitumor and antibiotic agents ^[23–26]. These results highlight the potential of enzymatic processes for the implementation of sustainable methodologies targeted at improving dye-containing wastewaters treatment, management and most importantly their valorization.

Table 2.1 Dyes used in this study expected and identified products obtained after incubation with the PpAzoR azoreductase (1st step) and CotA-laccase enzymes (2nd step), as identified by NMR.

Azo Dye	Decolorization after 1 st step (%)	Expected products from 1 st step	Identified Products	
			1 st step	2 nd step
Mordant black 9 	90 ± 2		 1 (SAHBS)	 7
Mordant black 3 	85 ± 4		 2 (SAHNS)	 8
Acid Red 266 	87 ± 1		 3 (SDAHNS)	ND
Reactive Yellow 145 	90 ± 3		 4 (SANT)	nd
Direct Red 80 	96 ± 2		 5 (SABS) 6 (SDBS)	 9

ND not determined nd not detected

2.3.2. Set-up of free and immobilized whole-cells systems for the sequential degradation and valorization of MB9

In order to develop not only environmentally friendly but also cost-effective bioprocesses, we set-up dye decolorization assays using free and immobilized whole-cells that overproduced the enzymes of interest. The use of whole-cells as biocatalysts is very advantageous since it not only reduces direct operational costs associated to enzyme purification and the supply of expensive co-factors such as NAD(P)H, but also reduces indirect costs associated with the presence and protective nature of the cellular envelope that helps to stabilize the enzymes enabling longer and/or recycling reactions ^[39,40].

The use of whole cells as biocatalysts can be limited by the cell membrane which impairs the permeation of substrates and/or products to and from the cell core ^[39]. Different methods have been shown to improve cell permeation, that typically include incubation in slightly adverse conditions such as in organic solvents, detergents, and/or at different temperatures ^[41]. Reactive Black 5 (RB5) was used as a model to access the effect on decolorization rate of incubating *E. coli* Tuner overproducing PpAzoR with 2% toluene, 10 % ethanol and 100 mM sodium phosphate buffer pH 7, at 15 and 37 °C for 20 min. After incubation, supernatants were analyzed for protein content and enzymatic activity (Fig. 2.6A). The incubation with organic solvents led

to an increased release of total protein to the supernatant, that exhibited higher activity for PpAzoR than in control conditions (where no incubation protocol was applied) (Fig. 2.6A). This indicates that cell integrity might have been affected more than intended. The treated cells were also used to decolorize RB5 using a time course assay. Good decolorization levels were reached in all conditions after 48 to 72 h of incubation (Fig 2.6B). Nonetheless, in conditions that no treatment was applied (control) or upon incubation at 15 °C (in the presence or absence of solvents) resulted in faster reaction rates (Fig. 2.6B). These results led us to decide to not apply any permeabilization protocol to *E. coli* cells prior to use. These results are in accordance with the reported non-dependence of dyes degradation on its crossing along the cell membrane [11,42–44].

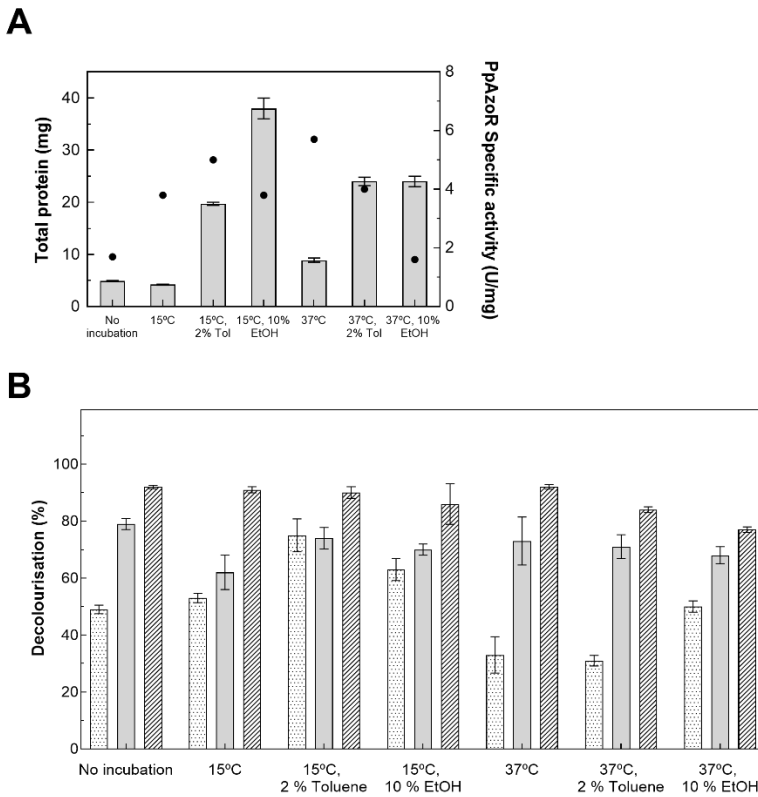


Figure 2.6 Assessment of *E. coli* Tuner permeabilization assays through evaluation of total protein (A, grey bars) and PpAzoR specific activity (A, dots) released to the supernatant during incubation; and through a time course decolorization assay of RB5 with permeabilized *E. coli* Tuner cells: 24h (dotted bars), 48h (grey bars) and 72h (dashed bars).

Time-course decolorization assays of MB9 were performed using different *E. coli* strains overproducing a PpAzoR evolved variant, 2A1-Y179H that shows 4-fold higher activity than the wild-type enzyme ^[45] (Fig 2.7).

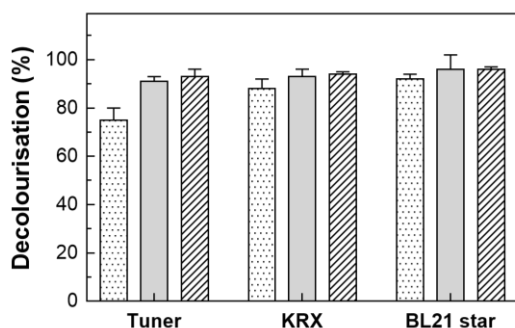


Figure 2.7 Time course bioconversion of MB9 using different *E. coli* strains (60 mg DCW mL⁻¹) containing PpAzoR azoreductase after 24 h (dotted bars), 48 h (grey bar) and 72 h (dashed bars) of reaction at 30°C in static conditions.

Whole-cell reactions using Tuner, KRX and BL21 star *E. coli* strains lead to decolorization values after 24 h of reaction close to 95% with 70-91 % product yields (0.66 to 0.87 mM of SAHBS; Table 2.2). In general, it was observed that the levels of decolorization are higher than product yields most likely related to the occurrence of non-enzymatic decolorization, for example, adsorption of dyes to cell surfaces [46].

Table 2.2 Decolorization of MB9 using different free or immobilized *E. coli* cells (Tuner, BL21 star and KRX strains) containing the PpAzoR 2A1-Y179H variant (60 mg DCW mL⁻¹) in static conditions for 72 h at 30°C.

<i>E. coli</i> cells	Immobilization	Decolorization (%)	SAHBS (mM)	Yield (%)
Tuner	No	90 ± 2	0.87	91
BL21 star	No	91 ± 1	0.66	70
KRX	No	92 ± 2	0.76	80
Tuner	Yes	68 ± 4	0.33	34
BL21 star	Yes	84 ± 5	0.87	92
KRX	Yes	89 ± 2	0.94	99

As expected, the ^1H NMR analysis of the reaction mixtures showed the resonances of SAHBS and no signals of NADPH or its oxidized products were observed, as expected, and in contrast to the reactions using purified enzymes where the co-factor was added to the reaction mixture (see Figs. 2.1Cb and 2.8). The ^1H NMR spectra showed, however, the presence of other signals, due most probably to intracellular metabolites derived from cells. A lower amount of 'contaminant' signals was present in reactions with KRX, as compared to Tuner or BL21 star cells (Fig 2.8).

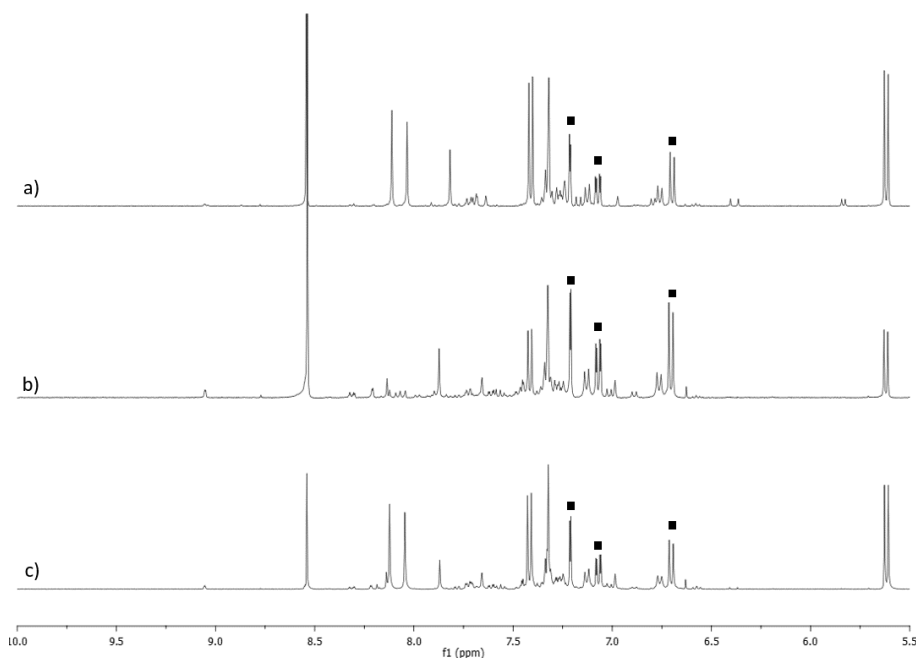


Figure 2.8 ^1H NMR spectra (aromatic region) of the bioconversion of MB9 using (a) *E. coli* Tuner, (b) *E. coli* KRX or (c) *E. coli* BL21 star cells containing PpAzoR azoreductase, after 72 h of reaction at 30 °C, in static conditions. Resonances due to SAHBS (filled square) are labelled.

Immobilization of cells is known to bring advantages to the efficiency of bioprocesses since it protects biocatalysts by improving their stability^[47]. This is particularly important in processes targeted at dye-containing wastewaters which are rich in salts, additives, surfactants, detergents and others that lead to enzyme denaturation^[48,49]. Moreover, immobilization allows the biocatalysts (cells) to be used in repeated cycles, which is critical when applying at industrial scale. We have first compared the performance in time-course MB9 decolorization assays of free and immobilized *E. coli* cells (60 mg DCW ml⁻¹). The alginate-immobilized cells showed lower decolorization rates as compared to free cells, most likely due to the presence of the alginate matrix that restricts diffusion of substrate through the beads^[50], and only after 72 h of reaction, decolorization with immobilized cells reached the levels obtained with free cells after 24 h of reaction (~ 90%; Fig. 2.9A). Notably, the reaction mixture performed with immobilized cells resulted in a cleaner ¹H-NMR spectrum indicating that cell encapsulation prevented leakage of undesirable intracellular 'contaminants' (Fig 2.9B).

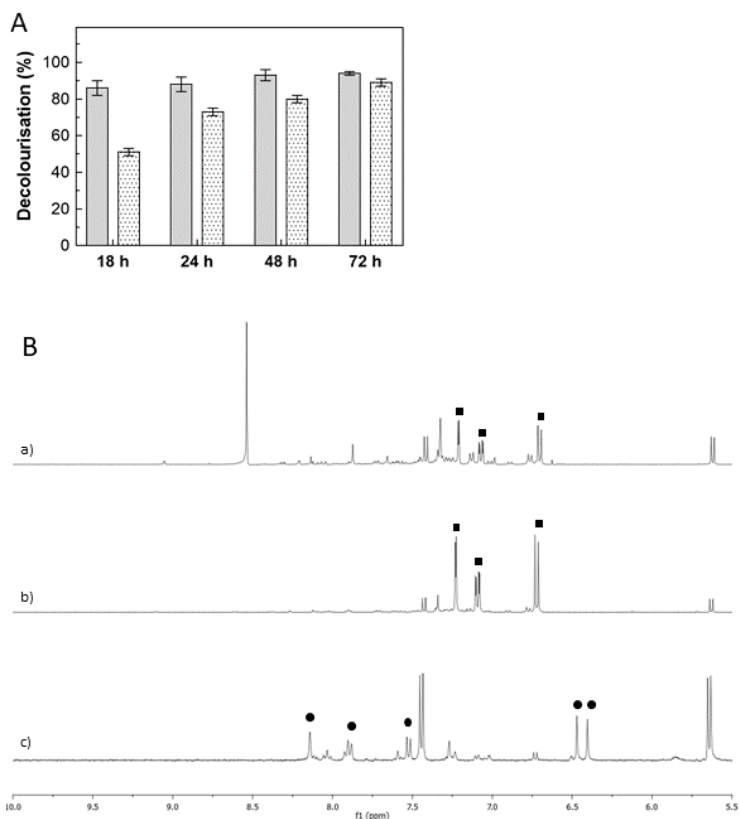
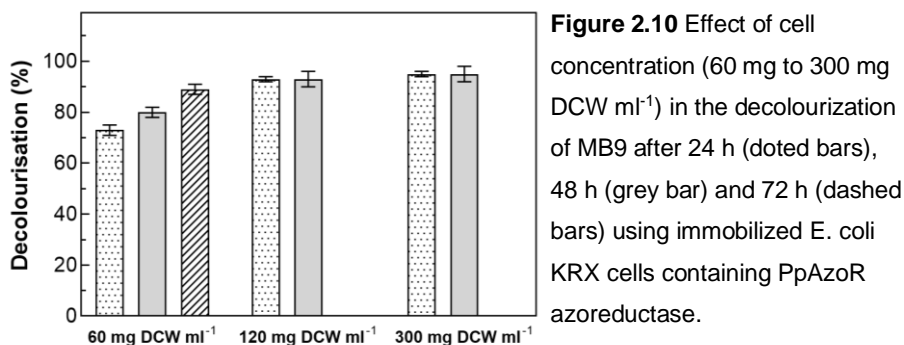


Figure 2.9 (A) Time-course decolorization of MB9 using free (light grey) and immobilized (dotted bars) cells containing PpAzor azoreductase ($60 \text{ mg DCW ml}^{-1}$) at 30°C in static conditions. (B) $^1\text{H-NMR}$ spectra (aromatic region) of reaction mixtures containing MB9 with (a) free or (b) immobilized *E. coli* KRX cells overproducing PpAzor in static conditions at 30°C , and (c) after addition of immobilized *E. coli* KRX cells overproducing CotA-laccase under shaking conditions at 37°C . Resonances due to SAHBS (filled squares) and compound **7** (filled circles) are labelled.

E. coli KRX cells were selected for further studies considering the superior performance as compared with BL21 star and Tuner cells (Table 2.2). To decrease the time of reaction the amount of cells immobilized in alginate beads was increased from 60 to 120 mg DCW ml⁻¹, which resulted in 90 ± 4 % MB9 decolorization after 24 h (Fig 2.10). Further increase in cell amounts did not lead to improved decolorization levels in shorter time periods (Fig. 2.10).



In these conditions (120 mg ml⁻¹), the MB9 enzymatic reductive process catalyzed by PpAzoR reached 77 % yield after 24 h of the aromatic amine SAHBS (Table 2.3). The slightly lower production yield as compared with free cells, relates to dye adsorption to the alginate matrix, as observed by the color of the alginate beads at the end of the reaction.

Table 2.3 Biotransformation of MB9 in two sequential steps using immobilized *E. coli* KRX whole-cells (120 mg DCW mL⁻¹) overproducing PpAzoR and CotA-laccase individually. The first step was performed in static conditions at 30°C (1 cycle or 4 cycles of 24 h each), and the second in shaking conditions, at 37°C for 24 h. Reactions were performed in water (1, 3) and 20 mM phosphate buffer, pH 7 (2, 4).

	1 st step			2 nd step		Overall yield (%)
	Decolorization (%)	SAHBS (mM)	Yield (%)	Compound 7 (mM)	Yield (%)	
1	89 ± 2	0.71	74	0.36	99	74
2	91 ± 3	0.73	77	0.36	99	75
3	91; 70; 55; 37	0.76	80	0.37	97	78
4	91; 70; 51; 38	0.78	82	0.38	95	80

The addition to the reaction mixture of immobilized cells containing CotA-laccase, lead to full conversion (99 %) of the amine to the phenoxazinone (**7**) (Fig. 2.9 and Table 2.3). These results clearly show that the first step is the limiting step of the enzymatic conversion of the MB9 dye into a phenoxazinone. Importantly, the overall yield of the two-step biotransformation reaction was very similar when using water (74 %) or 20 mM phosphate buffer pH 7 (75 %) in the reaction mixtures, a result that further highlights the cost-effectiveness and environmental-friendly character of the developed system.

Next, we have tested the recycled utilization of immobilized cells containing the PpAzoR azoreductase through a 24 h-stepwise addition of a 2 mM MB9 dye solution, under static conditions in water and in buffer (20 mM phosphate buffer, pH 7). In these conditions, the levels

of decolorization decreased stepwise from 91 after 24 h to 37-38 % after 96 h of reaction (Fig. 2.11). Notably, along the recycling process the final product yields increased from 74 to 78% in water and from 75 to 80% in buffer (Table 2.3), probably due to a time-dependent increase in cell permeabilization. Although higher yields of SAHBS were obtained in the buffered reaction, alginate beads were not sufficiently stable, and slow disintegration was visible during the recycling cycles. The addition of immobilized whole-cells containing CotA-laccase resulted in comparable yields in all tested conditions (between 97 to 99 %) and the slightly higher final overall yields of phenoxazinone production in the recycled system (78 and 80 %) as compared to the one-cycle system (74 and 75 %) (Table 2.3).

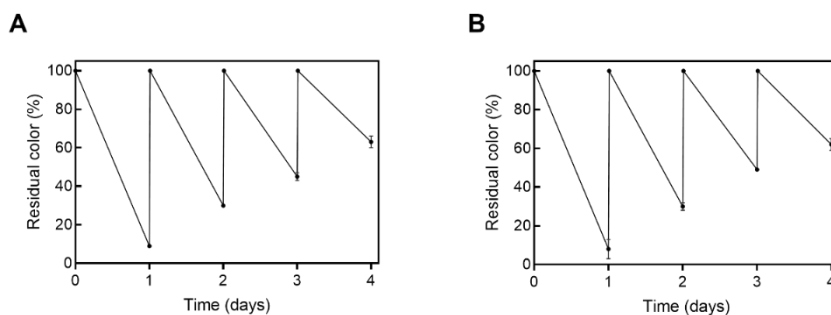


Figure 2.11 Whole-cell biocatalysis residual color in sequential batches for MB9 decolorization reaction using different mediums: (A) water or (B) 20 mM sodium phosphate buffer pH 7.

Finally, we have tested *E. coli* cells co-producing simultaneously the enzymes PpAzoR and CotA (Table 2.4) ^[15,51,52]. This approach reduces two-fold the time and cost associated with cell production. The dye conversion bioprocess was first performed by subjecting reaction mixtures to 24 h static followed by a 24 h shaken treatment, *i.e.* anaerobic conditions where the first enzyme PpAzoR is active and aerobic conditions where CotA is active, respectively. This approach resulted in significantly lower phenoxazinone yields (50%) than the process using *E. coli* cells producing separately the PpAzoR and the CotA-laccase enzymes (Table 2.4). However, when the first step was performed in a recycled manner, adding dye solution in a 24 h stepwise manner, the overall performance improved significantly, affording 90% product yields, showing an enormous potential for dye-containing wastewaters sustainable and eco-friendly valorization.

Table 2.4 Biotransformation of MB9 in two sequential steps using immobilized *E. coli* KRX whole-cells (120 mg DCW mL⁻¹) overproducing PpAzoR and CotA-laccase simultaneously. The first step was performed in static conditions at 30°C (1 cycle or 4 cycles of 24 h each), and the second in shaking conditions, at 37°C for 24 h. Reactions were performed in water.

1 st step	2 nd step	
Decolorization (%)	Compound 7 (mM)	Yield (%)
89 ± 5	0.24	50
90; 67; 53; 40	0.44	91

2.4. Conclusion

Azo-dyes are xenobiotic molecules whose structures designed to resist decolorization and degradation which turns challenging its sustainable and efficient eradication from the environment. We had proven that the sequential use of PpAzoR azoreductase and CotA-laccase enzymes resulted in the decolorization, degradation and conversion into valuable compounds of a set of azo dyes, mordant, acid, reactive and direct, that are cheap feedstock's, commonly found in dye-containing wastewaters of textile-related industries. For the set-up of the biocatalytic bioprocess, we took advantage of the previously known complementary catalytic properties of both azoreductases and CotA-laccase enzymes, *i.e.* the first enzyme converts the azo dyes into aromatic amines, which are substrates of the second enzyme that promotes their oxidative coupling into precursors of biologically active molecules. Free and immobilized whole-cells of *E. coli* containing these enzymes allowed developing an economically feasible bioprocess resulting in less contaminated reaction mixtures with final product yields that goes up to ~ 90%. The optimized biocatalytic systems offer a sustainable and promising approach for cleaning-up dye-containing wastewaters while producing valuable chemicals with a range of applications in the pharmaceutical and chemical industries.

2.5. Experimental Section

2.5.1. Chemicals

All reagents and solvents are commercially available. The dyes used in this study were: mordant black 9 (MB9; λ_{\max} = 550 nm; purity of 48 %), mordant black 3 (MB3; λ_{\max} = 550 nm; purity of 40 %), acid red 266 (AR266; λ_{\max} = 470 nm; purity of 30 %), reactive yellow 145 (RY145; λ_{\max} = 420 nm; purity of 50 %) and direct red 80 (DR80; λ_{\max} = 530 nm; purity of 50 %). MB9 was purchased at DyStar Textilfarben (Germany), MB3 was purchased at Honeywell Fluka (Bucharest, Romania) and AR266, RY145 and DR80 were purchased at Town End (Leeds, UK). All dyes were used as purchased without purification.

2.5.2. Bacterial strains and plasmids

Escherichia coli strain DH5 α (Novagen) was used for routine propagation and amplification of plasmid constructs and *E. coli* Tuner (DE3, Novagen), *E. coli* KRX (Promega), and *E. coli* BL21 star (DE3, Novagen) were used as host of plasmids for gene expression. Three plasmids were used: pLOM10, coding for CotA-laccase from *Bacillus subtilis* ^[53], pVB-8, coding for the evolved variant 2A1-Y179H of *Pseudomonas putida* MET94 PpAzoR azoreductase ^[45], and pAIF-2, a pET-Duet-1 construct, coding for both wild-type PpAzoR azoreductase and CotA-laccase genes ^[15].

2.5.3. Preparation of purified enzymes and whole-cell systems

E. coli recombinant cells overproducing the enzymes of interest were cultivated in Luria-Bertani media (LB) supplemented with 100 $\mu\text{g mL}^{-1}$ ampicillin following previously described procedures [15,16,54]. The cells were harvested by centrifugation ($8000 \times g$, 10 min, 4°C) and washed with 0.9% (w/v) NaCl.

(i) For reactions using purified enzymes, cells were disrupted using a French-Press, cell debris removed by centrifugation ($18000 \times g$, 2 h, 4°C) and enzymes were purified from supernatants using well-established chromatographic methods [16,55]. Laccase (CotA) activity was determined at 37°C using 0.1 mM ABTS as substrate ($\epsilon_{420} = 36,000 \text{ M}^{-1} \text{ cm}^{-1}$) in 0.1 M sodium acetate buffer, pH 4.3 [53]. The activity of azoreductase (PpAzoR) was measured in 0.1 M sodium phosphate buffer, pH 7, using 0.1 mM anthraquinone-2-sulfonate (AQS) and 0.25 mM β -nicotinamide adenine dinucleotide phosphate (NADPH; $\epsilon_{340} = 6,200 \text{ M}^{-1} \text{ cm}^{-1}$) at 30°C. One unit (U) of enzymatic activity was defined as the amount of enzyme required to convert 1 μmol of substrate per min. Aliquots of purified enzymes were stored at -20°C prior to use. The protein concentration was determined by using the Bradford assay with bovine serum albumin as the standard.

(ii) For reactions using free and immobilized whole-cell systems, cells were suspended in distilled water, the optical density was measured at 600 nm (OD_{600}). A calibration curve of OD_{600} versus DCW (mg mL^{-1}) was performed after drying cell suspensions (at different OD_{600}) at 100°C until no variation in weight was observed. Aliquots of cell suspensions containing around 300 mg dry cell weight (DCW) were prepared, centrifuged and pellets stored at -20°C prior to use. Immobilization was performed after suspending cell pellets (300 or 600 mg DCW) in 2 mL of a 2 % sodium alginate solution, followed by dropwise addition to a 0.15 M CaCl_2 solution under continuous agitation. The spheres solidified for 90 min, were washed with distilled water and stored at 4°C until used.

2.5.4. Two-step enzymatic bioprocesses using purified enzymes

The first step of bioconversion of dyes using purified enzymes was performed in serum bottles (20 mL) containing 2 mM of β -nicotinamide adenine dinucleotide hydrogen (NADH) and 2 mM of azo dyes (MB9, MB3, AR266, RY145 and DR80) in 0.1 M sodium phosphate buffer, pH 7, made anaerobic by nitrogen bubbling followed by sealing with rubber stoppers. The 10 mL-mixtures were incubated at 30°C and reactions started by adding 5 U mL^{-1} of an anoxic preparation of purified PpAzoR azoreductase. Decolorization was monitored at the maximum

wavelength of each dye. When decolorization was $\geq 85\%$ (after 24 h), reaction mixtures were transferred to 50 mL-Erlenmeyer's, 1 U mL⁻¹ of CotA-laccase was added and these were shaken at 170 rpm at 37°C for 24 h.

2.5.5. Two-step enzymatic bioprocesses using free or immobilized whole-cells

The first PpAzoR enzymatic step was performed in 5-mL of water or 20 mM sodium phosphate buffer (pH 7) at 30°C in the presence of free or immobilized cells (60 or 120 mg DCW mL⁻¹). Reactions started by adding MB9 to a final concentration of 2 mM. Decolorization was monitored at 550 nm (λ_{\max} for MB9) and when reached $\geq 85\%$ (after ~ 24 h of reaction) mixtures were shaken at 170 rpm, 37°C for 24 h. Experiments recycling the biocatalysts were tested for the first-enzymatic step as follows: after 24 h of reaction, 5 mL of 2 mM of MB9 was added to the reaction mixture and this procedure was repeated 4 times, after 24 h-periods, up to 96 h of reaction. After this time the second step with CotA-laccases was performed similarly to the described above. Each experience was performed with at least 5 replicas, with standard deviations not superior to 15%. The products of reactions after the first and second step were quantified by HPLC through a calibration curve of compound concentration versus area of signal.

2.5.6. Products separation and characterization

UV-visible spectra of substrates and reaction mixtures were obtained on a Nicolet Evolution 300 spectrophotometer. HPLC analysis was performed on a Waters Alliance 2695 equipped with a Waters photodiode array detector. The separations were performed in a Purospher STAR RP-18e column (250 x 4 mm), 5 μm particle size (Merck, KGaA, Germany). The injection volume was 60 μl , the flow rate, 0.8 mL min^{-1} , at a column oven temperature of 40°C. The eluent A, was 0.1 M ammonium acetate pH 6.7, and the eluent B was a mixture of methanol: acetonitrile (70:30, v/v). The following gradient was used for products separation: 0-2 min - isocratic elution of 100% eluent A; 2-16 min - linear gradient from 100% to 60% of eluent A; 16-24 min - linear gradient from 60% to 45% of eluent A; 24-28 min - linear gradient from 45% to 20% of eluent A; 28-32 min - isocratic elution of 20% eluent A; 32-30 min - linear gradient from 20% to 100% of eluent A; 33-43 min - equilibrium to the initial conditions of the following injection. The final product of MB9 conversion, after the sequential action of PpAzoR and CotA-laccase was purified by HPLC and its molecular extinction coefficient was determined in the concentration range of 0.05 – 0.8 mM at 430 nm using a Synergy 2, Biotek microplate reader. ^1H - and ^{13}C -NMR, and COSY, HSQC and HMBC NMR spectra were obtained at room temperature with an Advanced Bruker 400 MHz spectrometer in $\text{CD}_3\text{OD-d}_4$ solvent. The chemical shifts are reported in

part per million (ppm) using the solvent signal as internal reference. The identity of the products **4**, **7**, **8** and **9**, not commercially available, was established by comparison of their NMR spectral data with the reported in the literature ^[18,31,38,56]

1, ¹H NMR (CD₃OD-d₄): δ 7.22 (d, J = 2.0 Hz, H₂); 7.08 (dd, J=8.0, 2.0 Hz, H₆); 6.72 (d, J=8.0, H₅).

2, ¹H NMR (CD₃OD-d₄) δ 8.71 (dd, J = 7.8, 1.2 Hz, 1H, H₈), 7.93 (d, J = 7.8, 1.2 Hz, 1H, H₅), 7.84 (s, 1H, H₂), 7.38 (m, 2H, H₆, H₇). ¹³C NMR (CD₃OD-d₄): δ: 138.8 (C₄), 132.3 (C_{4a}), 131.3 (C₁), 127.7 (C₈), 126.1 (C₇), 126.1 (C₃), 125.8 (C_{8a}), 124.7 (C₆), 121.9 (C₅), 118.9 (C₂).

3, ¹H NMR (CD₃OD-d₄): δ 7.95 (d, J = 1.2 Hz, 1H, H₄), 7.69 (d, J = 8.8 Hz, 1H, H₅), 7.65 (d, J = 8.8 Hz, 1H, H₆), 7.37 (d, J = 1.2 Hz, 1H, H₂). ¹³C NMR (CD₃OD-d₄): 152.9 (C₁), 141.1 (C₃), 130.6 (C₈), 130.4 (C₇), 122.7 (C₅), 117.9 (C₆), 116.6 (C₄), 114.2 (C_{4a}), 113.9 (C_{8a}), 105.2 (C₂).

4, ¹H NMR (CD₃OD-d₄): δ 8.53 (s, 1H, H₂), 8.34 (s, 1H, H₄), 8.27 (s, 1H, H₅), 7.98 (s, 1H, H₈).

5, ¹H NMR (CD₃OD-d₄): δ 7.55 (d, J= 8.8 Hz, 2H, H₃, H₅), 6.68 (d, J= 8.8 Hz, 2H, H₂, H₆).

6, ¹H NMR (CD₃OD-d₄): δ 7.19 (d, J = 2.8 Hz, 1H, H₆); 6.72 (dd, J = 8.4 Hz, 2.4 Hz, 1H, H₄); 6.67 (d, J = 8.4 Hz, 1H, H₃). ¹³C NMR (CD₃OD-

d₄): 137.4 (C2), 136.8 (C5), 129.3 (C1), 120.2 (C4), 118.6 (C3), 115.0 (C6).

7, ¹H NMR (CD₃OD-d₄): δ 8.14 (d, J= 2.0, H9); 7.89 (dd, J = 8.4; 2.0 Hz, H7); 7.52 (d, J=8.4 Hz, H6); 6.49 (s, H5); 6.43 (s, H8). UV-Vis (H₂O): 430 nm, 2852 M⁻¹ cm⁻¹

8, ¹H NMR (CD₃OD-d₄) [38] δ 8.76 (dd, J = 8.4 , 1.0 Hz, 1H, H8), 8.15 (dd, J = 7.8 , 1.5 Hz, 1H, H5), 7.61 (dt, J = 8.0 , 1.5 Hz, 1H, H6), 7.51 (dt, J = 8.4 , 1.0 Hz, 1H, H7), 6.91 (s, 1H, H2). ¹³C NMR (D₂O)^a: 183.5 (C4), 180.1 (C3), 155.2 (C1), 137.0 (C7), 132.2 (C6), 131.8 (C4a), 131.5 (C5), 130.9 (C8a), 130.2 (C2), 126.5 (C8).

9, ¹H NMR (D₂O)^{[18].a}: δ 7.04 (d, 2H, J = 9.5 Hz, H4, H9); 6.38 (d, 2H, J = 9.5 Hz, H3, H8). ¹³C NMR (D₂O)^a: δ 146.6 (C2, C7); 139.5 (C1a, C5a); 137.9 (C4a, C9a); 132.9 (C4, C9); 127.2 (C3, C8); 111.3 (C1, C6).

^a referenced to (CD₃)₂CO-*d*₆ solvent.

2.6. References

- [1] R. A. D. Arancon, C. S. K. Lin, K. M. Chan, T. H. Kwan, R. Luque, *Energy Sci. Eng.* **2013**, *1*, 53–71.
- [2] M. Geissdoerfer, P. Savaget, N. M. P. Bocken, E. J. Hultink, *J. Clean. Prod.* **2017**, *143*, 757–768.
- [3] Z. Carmen, S. Daniel, in *Org. Pollut. Ten Years After Stock. Conv. - Environ. Anal. Updat.* (Ed.: T. Pusyn), InTech, **2012**, pp. 55–86.
- [4] R. Kant, *Nat. Sci.* **2012**, *04*, 22–26.
- [5] D. Rawat, V. Mishra, R. S. Sharma, *Chemosphere* **2016**, *155*, 591–605.
- [6] M. A. Hassaan, A. El Nemr, *Am. J. Environ. Sci. Eng.* **2017**, *1*, 64–67.
- [7] L. Pereira, M. Alves, in *Environ. Prot. Strateg. Sustain. Dev.* (Eds.: A. Malik, E. Grohmann), Springer Netherlands, Dordrecht, **2012**, pp. 111–162.
- [8] K. Vikrant, B. S. Giri, N. Raza, K. Roy, K. H. Kim, B. N. Rai, R. S. Singh, *Bioresour. Technol.* **2018**, *253*, 355–367.
- [9] H. S. Rai, M. S. Bhattacharyya, J. Singh, T. K. Bansal, P. Vats, U. C. Banerjee, *Crit. Rev. Environ. Sci. Technol.* **2005**, *35*,

219–238.

- [10] R. G. Saratale, G. D. Saratale, J. S. Chang, S. P. Govindwar, *J. Taiwan Inst. Chem. Eng.* **2011**, *42*, 138–157.
- [11] R. Khan, P. Bhawana, M. H. Fulekar, *Rev. Environ. Sci. Biotechnol.* **2013**, *12*, 75–97.
- [12] S. Rodríguez-Couto, J. F. Osma, J. L. Toca-Herrera, *Eng. Life Sci.* **2009**, *9*, 116–123.
- [13] S. Mendes, M. P. Robalo, L. O. Martins, in *Microb. Degrad. Synth. Dye. Wastewaters* (Ed.: S.N. Singh), Springer, Switzerland, Cham, **2015**, pp. 27–55.
- [14] R. L. Singh, P. K. Singh, R. P. Singh, *Int. Biodeterior. Biodegradation* **2015**, *104*, 21–31.
- [15] S. Mendes, A. Farinha, C. G. Ramos, J. H. Leitão, C. A. Viegas, L. O. Martins, *Bioresour. Technol.* **2011**, *102*, 9852–9859.
- [16] S. Mendes, L. Pereira, C. Batista, L. O. Martins, *Appl. Microbiol. Biotechnol.* **2011**, *92*, 393–405.
- [17] A. C. Sousa, L. O. Martins, M. P. Robalo, *Adv. Synth. Catal.* **2013**, *355*, 2908–2917.
- [18] A. C. Sousa, M. C. Oliveira, L. O. Martins, M. P. Robalo, *Green*

- Chem.* **2014**, *16*, 4127–4136.
- [19] A. C. Sousa, M. F. M. M. Piedade, L. O. Martins, M. P. Robalo, *Green Chem.* **2015**, *17*, 1429–1433.
- [20] A. C. Sousa, M. F. M. M. Piedade, L. O. Martins, M. P. Robalo, *Green Chem.* **2016**, *18*, 6063–6070.
- [21] A. C. Sousa, M. Conceição Oliveira, L. O. Martins, M. P. Robalo, *Adv. Synth. Catal.* **2018**, *360*, 575–583.
- [22] A. C. Sousa, S. R. Baptista, L. O. Martins, M. P. Robalo, *Chem. - An Asian J.* **2019**, *14*, 187–193.
- [23] M. McDonald, B. Wilkinson, C. W. Van't Land, U. Mocek, S. Lee, H. G. Floss, *J. Am. Chem. Soc.* **1999**, *121*, 5619–5624.
- [24] P. Corona, A. Carta, M. Loriga, G. Vitale, G. Paglietti, *Eur. J. Med. Chem.* **2009**, *44*, 1579–1591.
- [25] A. Bolognese, G. Correale, M. Manfra, A. Lavecchia, O. Mazzoni, E. Novellino, V. Barone, P. La Colla, R. Loddo, *J. Med. Chem.* **2002**, *45*, 5217–5223.
- [26] L. Vairavelu, M. Zeller, K. J. Rajendra Prasad, *Bioorg. Chem.* **2014**, *54*, 12–20.
- [27] B. Piro, S. Reisberg, G. Anquetin, H. T. Duc, M. C. Pham, *Biosensors* **2013**, *3*, 58–76.

- [28] C. M. H. Cho, A. Mulchandani, W. Chen, *Appl. Environ. Microbiol.* **2004**, *70*, 4681–4685.
- [29] M. C. Cholo, H. C. Steel, P. B. Fourie, W. A. Germishuizen, R. Anderson, *J. Antimicrob. Chemother.* **2012**, *67*, 290–298.
- [30] O. J. X. Morel, R. M. Christie, *Chem. Rev.* **2011**, *111*, 2537–2561.
- [31] S. Forte, J. Polak, D. Valensin, M. Taddei, R. Basosi, S. Vanhulle, A. Jarosz-Wilkolazka, R. Pogni, *J. Mol. Catal. B Enzym.* **2010**, *63*, 116–120.
- [32] R. Pauliukaite, M. E. Ghica, M. M. Barsan, C. M. A. Brett, *Anal. Lett.* **2010**, *43*, 1588–1608.
- [33] J. B. Laursen, J. Nielsen, *Chem. Rev.* **2004**, *104*, 1663–1685.
- [34] Shruti, J. Dwivedi, D. Kishore, S. Sain, *Synth. Commun.* **2018**, *48*, 1377–1402.
- [35] H. M. Pinheiro, E. Touraud, O. Thomas, *Dye. Pigment.* **2004**, *61*, 121–139.
- [36] N. Dafale, S. Wate, S. Meshram, N. R. Neti, *Environ. Rev.* **2010**, *18*, 21–36.
- [37] M. Kudlich, M. J. Hetheridge, H. J. Knackmuss, A. Stolz, *Environ. Sci. Technol.* **1999**, *33*, 896–901.

- [38] A. C. Sousa, Biotransformação de Aminas Aromáticas Catalisada Por Laccases, PhD Thesis, Universidade de Lisboa, Instituto Superior Técnico, **2015**.
- [39] B. Lin, Y. Tao, *Microb. Cell Fact.* **2017**, *16*, 1–12.
- [40] C. C. C. R. de Carvalho, *Microb. Biotechnol.* **2017**, *10*, 250–263.
- [41] R. R. Chen, *Appl. Microbiol. Biotechnol.* **2007**, *74*, 730–738.
- [42] A. Pandey, P. Singh, L. Iyengar, *Int. Biodeterior. Biodegrad.* **2007**, *59*, 73–84.
- [43] T. Robinson, G. McMullan, R. Marchant, P. Nigam, *Bioresour. Technol.* **2001**, *77*, 247–255.
- [44] M. A. Rauf, S. Salman Ashraf, *Chem. Eng. J.* **2012**, *209*, 520–530.
- [45] V. Brissos, N. Gonçalves, E. P. Melo, L. O. Martins, *PLoS One* **2014**, *9*, e87209.
- [46] V. Prigione, V. Tigrini, C. Pezzella, A. Anastasi, G. Sannia, G. C. Varese, *Water Res.* **2008**, *42*, 2911–2920.
- [47] R. G. Willaert, in *Ferment. Microbiol. Biotechnol.* (Eds.: E.M.T. El-Mansi, J. Nielsen, D. Mousdale, R.P. Carlson), Taylor & Francis, **2018**, pp. 313–347.

- [48] V. Faraco, C. Pezzella, A. Miele, P. Giardina, G. Sanna, *Biodegradation* **2009**, *20*, 209–220.
- [49] P. Devi, S. Wahidullah, F. Sheikh, R. Pereira, N. Narkhede, D. Amonkar, S. Tilvi, R. M. Meena, *Mar. Drugs* **2017**, *15*, 1–14.
- [50] J. S. Chang, C. Chou, S. Y. Chen, *Process Biochem.* **2001**, *36*, 757–763.
- [51] J. M. Sperl, V. Sieber, *ACS Catal.* **2018**, *8*, 2385–2396.
- [52] M. Sydnnes, *Curr. Green Chem.* **2014**, *1*, 216–226.
- [53] L. O. Martins, C. M. Soares, M. M. Pereira, M. Teixeira, T. Costa, G. H. Jones, A. O. Henriques, *J. Biol. Chem.* **2002**, *277*, 18849–18859.
- [54] P. Durão, Z. Chen, A. T. Fernandes, P. Hildebrandt, D. H. Murgida, S. Todorovic, M. M. Pereira, E. P. Melo, L. O. Martins, *J. Biol. Inorg. Chem.* **2008**, *13*, 183–193.
- [55] I. Bento, L. O. Martins, G. Gato Lopes, M. Arménia Carrondo, P. F. Lindley, *Dalt. Trans.* **2005**, *4*, 3507.
- [56] J. Jirman, *Collect. Czechoslov. Chem. Commun.* **1993**, *58*, 1378–1387.

Chapter 3

3. Water-Soluble Iridium N-Heterocyclic Carbene Complexes for the Alkylation of Amines with Alcohols

The work described in this chapter has been published in:

Ana Fernandes and Beatriz Royo (2017), Water-soluble Iridium N-Heterocyclic Carbene Complexes for the Alkylation of Amines with Alcohols, *ChemCatChem*, 9, 3912-3917.

Acknowledgements and contributions

Ana Fernandes performed all the experiments described in this chapter and participated in the writing of the manuscript. Beatriz Royo directed the research and wrote the manuscript. M. C. Almeida is acknowledged for elemental analyses (ITQB) and Dr. A. L. Llamas-Saiz from University of Santiago de Compostela, Spain, for the X-Ray studies.

3.1. Abstract

A new series of water-soluble $\text{Cp}^*\text{Ir}(\text{NHC})\text{Cl}_2$ complexes with N-heterocyclic carbene (NHC) ligands bearing ester- and amide-groups have been obtained and fully characterized. The new complexes are highly reactive and selective catalysts for the alkylation of amines with alcohols, using 1:1 ratio of reactants, in water and in the absence of base or other additives. The catalytic system has a broad substrate scope, allowing the synthesis of a variety of primary and secondary amines in excellent yields. Tolerance to a large range of functional groups was obtained.

3.2. Introduction

The development of water-soluble catalysts has gained increasing attention in the last years ^[1]. The use of water as a solvent in synthetic organic chemistry plays a key role in green chemistry since water is relatively inexpensive, non-toxic, and non-flammable. The most general approach for designing water-soluble catalysts is the functionalization of ligands with organic groups capable to form H-bonds with water, commonly P- and N-based ligands ^[2–5]. N-heterocyclic carbene (NHC) ligands offer attractive features for the development of water-soluble metal catalysts, because they can be easily functionalized, and confer great stability to their metal complexes ^[6–8]. However, this area of research is still in its early stage, and few transition metals containing water-soluble NHCs have been described in the literature ^[5,9,10]. In particular, reports on aqueous catalysis with iridium N-heterocyclic carbenes are scarcely found in the literature, despite the prominent role of iridium NHCs in homogeneous catalysis ^[11–15]. Catalytic applications using Ir-NHC complexes in water includes hydroamination ^[16], hydrogenation ^[17–19], C-H activation ^[17,20] and water oxidation reactions ^[21–30].

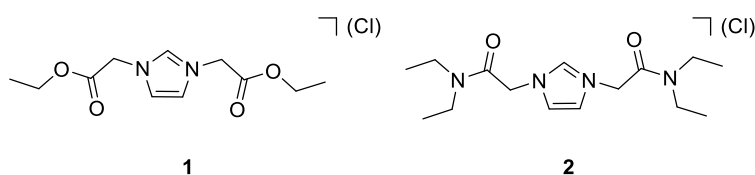
Recently, interest has aroused in developing water-soluble Ir-NHC complexes for their application in catalytic dehydrogenative processes. Direct *N*-alkylation of amines with alcohols provides a green and atom

economy method for the synthesis of substituted amines, which are important building blocks in different industries, such as the pharmaceutical industry ^[3,4,31–34]. Since the first reports independently disclosed by Watanabe and Grigg ^[35,36], significant progress has been made in this field ^[2–4,31,33–39], and a variety of successful catalytic systems have been developed using Ir(III)-NHC complexes ^[40–52]. However, little work has been done towards the development of catalytic systems operating in water ^[53–57]. To the best of our knowledge, this work represents the first examples of iridium NHC-based catalysts for alkylation of amines with alcohols operating in water. Herein, we report the preparation of iridium(III) complexes having ester-, and amide-functionalized NHC ligands and their catalytic activity in the alkylation of amines with alcohols in water.

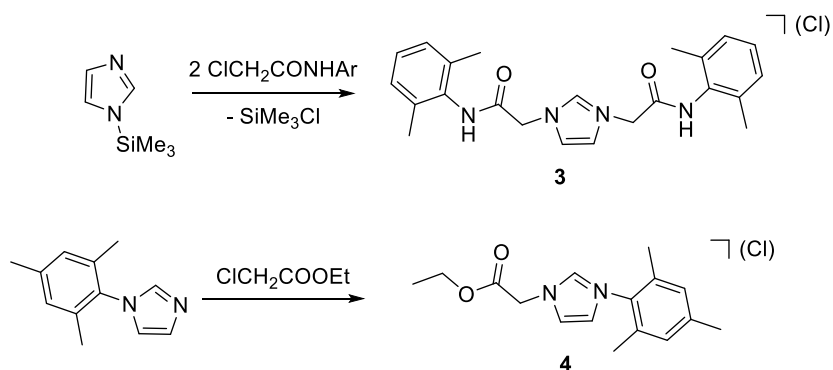
3.3. Results and Discussion

3.3.1. Synthesis and characterization

The synthesis of the NHC ligand precursors **1** and **2** (Scheme 3.1) was performed as previously described in the literature ^[58]. The novel NHC proligand **3** was prepared following a similar approach by reacting N-(2,6-dimethylphenyl) chloroacetamide with 1-(trimethylsilyl) imidazole (Scheme 3.2). The new unsymmetrical NHC proligand **4** was synthesized by refluxing 1-(mesityl) imidazole with ethyl chloroacetate (Scheme 2). Compounds **3** and **4** were isolated as pale-yellow solids in good yield (85 % and 80%, respectively). They were soluble in water, chlorinated solvents, methanol, acetonitrile, and dimethylsulfoxide and insoluble in diethyl ether and hexane.

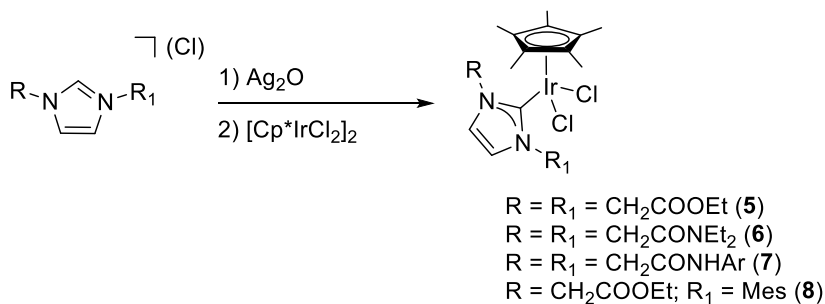


Scheme 3.1 NHC proligands **1** and **2**



Scheme 3.2 Synthesis of NHC proligands **3** and **4**.

The iridium NHC complexes **5-8** were successfully synthesized via a transmetallation procedure, involving a stepwise reaction of the appropriate proligand **1-4** with Ag₂O followed by addition of [Cp*IrCl₂]₂ (Cp* = η⁵-C₅Me₅) (Scheme 3.3). The identity of all complexes was established by spectroscopic methods, mass spectrometry (HRMS-ESI), and elemental analysis. The ¹³CNMR spectra confirmed that coordination of the NHC had occurred, showing the characteristic signal of Ir-C_{NHC} at 166 ppm (for complexes **5-7**) and at 169 ppm (for complex **8**). All iridium NHC complexes were soluble in water (pH = 7) at 20 °C. Yellow solutions were obtained after stirring for 10 min, giving solubility values of 17, 56, 10 and 7 mg mL⁻¹ for complexes **5**, **6**, **7**, and **8**, respectively. Complex **6**, bearing an acetamide group on the NHC wingtip, displayed the highest solubility in water. Remarkable, all complexes resulted to be stable in water for at least 24 h.



Scheme 3.3 Synthesis of iridium (III) NHC complexes **5-8**.

X-ray diffraction analyses of single crystals of **6** and **8** confirmed the expected three-legged piano-stool geometry of the complexes. Figures 3.1 and 3.2 show the ORTEP diagrams of **6** and **8**, respectively, and the more relevant bond lengths and angles. The molecular structure of complex **6** (Figure 3.1) has a symmetrically substituted NHC ligand coordinated to iridium, and two chlorides and a Cp* ligand completing the coordination sphere of the metal. The Ir-C_{NHC} distance of 2.04 Å, lies in the expected range [59–62]. The Ir-Cl (2.41 Å and 2.42 Å) and Ir-Cp* (centroid) (2.18 Å) distances are within the found ranges for other known Cp*Ir(NHC) complexes [59–62]. The molecular structure of **8** (Figure 3.2) showed the unsymmetrically substituted NHC ligand coordinated to iridium (Ir-C_{NHC} distance of 2.06 Å), and two chlorides (Ir-Cl, 2.41 Å, and 2.38 Å) and a Cp* (2.16 Å) completing the coordination sphere about the metal. All distances and angles lie on the expected range and compare well with other half-sandwich iridium(III) complexes reported in the literature [60–63].

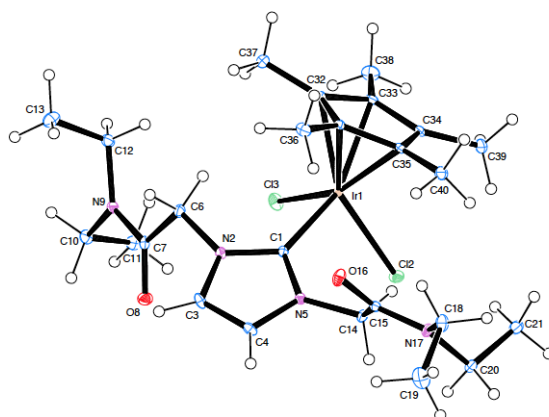


Figure 3.1 ORTEP-3 diagram of **6**, using 30% probability level ellipsoids. Selected distances (Å): Ir(1)-C(1) 2.0440(2), Ir(1)-Cl(2) 2.4121(4), Ir(1)-Cl(3) 2.4223(4), Ir(1)-Cpcentroid* 2.1831(6). Selected angles (°): C(1)-Ir(1)-Cl(2) 90.11(5), C(1)-Ir(1)-Cl(3) 91.16(5), Cl(1)-Ir(1)-Cl(2) 86.010(2), Cpcentroid*-Ir(1)-C(1) 115.66(8), Cpcentroid*-Ir(1)-Cl(2) 141.37(5), Cpcentroid*-Ir(1)-Cl(3) 132.07).

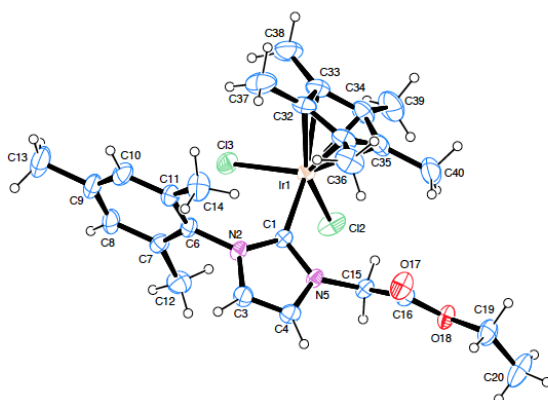


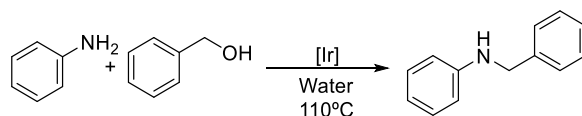
Figure 3.2 ORTEP-3 diagram of **8**, using 30% probability level ellipsoids. Selected distances (Å): Ir(1)-C(1) 2.062(3), Ir(1)-Cl(2) 2.4140(1), Ir(1)-Cl(3) 2.3868(4), Ir(1)-Cpcentroid* 2.161(4). Selected angles (°): C(1)-Ir(1)-Cl(2) 94.35(9), C(1)-Ir(1)-Cl(3) 89.56(9), Cl(1)-Ir(1)-Cl(2) 84.86(4), Cpcentroid*-Ir(1)-C(1) 113.47(1).

3.3.2. Catalytic studies

3.3.2.1. Conditions optimization

The catalytic activity of the iridium (III) NHC complexes **5-8** in *N*-alkylation of amines with alcohols was studied using aniline and benzyl alcohol as a model reaction. The reaction was performed in water, in a closed vessel, using 2 mol % of catalyst in a 1:1 ratio of aniline: benzyl alcohol. Results are summarized in Table 3.1. Complexes **6** and **7** resulted to be the most active catalysts, affording quantitative yield of *N*-benzyl aniline in 16 h at 110 °C (Table 3.1, entries 2 and 3). Under similar conditions, complexes **5** and **8** achieved lower yields of *N*-benzyl aniline (51 % and 38%, respectively, Table 3.2, entries 1 and 4). The presence of the amide group on the wingtip of the NHC seems to have a beneficial effect on the catalytic performance of the catalyst. When the catalyst loading was lowered to 1 and 0.5 mol %, a decrease of the catalytic activity was observed (Table 3.1, entry 6). An attempt to reduce the temperature to 70 °C resulted in a decrease in the activity (42 % yield, Table 3.1, entry 7). Notable, complexes **6** and **7** displayed good activity in the absence of base or other additives, using stoichiometric amount of alcohol. No reaction occurred in the absence of catalyst (Table 3.1, entry 8), and low yield was obtained using $[\text{Cp}^*\text{IrCl}_2]_2$ as catalyst (Table 3.1, entry 9).

Table 3.1 *N*-Alkylation of aniline with benzyl alcohol catalyzed by Ir-NHC complexes
5-8



Entry ^[a]	Catalyst	Loading (%)	Time (h)	Yield (%) ^[b]
1	5	2	16	51
2	6	2	16	99
3	7	2	16	99
4	8	2	16	38
5	6	1	24	57
6	6	0.5	24	38
7	6	2	24	42 ^[c]
8	None	-	24	0
9	[Cp*IrCl ₂] ₂	2	16	20

[a] Reaction conditions: benzyl alcohol (1 mmol), aniline (1 mmol), catalyst, water (0.25 mL), 110 °C. [b] Yield determined by ¹H NMR using 1,4-di-*tert*-butylbenzene as an internal standard. [c] Reaction carried out at 70 °C.

Catalyst **6** was recycled and reused for three catalytic cycles without losing its activity. The catalyst was recovered by a simple phase separation (water/CH₂Cl₂). Examination of the ¹H and ¹³C NMR spectra of the recovered catalyst confirmed the identity of the Ir species **6**.

Furthermore, the activity of catalyst **6** was studied in a buffered medium to assess the viability of the use of this system under biological conditions. Aniline and benzyl alcohol (1:1 ratio) were used as substrates with 2 mol % of catalyst **6** at 110°C in 0.1 M sodium phosphate buffer pH 6, 7 and 8. In all buffered mediums, catalysts **6** maintained its high activity with a quantitative yield of N-benzyl aniline in 16 h (97 %).

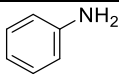
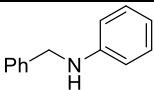
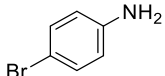
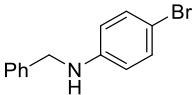
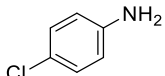
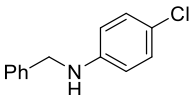
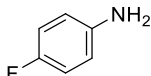
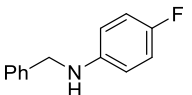
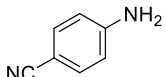
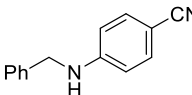
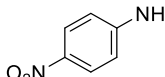
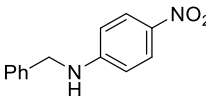
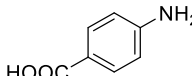
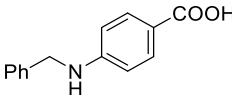
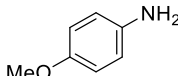
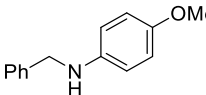
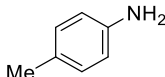
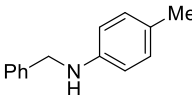
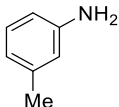
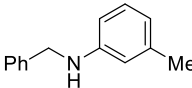
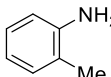
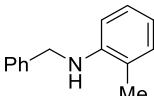
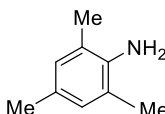
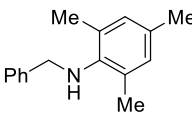
3.3.2.2. Substrate scope with monosubstituted aromatic amines, aliphatic amines, and primary and secondary alcohols

Then, we decided to explore the scope of the reaction, and we chose complex **6** for this study due to its high reactivity, better accessibility, and lower cost than other complexes. The scope of the reaction was explored using 2 mol % of catalyst **6** at 110 °C in water. Results are summarized in Table 3.2. A variety of substituted anilines were selectively alkylated with benzyl alcohol (in a ratio 1:1) to yield the corresponding N-benzyl anilines in good yields (>88 %). Electron-donating and electron-withdrawing groups were well tolerated; high

yields of N-benzyl anilines were obtained in all cases (Table 3.2, entries 1-10). Anilines containing *ortho* and *meta* substituents were also quantitatively alkylated with benzyl alcohol (Table 3.2, entries 9 and 10). An exception was the bulky 2,4,6-trimethylaniline, which was alkylated in a lesser extent, giving a 44% yield of the corresponding N-benzyl aniline after 24 hours of reaction (Table 3.2, entry 11).

Complex **6** displayed a comparable catalytic activity to the iridium(III) complex $[\text{Cp}^*\text{Ir}(\text{Pro})\text{Cl}]$ (Pro = prolinato), recently described by Limbach and co-workers^[14d] as the first iridium complex catalyzing this reaction without additives at 95 °C in water. Both **6** and $[\text{Cp}^*\text{Ir}(\text{Pro})\text{Cl}]$ complexes are identified among $\text{Cp}^*\text{Ir}(\text{III})$ state-of-the-art catalysts, as highly reactive catalysts for the alkylation of amines with alcohols in water under base-free conditions. Other base-free catalytic systems are known, but in all cases temperature higher than 100 °C and activation by inorganic salts is required.^[53–55,64]

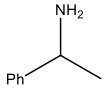
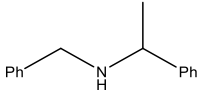
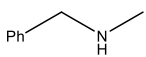
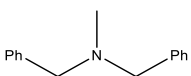
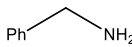
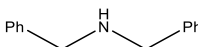
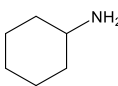
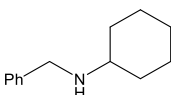
Table 3.2 *N*-Alkylation of anilines with benzyl alcohol using complex **6** [a]

Entry	Amine	Product	Time (h)	Yield (%)
1			16	95 (99)
2			24	93 (98)
3			16	86 (93)
4			16	83 (92)
5			24	92 (99)
6			16	87 (92)
7			24	84 (90)
8			24	84 (88)
9			24	90 (94)
10			24	93 (99)
11			16	91 (96)
12			24	(44)

[a] Reaction conditions: benzyl alcohol (1 mmol), amine (1 mmol), catalyst **6** (2 mol%), water (0.25 mL), 110 °C. [b] Isolated yields. In parenthesis, yield determined by ¹H NMR using 1,4-di-*tert*-butylbenzene as an internal standard.

The catalytic system has also been tested with aliphatic amines such as α -methylbenzylamine, N-benzylmethylamine, benzyl amine, and cyclohexylamine (Table 3.3). Good to moderate yields of the corresponding secondary and tertiary amines were obtained, except in the alkylation of cyclohexylamine with benzyl alcohol that afforded 35% yield of N-benzylcyclohexylamine.

Table 3.3 *N*-alkylation of primary and secondary aliphatic amines and benzyl alcohol using complex **6** [a].

Entry	Amine	Product	Time (h)	Yield (%) ^[b]
1			16	60 (64)
2			16	87 (93)
3			24	69 (77)
4			24	(35)

[a] Reaction conditions: benzyl alcohol (1 mmol), primary or secondary amine (1 mmol), 2 mol % catalyst **6**, water (0.25 mL). [b] Isolated yield. In parenthesis, yield determined by ¹H NMR using 1,4-di-*tert*-butylbenzene as an internal standard.

In addition, secondary amines were obtained in high yields by alkylation of aniline with 2-methoxybenzyl alcohol, cyclohexanol, and cyclopentanol (Table 3.4, entries 1-3).

Table 3.4 N-Alkylation of aniline with primary and secondary alcohols using complex **6** ^[a]

Entry	Alcohol	Product	T (h)	Yield (%) ^[b]
1			16	75 (80)
2			24	90 (99)
3			16	88 (95)

[a] Reaction conditions: alcohol (1 mmol), aniline (1 mmol), catalyst **6** (2 mol%), water (0.25 mL), 110 °C. [b] Isolated yield. In parenthesis, yield determined by ¹H NMR using 1,4-di-tert-butylbenzene as an internal standard.

3.3.2.3. Substrate scope of sulfonated aromatic amines

Since one of the goals of this thesis was the development of cooperative organometallic and enzymatic catalysis, we explored the possibility of alkylating the amines obtained in the decolorization of dyes by azoreductases using the iridium complex **6**. The final aim was to develop a one-pot catalytic system in which the amines obtained by azoreductase could be alkylated with alcohols using **6**. Therefore, the activity of complex **6** in the alkylation of the sulfonated aromatic amines

shown in Figure 3.3 were tested using benzyl alcohol and 2 mol % of catalyst **6** at 110 °C in water. The sulfonated aromatic amine SABS yielded the expected N-alkylated amine in 16 h with 90% yield. However, the diamines SDBS and SAHBS did not react; the intact substrate was retrieved after 24 h of reaction.

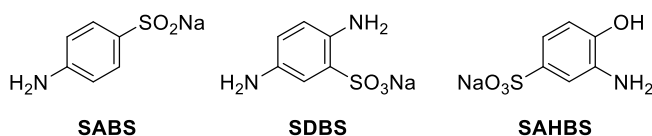


Figure 3.3 Sulfonate aromatic amines used in this study.

3.3.2.4. Sequential reaction of enzymatic azo reduction and organometallic N-alkylation of amines

It was demonstrated in Chapter 2 of this thesis that the enzyme PpAzoR reduces dye DR80 into two aromatic amines (Figure 3.4). Furthermore, the amine SABS can be alkylated with benzyl alcohol using **6** as a catalyst, while the amine SDBS is not a substrate for this reaction.

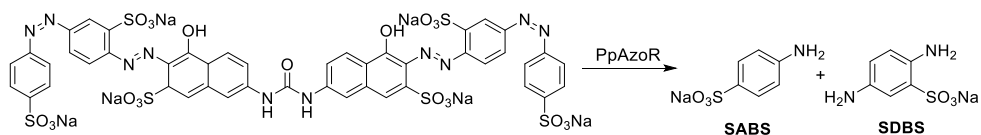


Figure 3.4 Azo reduction of direct red 80 by the action of PpAzoR.

In order to investigate the cooperative action of catalysts **6** and the enzyme PpAzoR, we assessed the sequential reaction of the enzymatic azo reduction of DR80 and the organometallic *N*-alkylation of the amines obtained from the azo reduction. First, the reaction was studied using the organometallic catalysis optimized conditions: SABS, SDBS and benzyl alcohol (1:1:1 ratio, 1 mmol), 2 mol % catalyst **6** in water (0.25 ml). This reaction mixture was reacted at 110°C for 16 h. At the end of the reaction, amine SABS was fully converted to the corresponding alkylated product, while amine SDBS remained intact. Interestingly, PpAzoR was not inactivated by the presence of **6**.

Since the amine SDBS can be converted into a phenazine by action of CotA laccase, we decided to study the simultaneous alkylation of SABS by catalyst **6** and the self-coupling oxidation of SDBS catalyzed by CotA-laccase. The reaction was performed with 2 mM of SABS, SDBS and benzyl alcohol (1:1:1 ratio) in 0.1 mM sodium phosphate buffer pH 7. Upon addition of 2 mol % of catalyst **6** and 1 U ml⁻¹ of CotA-laccase the mixture was heated at 110°C for 24 h. After this time, the amine SDBS was fully converted by CotA laccase into the phenazine, while amine SABS remained intact. Unfortunately, this findings seem to indicate the inactivation of the iridium catalyst by the presence of the enzyme CotA laccase.

3.4. Conclusion

A versatile catalytic system for the alkylation of amines with alcohols in water using a series of new water-soluble $\text{Cp}^*\text{Ir}(\text{NHC})\text{Cl}_2$ (Cp^* =pentamethylcyclopentadienyl, NHC=N-heterocyclic carbene) complexes that bear ester- and amide-functionalized NHCs has been developed. For the first time, iridium NHC complexes have been applied as catalysts for the alkylation of amines with alcohols in water. All the Ir complexes were stable in water solutions for at least 24 h. The best catalyst displayed a broad substrate scope for various alcohols and amines, which allowed the synthesis of a diverse range of secondary aromatic and aliphatic amines in excellent yields and selectivity. Notably, the catalytic system operates under base free conditions without additives.

3.5. Experimental Section

3.5.1. General Information

All experiments were carried out under nitrogen using standard Schlenk techniques and high vacuum, unless otherwise stated. Compounds $[\text{Cp}^*\text{IrCl}_2]_2$ ^[67], **1**^[58], **2**^[58], and 1-(mesityl)imidazole^[68], were synthesized according to literature procedures. All other reagents were used as purchased. ¹H and ¹³C NMR spectra were recorded on a Bruker Avance III 400 MHz. Assignment of resonances was made from HMQC and HMBC experiments. CCDC-1531731 and CCDC-1531733 contain the supplementary crystallographic data. These can be obtained free of charge from The Cambridge Crystallographic Data Centre via http://www.ccdc.cam.ac.uk/data_request/cif.

Synthesis of compound 3. A mixture of N-(2,6-Dimethylphenyl)chloroacetamide (1.5 g, 8.6 mmol) and 1-(trimethylsilyl)-imidazole (0.5 g, 3.2 mmol) was heated to 60 °C and stirred for 24 h to obtain a yellow solid. The solid was cooled to room temperature, washed with diethyl ether (3 x 20 mL), filtered off, and dried under vacuo to yield **3** as a pale yellow solid in 70% yield. Data for **3**: ¹H NMR (298K, 400 MHz, DMSO-d₆): δ = 9.98 (s, 1H, *NH*), 9.28 (s, 1H, *NCHN*), 7.80 (s, 2H, *NCHCHN*), 7.08 (m, 6H, Ph), 5.37 (s, 4H, *NCH₂CO*), 2.17 (s, 12H, PhCH₃). ¹³C NMR (298K, 400 MHz, DMSO-

δ 163.63 (CO), 138.72 (NCHN), 136.25 (Ph, C_{ipso}), 134.18 (Ph, CH), 127.92 (Ph, CH), 126.99 (Ph, C_{ipso}), 123.58 (NCHCHN), 50.78 (NCH₂CO), 18.25 (CH₃Ph). HRMS (ESI-TOF) in acetonitrile: m/z [M]⁺ calcd for [C₂₃H₂₇N₄O₂]⁺, 391.2134, found: 391.2133.

Synthesis of compound 4. A mixture of ethyl chloroacetate (0.66 g, 54 mmol) and 1-(mesityl)imidazole (1 g, 54 mmol) was heated to 60 °C and stirred for 24 h to afford a yellow solid. The solid was washed with diethyl ether (3 x 20 mL), filtered off, and dried under vacuo to yield 4 in 77% yield. Data for 4: ¹H NMR (298K, 400 MHz, CDCl₃): δ = 10.31 (s, H, NCHN), 7.94 (s, H, NCH), 7.14 (s, H, NCH), 6.99 (s, 2H, CHPh), 5.90 (s, 2H, NCH₂CO), 4.28-4.23 (m, 2H, CH₂CH₃), 2.33 (s, 3H, CH₃Ph), 2.08 (s, 6H, PhCH₃), 1.30 (t, 3H, ³J_{HH} = 7.1 Hz, CH₂CH₃). ¹³C NMR (298K, 400 MHz, CDCl₃): δ = 166.80 (CO), 141.47 (NCHN), 139.82 (Ph, C_{ipso}), 134.49 (Ph, C_{ipso}), 129.92 (Ph), 124.63 (NCHCHN), 122.46 (NCHCHN), 62.95 (CH₂CH₃), 50.76 (NCH₂CO), 21.21 (Ph, CH₃), 17.61 (Ph, CH₃), 14.14 (CH₂CH₃). HRMS (ESI-TOF) in acetonitrile: m/z [M]⁺ calcd for [C₁₆H₂₁N₂O₂]⁺, 273.1603, found: 273.1603.

3.5.2. General procedure for the synthesis of iridium complexes 5-8

Silver oxide was added to a solution of the appropriated proligand 1-4 in dichloromethane (10 mL). The suspension was stirred at room

temperature for 1 h under the exclusion of light. Then, $[\text{Cp}^*\text{IrCl}_2]_2$ was added, and the reaction mixture was stirred at room temperature for 4 h. The suspension was filtered through Celite, and the solvent was evaporated. The crude solid was purified by column chromatography on silica gel with a mixture dichloromethane/acetone (10/1).

Preparation and characterization of $\text{Cp}^*\text{Ir}(\text{NHC})\text{Cl}_2$, 5. Following the general procedure, proligand 1 (0.5 g, 1.8 mmol), Ag_2O (0.32 g, 1.37 mmol), and $[\text{Cp}^*\text{IrCl}_2]_2$ (0.72 g, 0.9 mmol) afforded 5 as a yellow solid. Yield: 918 mg, 80%. Data for 5: ^1H NMR (298 K, 400MHz, CDCl_3): δ = 6.95 (s, 2H, NCHCHN), 5.96 (dd, 2H, NCH_2CO , AB pattern, $J_{\text{HH}} = 18.49$ Hz), 4.70 (dd, 2H, NCH_2CO , AB pattern, $J_{\text{HH}} = 18.49$ Hz), 4.23-4.15 (m, 4H, CH_2CH_3), 1.53 (s, 15H, CH_{3Cp^*}), 1.26-1.22 (t, 6H, CH_2CH_3) ^{13}C NMR (298 K, 400MHz, CDCl_3): δ 169.40 (CO), 159.80 (Clr), 123.50 (NCHCHN), 89.75 (C_{Cp^*}), 61.87 (CH_2CH_3), 52.48 (NCH_2CO), 14.32 (CH_2CH_3), 8.88 (CH_{3Cp^*}). Anal. Calcd. for $\text{C}_{21}\text{H}_{31}\text{N}_2\text{O}_4\text{Cl}_2\text{Ir}$ (638.604): C, 39.50; H, 4.89; N, 4.39. Found: C, 39.27; H, 4.97; N, 4.26. HRMS (ESI-TOF) in acetonitrile: m/z $[\text{M}]^+$ calcd for $[\text{C}_{21}\text{H}_{31}\text{N}_2\text{O}_4\text{IrCl}]^+$, 603.1594, found: 603.1591.

Preparation and characterization of $\text{Cp}^*\text{Ir}(\text{NHC})\text{Cl}_2$, 6. Following the general procedure, proligand 2 (0.5 g, 1.7 mmol), Ag_2O (0.30 g, 1.30 mmol), and $[\text{Cp}^*\text{IrCl}_2]_2$ (0.72 g, 0.9 mmol) afforded 6 as a yellow solid. Yield: 962 mg, 82 %. Crystallization from dichloromethane-pentane led

to yellow crystals suitable for X-ray diffraction studies. Data for 6: ^1H NMR (298 K, 400MHz, CDCl_3): δ = 6.95 (s, 2H, NCHCHN), 6.23 (dd, 2H, NCH_2CO , AB pattern, $J_{\text{HH}} = 17.50$ Hz), 4.65 (dd, 2H, NCH_2CO , AB pattern, $J_{\text{HH}} = 17.50$ Hz), 3.60-3.57 (m, 2H, CH_2CH_3), 3.46-3.41 (m, 2H, CH_2CH_3), 3.32-3.19 (m, 4H, CH_2CH_3), 1.54 (s, 15H, CH_{3Cp^*}), 1.24 (t, 6H, CH_2CH_3), 1.11 (t, 6H, CH_2CH_3). ^{13}C NMR (298 K, 400MHz, CDCl_3): δ 166.75 (CO), 157.03 (NHCIr), 123.58 (NCHCHN), 89.67 (C_{Cp^*}), 52.39 (NCH₂CO), 41.29 (CH_2CH_3), 40.32 (CH_2CH_3), 14.15 (CH_2CH_3), 12.84 (CH_2CH_3), 8.62 (CH_{3Cp^*}). Anal. Calcd. for $\text{C}_{25}\text{H}_{41}\text{N}_4\text{O}_2\text{Cl}_2\text{Ir}$ (692.74): C, 43.34; H, 5.97; N, 8.09. Found: C, 43.45; H, 5.91; N, 7.81. HRMS (ESI-TOF) in acetonitrile: m/z $[\text{M}]^+$ calcd for $[\text{C}_{25}\text{H}_{41}\text{N}_4\text{O}_2\text{ClIr}]^+$, 657.2540, found: 657.2540.

Preparation and characterization of $\text{Cp}^*\text{Ir}(\text{NHC})\text{Cl}_2$, 7. Following the general procedure, proligand 3 (0.5 g, 1.2 mmol), Ag_2O (0.21 g, 0.9 mmol), and $[\text{Cp}^*\text{IrCl}_2]_2$ (0.48 g, 0.6 mmol) afforded 7 as a yellow solid. Yield: 741 mg, 78%. Data for 7: ^1H NMR (298 K, 400MHz, CDCl_3): δ = 9.0 (s, 2H, NH), 7.46 (s, 2H, NCHCHN), 7.06-6.98 (m, 6H, CHPh), 6.09 (dd, 2H, NCH₂CO, AB pattern, $J_{\text{HH}} = 12.96$ Hz), 4.478 (dd, 2H, NCH₂CO, AB pattern, $J_{\text{HH}} = 12.96$ Hz), 2.13 (s, 12H, CH_3Ph), 1.66 (s, 15H, CH_{3Cp^*}). ^{13}C NMR (298 K, 400MHz, CDCl_3): δ 164.23 (CO), 157.81 (Clr), 133.95 (CPh), 132.316 (CPh), 127.10 (CHPh), 126.26 (CHPh), 121.97 (NCHCHN), 88.90 (Ar_{Cp^*}), 53.68 (NCH₂CO), 28.67

(CPh), 17.57 (CH_3Ph), 8.10 (CH_3Cp^*). Anal. Calcd. for $\text{C}_{33}\text{H}_{41}\text{N}_4\text{O}_2\text{Cl}_2\text{Ir}$ (788.826): C, 50.25; H, 5.24; N, 7.01. Found: C, 49.87; H, 5.19; N, 6.92. MS (ESI-TOF) in acetonitrile: m/z $[\text{M}]^+$ calcd for $[\text{C}_{33}\text{H}_{41}\text{N}_4\text{O}_2\text{ClIr}]^+$, 753.2541, found: 753.2549.

Preparation and characterization of $\text{Cp}^*\text{Ir}(\text{NHC})\text{Cl}_2$, 8. Following the general procedure, proligand 4 (0.5 g, 1.6 mmol), Ag_2O (0.28 g, 1.2 mmol), and $[\text{Cp}^*\text{IrCl}_2]_2$ (0.662 g, 0.83 mmol) afforded 8 as a yellow solid. Yield: 804 mg, 75%. Crystallization from dichloromethane-pentane led to yellow crystals suitable for X-ray diffraction studies. Data for 8: ^1H NMR (298 K, 400MHz, CDCl_3): δ = 7.15 (s, 1H, NCHCHN), 6.84 (s, 2H, CPh), 6.70 (s, 1H, NCHCHN), 4.27-4.22 (m, 2H, CH_2CH_3), 2.30 (s, 3H, CH_3Ph), 2.08 (s, 6H, CH_3Ph), 1.49 (s, 15H, CH_3Cp^*), 1.30-1.27 (t, 3H, CH_2CH_3). ^{13}C NMR (298 K, 400MHz, CDCl_3): δ = 168.71 (CO), 155.19 (NHClr), 137.56 (CPh), 132.16 (CPh), 127.10 (CHPh), 126.26 (NCHCHN), 121.90 (NCHCHN), 88.27 (Ar_{Cp^*}), 60.79 (CH_2CH_3), 32.61 (NCH_2CO), 20.29 (CH_3Ph), 18.20 (CH_3Ph), 13.20 (CH_2CH_3), 7.98 (CH_3Cp^*). Anal. Calcd. for $\text{C}_{26}\text{H}_{35}\text{N}_2\text{O}_2\text{Cl}_2\text{Ir}$ (670.69): C, 46.56; H, 5.26; N, 4.18. Found: C, 46.26; H, 4.96; N, 3.87. MS (ESI-TOF) in acetonitrile: m/z $[\text{M}]^+$ calcd for $[\text{C}_{26}\text{H}_{35}\text{N}_2\text{O}_2\text{ClIr}]^+$, 635.2009, found: 635.2020.

3.5.3. General procedure of N-alkylation of amines with alcohols

A mixture of amine (1 mmol), alcohol (1 mmol), and catalyst, was heated in water (0.25 mL) to 110°C in a closed vessel for the time indicated in Tables 1-4. The yield was determined by ¹H NMR using 1,4-di-tert-butylbenzene as an internal standard. The corresponding amines were extracted in dichloromethane. The identity of the products was established by comparison of their NMR spectral data with the reported data found in the literature [46,55,69–73].

3.5.4. Procedure for the sequential organometallic N-alkylation of SABS and self-coupling oxidation of SDBS by CotA-laccase

To mimic the reaction mixture from the PpAzoR azoreduction of the azo dye DR80, a 5 ml mixture of 2mM of SABS and SDBS each was prepared in 0.1 mM sodium phosphate buffer pH 7. To the mixture one equivalent of benzyl alcohol, 1 U ml⁻¹ of CotA-laccase and 2 mol % of catalyst **6** was added. The reaction mixture was heated to 110 °C in a closed vessel for 24 h.

CotA-laccase was overproduced in *E. coli* recombinant cells following previously described procedures [74] and was purified using well established chromatographic methods [75]. One unit (U) of enzymatic activity was defined as the amount of enzyme required to convert 1 μmol of substrate per min.

3.6. References

- [1] P. H. Dixneuf, V. Cadierno, *Metal-Catalyzed Reactions in Water*, Wiley-VCH Verlag GmbH & Co. KGaA, Weinheim, Germany, **2013**.
- [2] Q. Yang, Q. Wang, Z. Yu, *Chem. Soc. Rev.* **2015**, *44*, 2305–2329.
- [3] C. Gunanathan, D. Milstein, *Science (80-.)*. **2013**, *341*, 1229712–1229712.
- [4] T. D. Nixon, M. K. Whittlesey, J. M. J. Williams, *Dalt. Trans.* **2009**, 753–762.
- [5] E. Levin, E. Ivry, C. E. Diesendruck, N. G. Lemcoff, *Chem. Rev.* **2015**, *115*, 4607–4692.
- [6] E. Peris, *Chem. Rev.* **2017**, acs.chemrev.6b00695.
- [7] M. N. Hopkinson, C. Richter, M. Schedler, F. Glorius, *Nature* **2014**, *510*, 485–496.
- [8] L. Benhamou, E. Chardon, G. Lavigne, S. Bellemin-Laponnaz, V. César, *Chem. Rev.* **2011**, *111*, 2705–2733.
- [9] L. A. Schaper, S. J. Hock, W. A. Herrmann, F. E. K??hn, *Angew. Chemie - Int. Ed.* **2013**, *52*, 270–289.
- [10] H. D. Velazquez, F. Verpoort, *Chem. Soc. Rev.* **2012**, *41*,

7032.

- [11] J. M. Brown, P. H. Dixneuf, A. Fürstner, L. S. Hegedus, P. Hofmann, P. H. P. Knochel, S. Murai, M. Reetz, G. Van Koten, J. M. B. P. H. Dixneuf, et al., *Iridium Catalysis*, Springer Berlin Heidelberg, Berlin, Heidelberg, **2011**.
- [12] L. A. Oro, C. Claver, *Iridium Complexes in Organic Synthesis*, Wiley, **2008**.
- [13] J. Choi, A. H. R. MacArthur, M. Brookhart, A. S. Goldman, *Chem. Rev.* **2011**, *111*, 1761–1779.
- [14] J. M. Thomsen, D. L. Huang, R. H. Crabtree, G. W. Brudvig, *Dalt. Trans.* **2015**, *44*, 12452–12472.
- [15] X.-Q. Guo, Y.-N. Wang, D. Wang, L.-H. Cai, Z.-X. Chen, X.-F. Hou, *Dalton Trans.* **2012**, *41*, 14557–67.
- [16] E. B. Bauer, G. T. S. Andavan, T. K. Hollis, R. J. Rubio, J. Cho, G. R. Kuchenbeiser, T. R. Helgert, C. S. Letko, F. S. Tham, *Org. Lett.* **2008**, *10*, 1175–1178.
- [17] A. Azua, S. Sanz, E. Peris, *Chem. - A Eur. J.* **2011**, *17*, 3963–3967.
- [18] H. Horváth, Á. Kathó, A. Udvardy, G. Papp, D. Szikszai, F. Joó, *Organometallics* **2014**, *33*, 6330–6340.

- [19] M. Albrecht, J. R. Miecznikowski, A. Samuel, J. W. Faller, R. H. Crabtree, *Organometallics* **2002**, *21*, 3596–3604.
- [20] Y. Feng, B. Jiang, P. A. Boyle, E. A. Ison, *Organometallics* **2010**, *29*, 2857–2867.
- [21] D. G. H. Hetterscheid, J. N. H. Reek, *Chem. Commun.* **2011**, *47*, 2712–2714.
- [22] O. Diaz-Morales, T. J. P. Hersbach, D. G. H. Hetterscheid, J. N. H. Reek, M. T. M. Koper, *J. Am. Chem. Soc.* **2014**, *136*, 10432–10439.
- [23] Z. Codolà, J. M. S. Cardoso, B. Royo, M. Costas, J. Lloret-Fillol, *Chem. - A Eur. J.* **2013**, *19*, 7203–7213.
- [24] T. P. Brewster, J. D. Blakemore, N. D. Schley, C. D. Incarvito, N. Hazari, G. W. Brudvig, R. H. Crabtree, *Organometallics* **2011**, *30*, 965–973.
- [25] A. R. Parent, T. P. Brewster, W. De Wolf, R. H. Crabtree, G. W. Brudvig, *Inorg. Chem.* **2012**, *51*, 6147–6152.
- [26] A. Volpe, A. Sartorel, C. Tubaro, L. Meneghini, M. Di Valentin, C. Graiff, M. Bonchio, *Eur. J. Inorg. Chem.* **2014**, 665–675.
- [27] R. Lalrempuia, N. D. McDaniel, H. Müller-Bunz, S. Bernhard, M. Albrecht, *Angew. Chemie - Int. Ed.* **2010**, *49*, 9765–9768.

- [28] D. Canseco-Gonzalez, A. Petronilho, H. Mueller-Bunz, K. Ohmatsu, T. Ooi, M. Albrecht, *J. Am. Chem. Soc.* **2013**, *135*, 13193–13203.
- [29] A. Petronilho, A. Llobet, M. Albrecht, *Inorg. Chem.* **2014**, *53*, 12896–12901.
- [30] A. Petronilho, J. A. Woods, H. Mueller-Bunz, S. Bernhard, M. Albrecht, *Chemistry* **2014**, *20*, 15775–15784.
- [31] J. Leonard, A. J. Blacker, S. P. Marsden, M. F. Jones, K. R. Mulholland, R. Newton, *Org. Process Res. Dev.* **2015**, *19*, 1400–1410.
- [32] G. Guillena, D. J. Ramón, M. Yus, *Chem. Rev.* **2010**, *110*, 1611–1641.
- [33] G. E. Dobereiner, R. H. Crabtree, E. Nucleophiles, **2010**, 681–703.
- [34] S. Bähn, S. Imm, L. Neubert, M. Zhang, H. Neumann, M. Beller, *ChemCatChem* **2011**, *3*, 1853–1864.
- [35] R. Grigg, T. R. B. Mitchell, S. Sutthivaiyakit, N. Tongpenyai, *J C S chem comm* **1981**, 611–612.
- [36] Y. Watanabe, Y. Tsuji, Y. Ohsugi, *Tetrahedron Lett.* **1981**, *22*, 2667–2670.

- [37] S. Rösler, M. Ertl, T. Irrgang, R. Kempe, *Angew. Chemie - Int. Ed.* **2015**, *54*, 15046–15050.
- [38] G. Guillena, D. Ramon, M. Yus, *Chem. Rev.* **2010**, *110*, 1611–1641.
- [39] S. Elangovan, J. Neumann, J.-B. Sortais, K. Junge, C. Darcel, M. Beller, *Nat. Commun.* **2016**, *7*, 12641.
- [40] A. Prades, R. Corberán, M. Poyatos, E. Peris, *Chem. - A Eur. J.* **2008**, *14*, 11474–11479.
- [41] C. Segarra, E. Mas-Marzá, J. A. Mata, E. Peris, *Adv. Synth. Catal.* **2011**, *353*, 2078–2084.
- [42] T. Hille, T. Irrgang, R. Kempe, *Angew. Chemie Int. Ed.* **2016**, 371–374.
- [43] X. H. Zhu, L. H. Cai, C. X. Wang, Y. N. Wang, X. Q. Guo, X. F. Hou, *J. Mol. Catal. A Chem.* **2014**, *393*, 134–141.
- [44] R. Zhong, Y. N. Wang, X. Q. Guo, Z. X. Chen, X. F. Hou, *Chem. - A Eur. J.* **2011**, *17*, 11041–11051.
- [45] A. P. Da Costa, M. Viciano, M. Sanaú, S. Merino, J. Tejada, E. Peris, B. Royo, *Organometallics* **2008**, *27*, 1305–1309.
- [46] A. Bartoszewicz, R. Marcos, S. Sahoo, A. K. Inge, X. Zou, B. Martín-Matute, *Chem. - A Eur. J.* **2012**, *18*, 14510–14519.

- [47] M. H. S. a Hamid, J. M. J. Williams, *Chem. Commun. (Camb)*. **2007**, 725–727.
- [48] A. J. A. Watson, A. C. Maxwell, J. M. J. Williams, *J. Org. Chem.* **2011**, 76, 2328–2331.
- [49] R. Martínez, D. J. Ramón, M. Yus, *Org. Biomol. Chem.* **2009**, 7, 2176–2181.
- [50] S. Michlik, T. Hille, R. Kempe, *Adv. Synth. Catal.* **2012**, 354, 847–862.
- [51] S. Imm, S. Bähn, M. Zhang, L. Neubert, H. Neumann, F. Klasovsky, J. Pfeffer, T. Haas, M. Beller, *Angew. Chemie - Int. Ed.* **2011**, 50, 7599–7603.
- [52] S. Ruch, T. Irrgang, R. Kempe, *Chem. - A Eur. J.* **2014**, 20, 13279–13285.
- [53] O. Saidi, A. J. Blacker, M. M. Farah, S. P. Marsden, J. M. J. Williams, *Chem. Commun. (Camb)*. **2010**, 46, 1541–3.
- [54] R. Kawahara, K. Fujita, R. Yamaguchi, S. Kyoto, *J. Am. Chem. Soc.* **2010**, 3, 15108–15111.
- [55] R. Kawahara, K. I. Fujita, R. Yamaguchi, *Adv. Synth. Catal.* **2011**, 353, 1161–1168.
- [56] A. Wetzel, S. Wöckel, M. Schelwies, M. K. Brinks, F.

- Rominger, P. Hofmann, M. Limbach, *Org. Lett.* **2013**, *15*, 266–269.
- [57] J. Norinder, A. Börner, *ChemCatChem* **2011**, *3*, 1407–1409.
- [58] M. Pellei, V. Gandin, M. Marinelli, C. Marzano, M. Yousufuddin, H. V. R. Dias, C. Santini, *Inorg. Chem.* **2012**, *51*, 9873–9882.
- [59] F. Hanasaka, K. Fujita, R. Yamaguchi, *Organometallics* **2004**, *23*, 1490–1492.
- [60] F. Hanasaka, Y. Tanabe, K. I. Fujita, R. Yamaguchi, *Organometallics* **2006**, *25*, 826–831.
- [61] R. Corberán, M. Sanaú, E. Peris, *J. Am. Chem. Soc.* **2006**, *128*, 3974–3979.
- [62] R. Corberán, M. Sanaú, E. Peris, *Organometallics* **2007**, *26*, 3492–3498.
- [63] F. Hanasaka, K. Fujita, R. Yamaguchi, *Organometallics* **2005**, *24*, 3422–3433.
- [64] W. Zhang, X. Dong, W. Zhao, *Org. Lett.* **2011**, *13*, 5386–5389.
- [65] L. Pereira, P. K. Mondal, M. Alves, in *Pollut. Build. Water Living Org.* (Eds.: E. Lichtfouse, J. Schwazbaeur, D. Robert), Springer International Publishing, **2015**, pp. 297–346.
- [66] R. Kant, *Nat. Sci.* **2012**, *04*, 22–26.

- [67] R. G. Ball, W. A. G. Graham, J. K. Hoyano, A. D. McMaster, B. M. Mattson, D. M. Heinekey, B. M. Mattson, S. T. Michel, *Inorg. Chem.* **1990**, *29*, 2023–2025.
- [68] M. G. Gardiner, W. A. Herrmann, C. P. Reisinger, J. Schwarz, M. Spiegler, *J. Organomet. Chem.* **1999**, *572*, 239–247.
- [69] D. Wang, X.-Q. Guo, C.-X. Wang, Y.-N. Wang, R. Zhong, X.-H. Zhu, L.-H. Cai, Z.-W. Gao, X.-F. Hou, *Adv. Synth. Catal.* **2013**, *355*, 1117–1125.
- [70] Q. Zou, C. Wang, J. Smith, D. Xue, J. Xiao, *Chem. - A Eur. J.* **2015**, *21*, 9656–9661.
- [71] M. M. Reddy, M. A. Kumar, P. Swamy, M. Naresh, K. Srujana, L. Satyanarayana, A. Venugopal, N. Narender, *Green Chem.* **2013**, *15*, 3474.
- [72] G. Zhang, Z. Yin, S. Zheng, *Org. Lett.* **2016**, *18*, 300–303.
- [73] N. Mittapelly, B. R. Reguri, K. Mukkanti, *Der Pharma Chem.* **2011**, *3*, 180–189.
- [74] P. Durão, Z. Chen, A. T. Fernandes, P. Hildebrandt, D. H. Murgida, S. Todorovic, M. M. Pereira, E. P. Melo, L. O. Martins, *J. Biol. Inorg. Chem.* **2008**, *13*, 183–193.
- [75] I. Bento, L. O. Martins, G. Gato Lopes, M. Arménia Carrondo, P. F. Lindley, *Dalt. Trans.* **2005**, *4*, 3507.

3.7. Supporting Information

3.7.1. NMR data for compounds 1-8

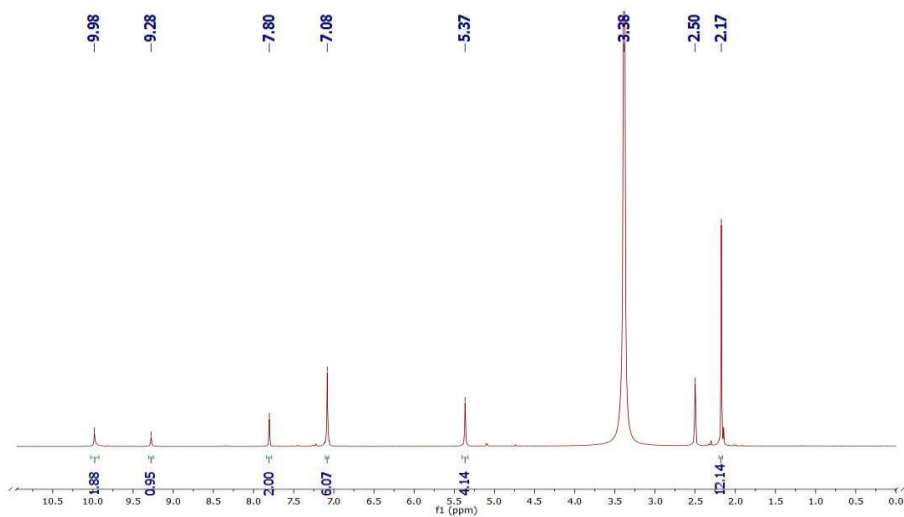


Figure 3.5 ¹H NMR (400 MHz) in DMSO-d₆ spectrum for compound 3

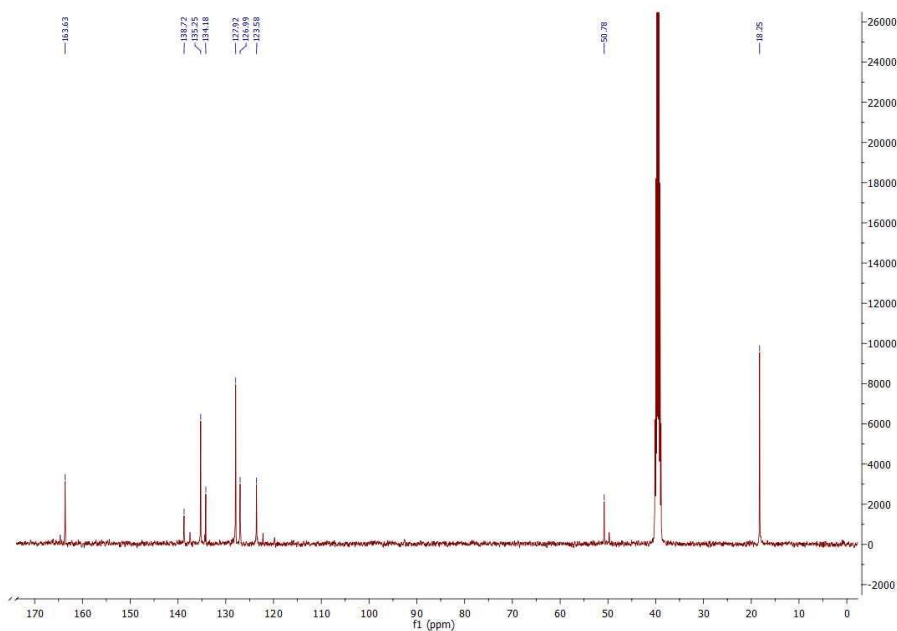


Figure 3.6 ¹³C NMR (400 MHz) in DMSO-d₆ spectrum for compound 3.

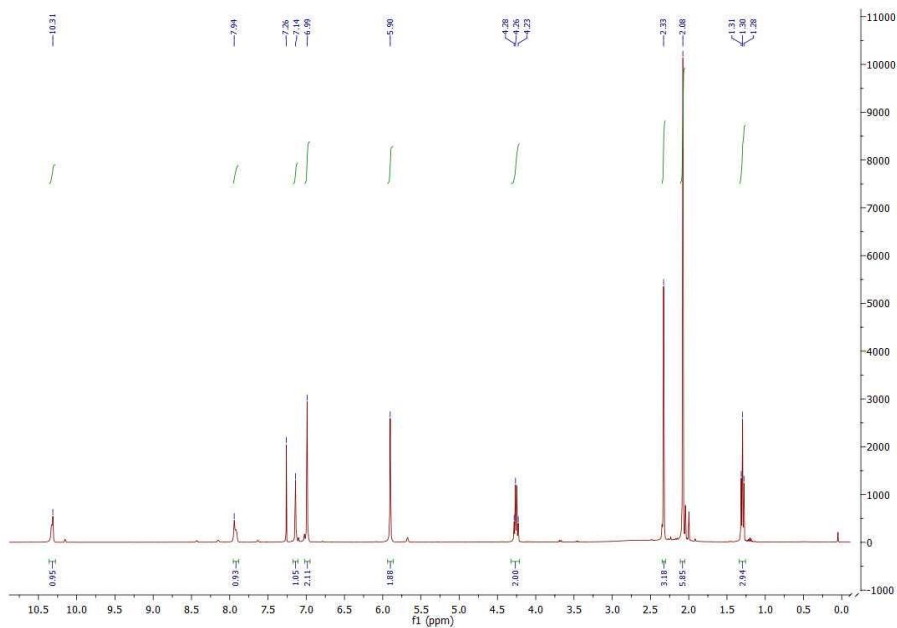


Figure 3.7 ¹H NMR (400 MHz) in CDCl₃ spectrum for compound 4

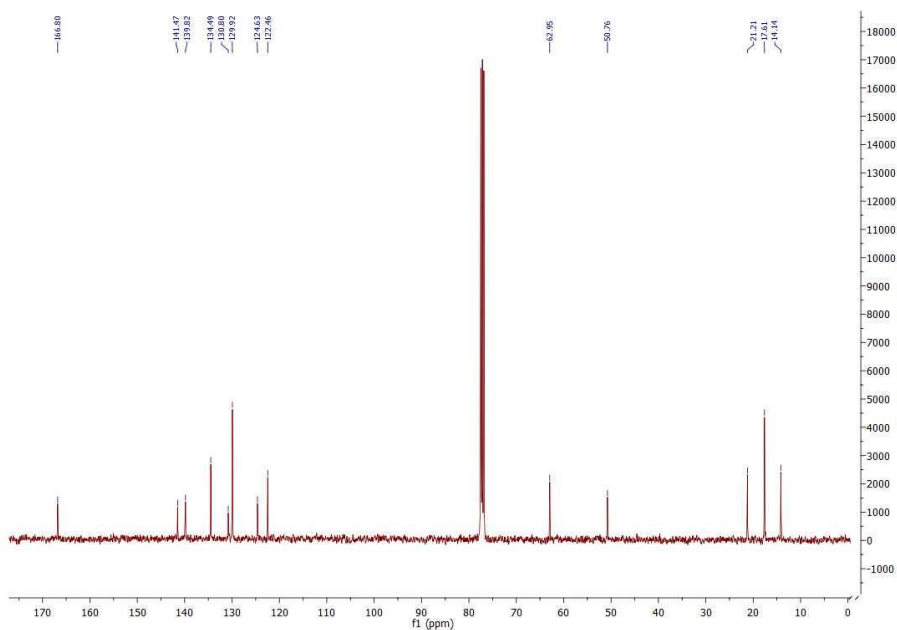


Figure 3.8 ¹³C NMR (400 MHz) in CDCl₃ spectrum for compound 4.

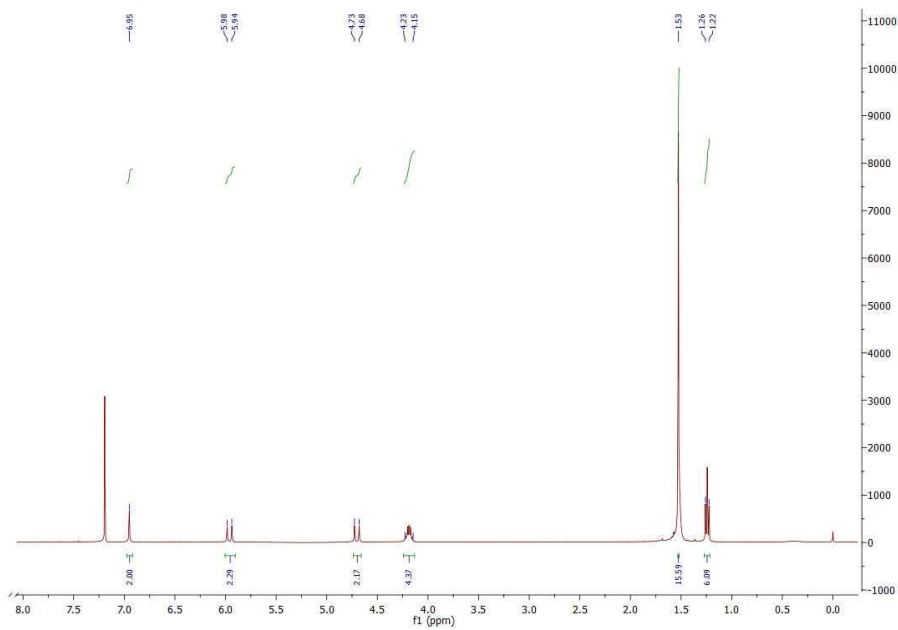


Figure 3.9 ^1H NMR (400 MHz) in CDCl_3 spectrum for compound 5

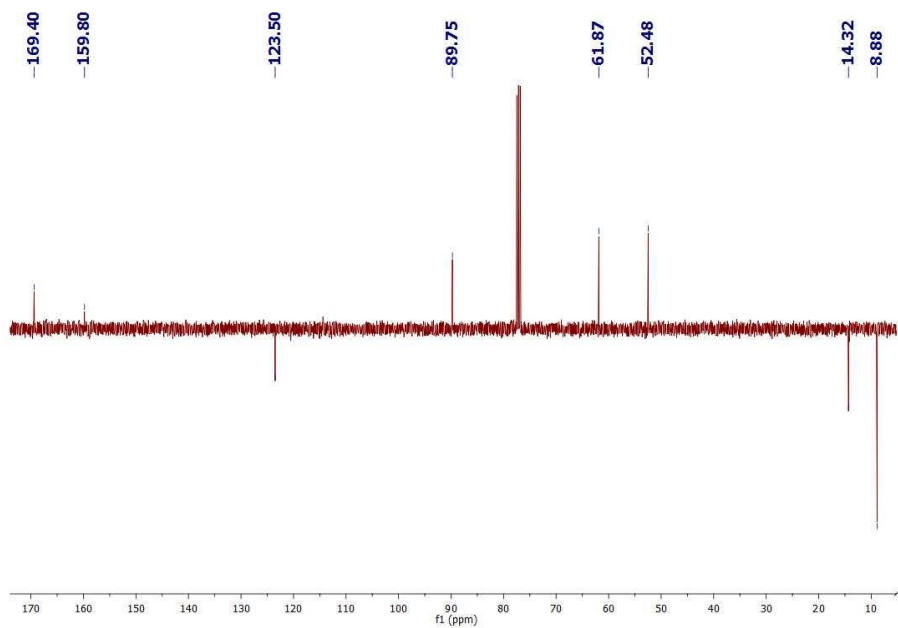


Figure 3.10 ^{13}C NMR (400 MHz) in CDCl_3 spectrum for compound 5.

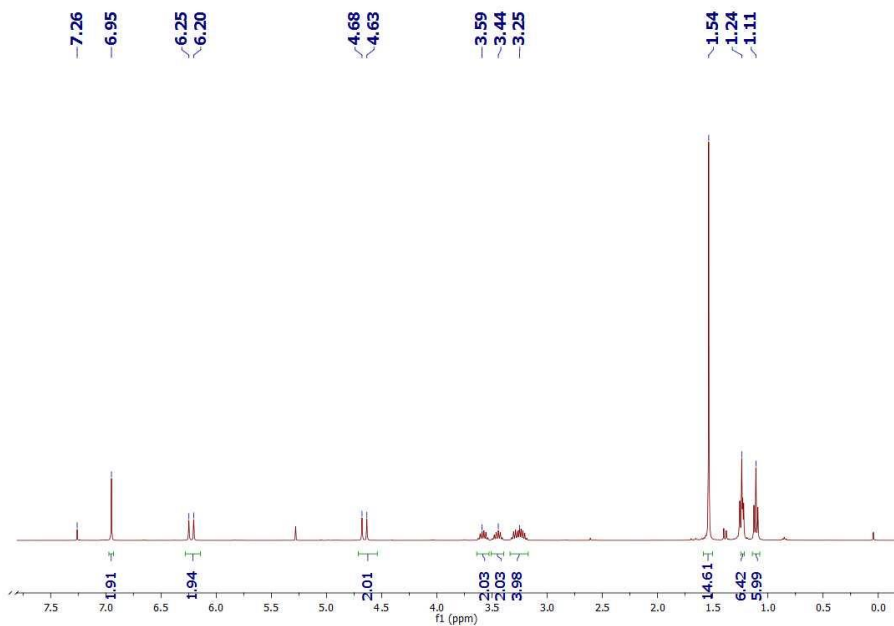


Figure 3.11 ¹H NMR (400 MHz) in CDCl₃ spectrum for compound 6

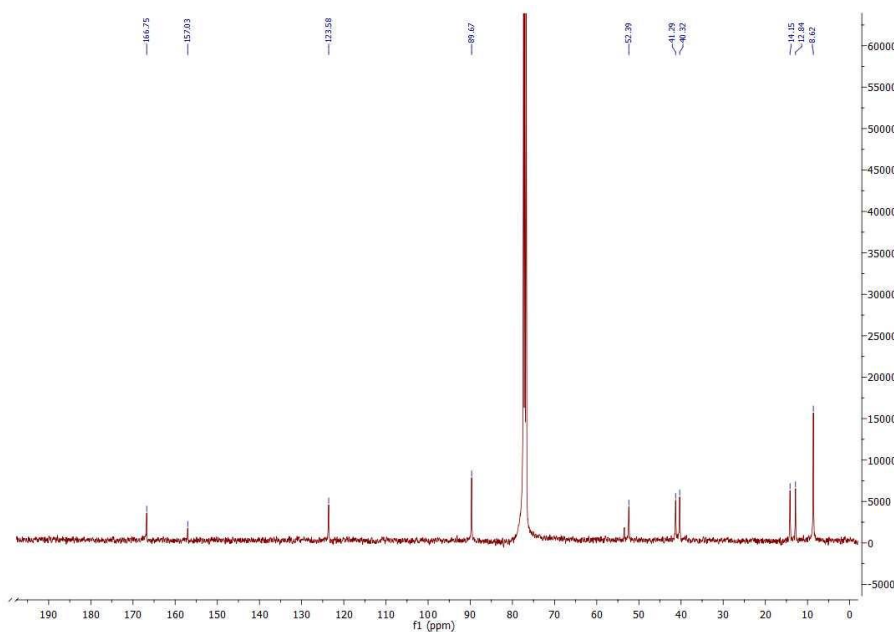


Figure 3.12 ¹³C NMR (400 MHz) in CDCl₃ spectrum for compound 6

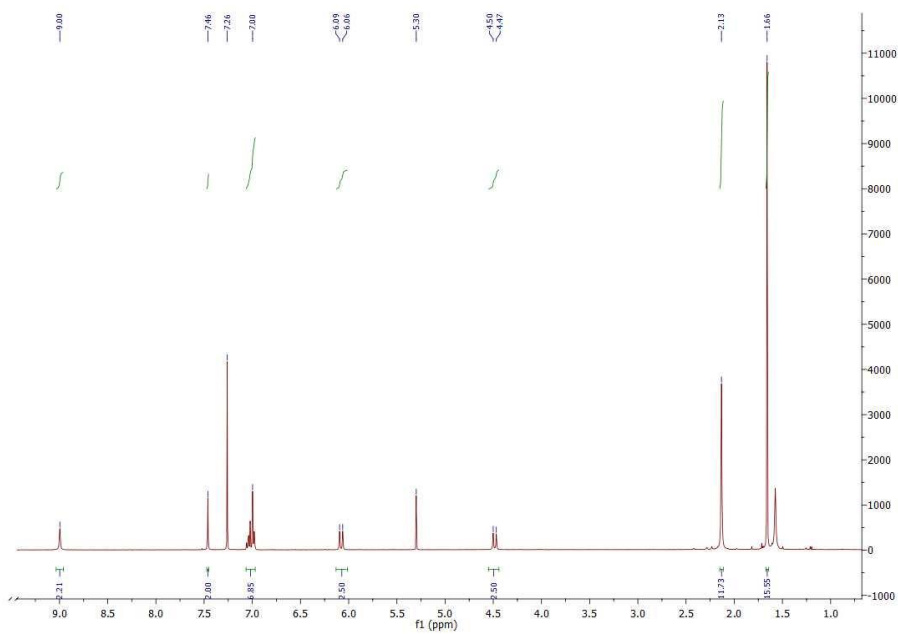


Figure 3.13 ^1H NMR (400 MHz) in CDCl_3 spectrum for compound 7

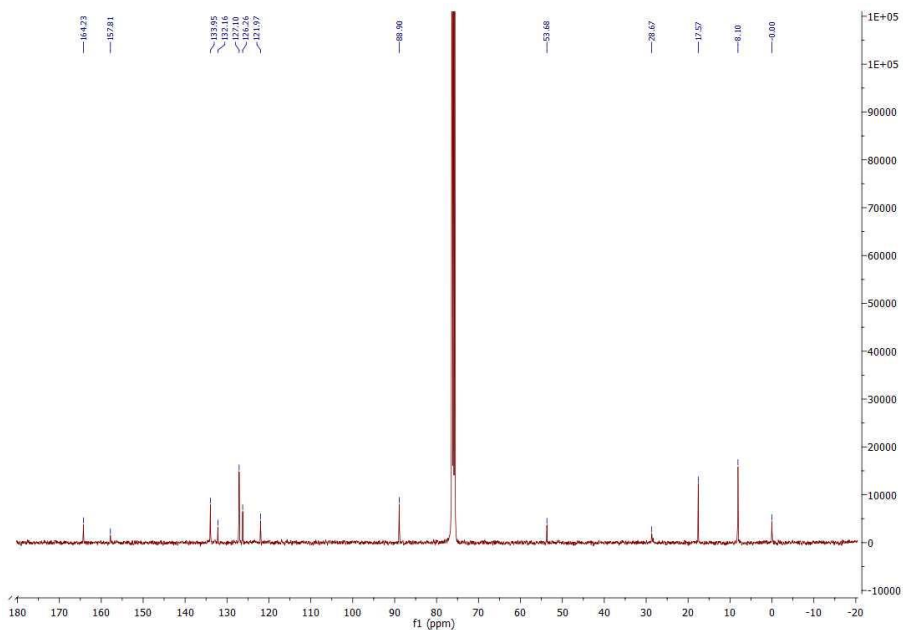


Figure 3.14 ^{13}C NMR (400 MHz) in CDCl_3 spectrum for compound 7

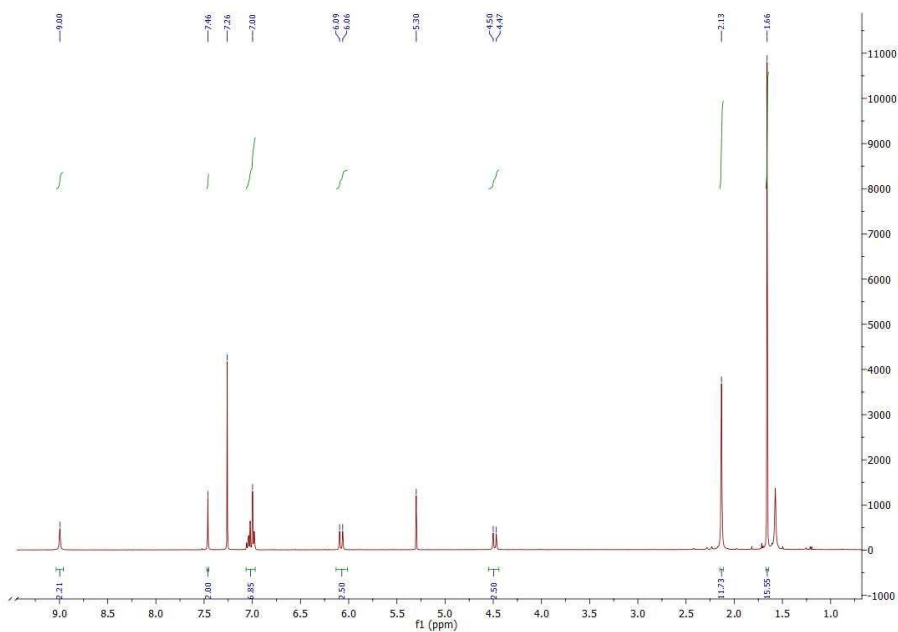


Figure 3.15 ¹H NMR (400 MHz) in CDCl₃ spectrum for compound **8**

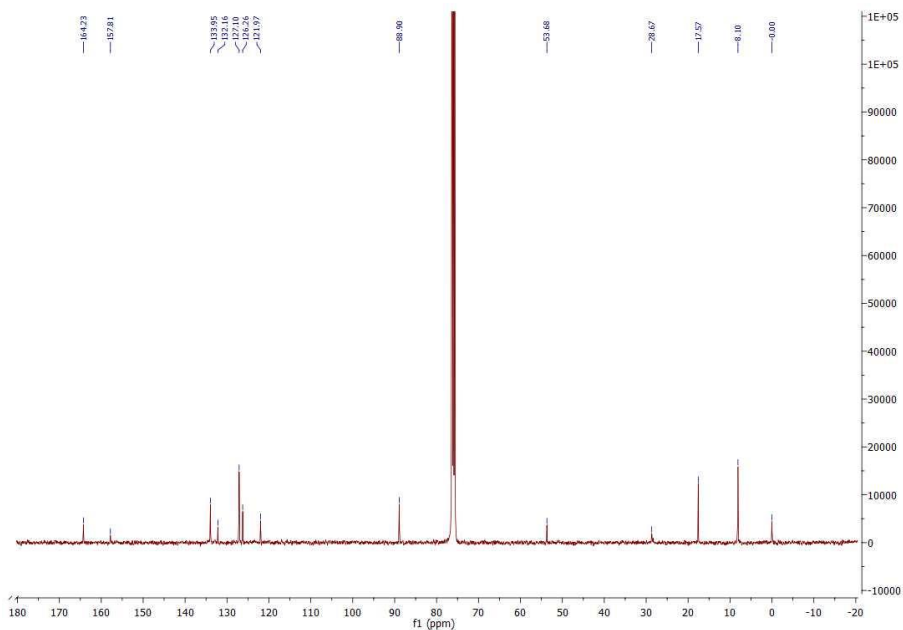


Figure 3.16 ¹³C NMR (400 MHz) in CDCl₃ spectrum for compound **8**

3.7.2. MS (ESI⁺) spectra for compounds 1-8

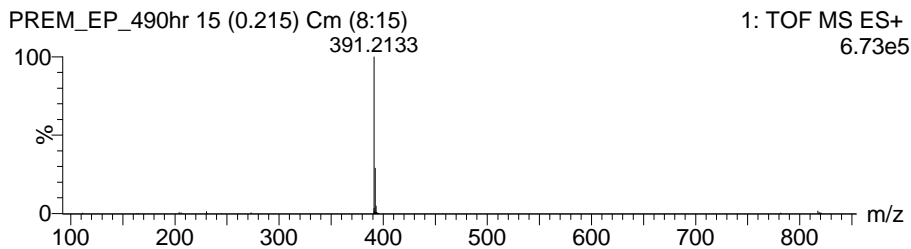


Figure 3.17 HRMS (ESI⁺) of compound 3

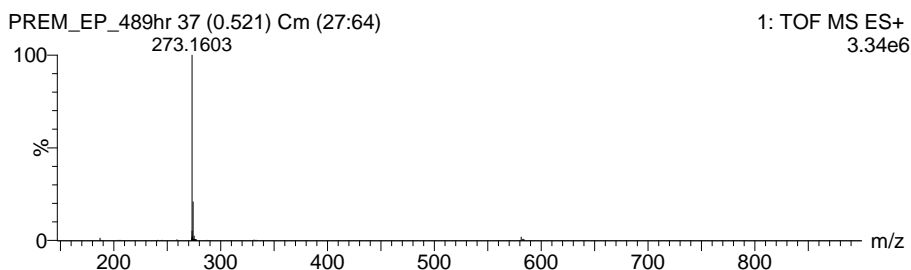


Figure 3.18 HRMS (ESI⁺) of compound 4

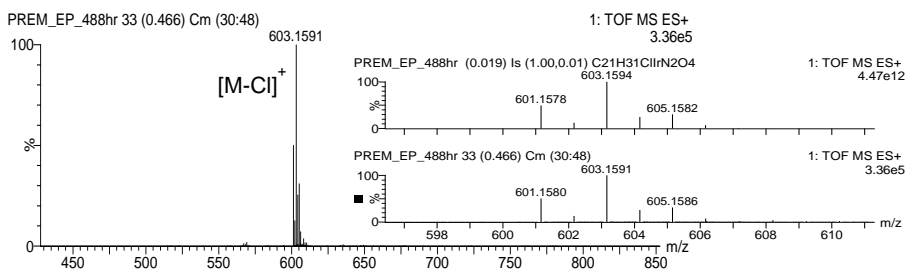


Figure 3.19 HRMS (ESI⁺) of compound 5

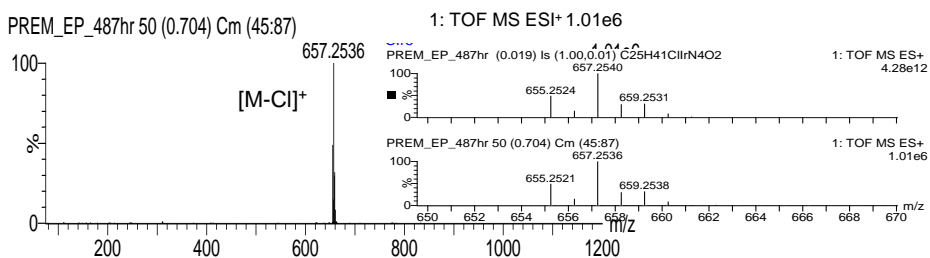


Figure 3.20 HRMS (ESI⁺) of compound 6

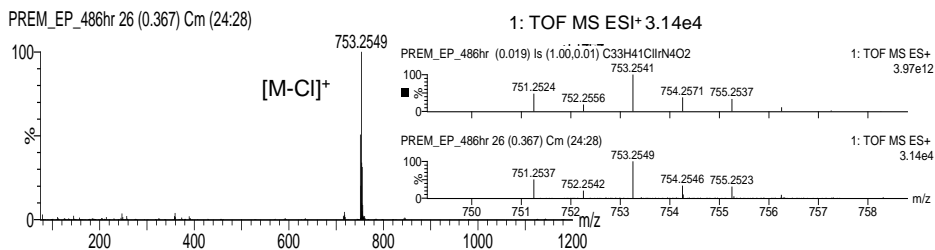


Figure 3.21 HRMS (ESI+) of compound 7

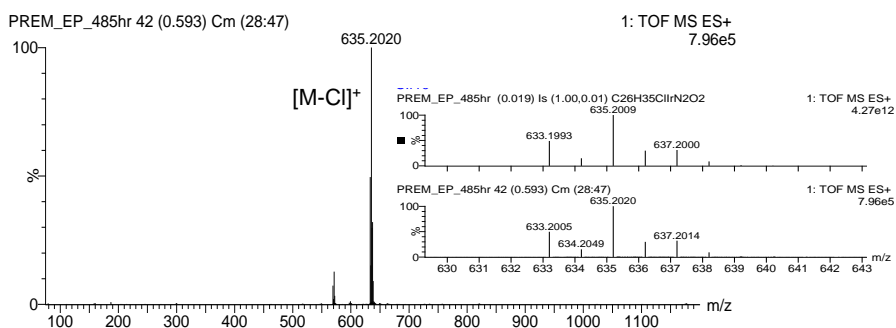


Figure 3.22 HRMS (ESI+) of compound 8

3.7.3. Crystallographic details for complexes 6 and 8

Table 3.5 Crystallographic details for complexes 6 and 8

	6	8
Empirical Formula	C ₂₅ H ₄₁ Cl ₂ IrN ₄ O ₂	C ₂₆ H ₃₅ Cl ₂ IrN ₂ O ₂
Mol wt	692.72	670.66
Radiation	Mo K α (monochr); 0.7107 λ (Å)	
T (K)	100(2)	293(2)
Cryst syst	Triclinic	Monoclinic
Space Group	P-1	P2 ₁ /n
a (Å)	10.7895(2)	9.7401(2)
b (Å)	11.6040(3)	20.9022(5)
c (Å)	11.7836(2)	13.5482(3)
α (deg)	83.1106(12)	90
β (deg)	68.0166(10)	95.5989
γ (deg)	81.1232(11)	90
V (Å ³)	1348.56(5)	2745.11(11)
Z	2	4
D _{calcd} (Mg m ⁻³)	1.706	1.623
Crystal size (mm ³)	0.220 x 0.190 x 0.150	0.440 x 0.410 x 0.030
F (000)	692	1328
θ range for data collection (deg)	1.780 to 30.544	1.797 to 29.633
μ (Mo K α) (mm ⁻¹)	1.706	5.083
Reflns collected	52894	74620
R _{int}	0.0423	0.0820
Independent reflections	8237	7734
R[F ² >2 σ (F ²)]	0.0183	0.0310
wR(F ²)	0.0347	0.0586
S	1.051	1.032

3.7.4. NMR data for recycled complex 6

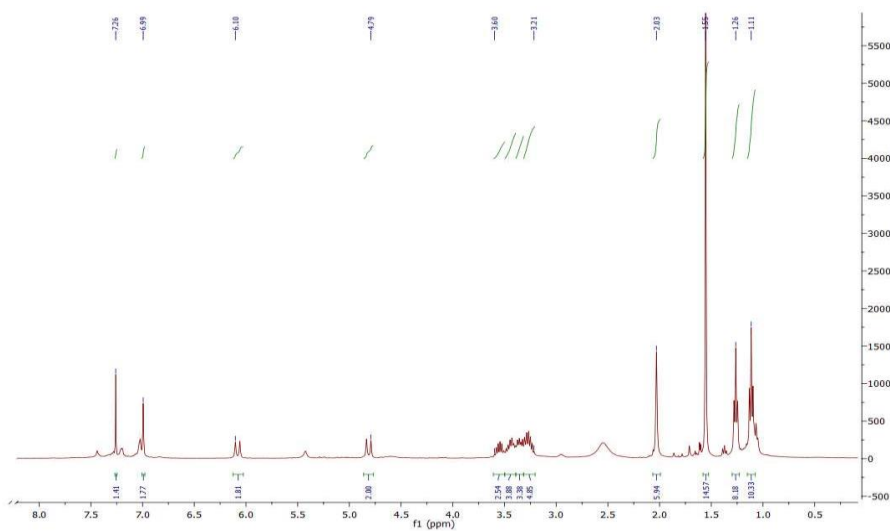


Figure 3.23 ^1H NMR (400 MHz) in CDCl_3 spectrum for complex **6** recycled from catalytic reaction

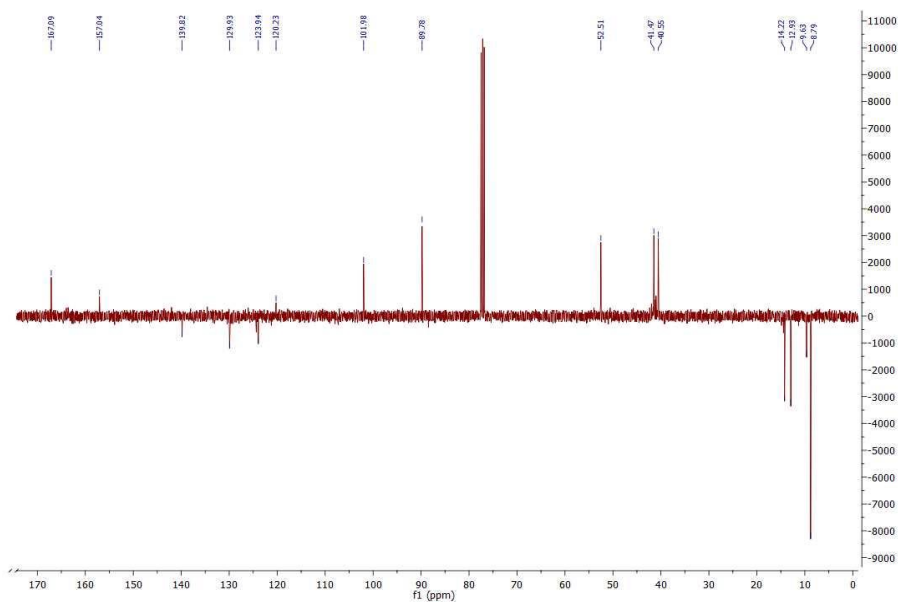


Figure 3.24 ^{13}C NMR (400 MHz) in CDCl_3 spectrum for complex **6** recycled from catalytic reaction

3.7.5. NMR data for isolated products of table 3.2

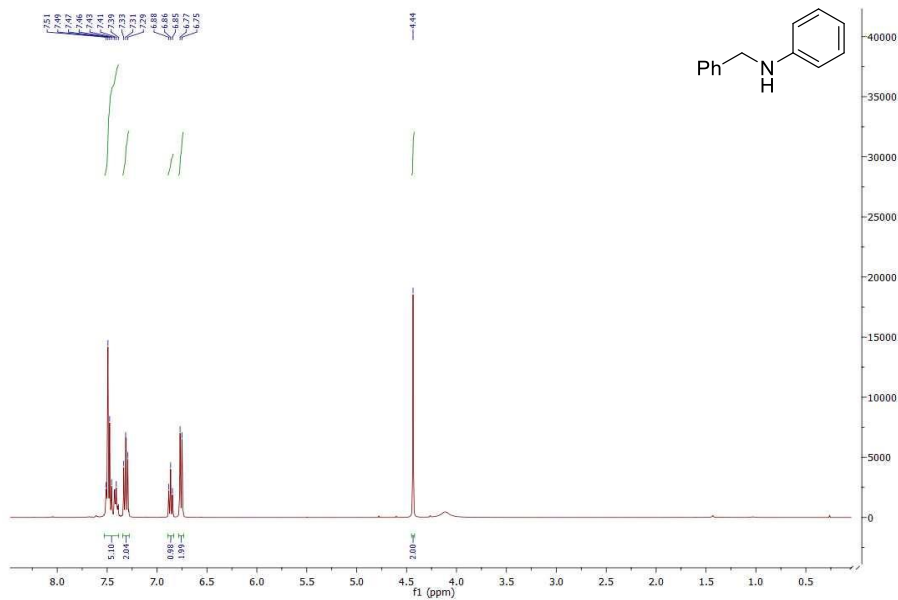


Figure 3.25 ¹H NMR (400 MHz) in CDCl₃ for N-benzylamine (table 2, entry 1)

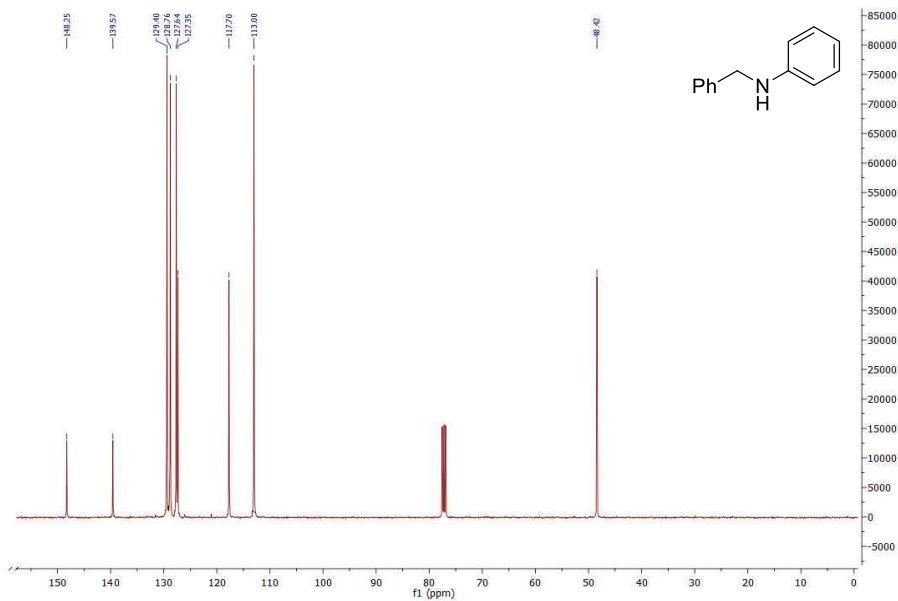


Figure 3.26 ¹³C NMR (400 MHz) in CDCl₃ for N-benzylamine (table 2, entry 1)

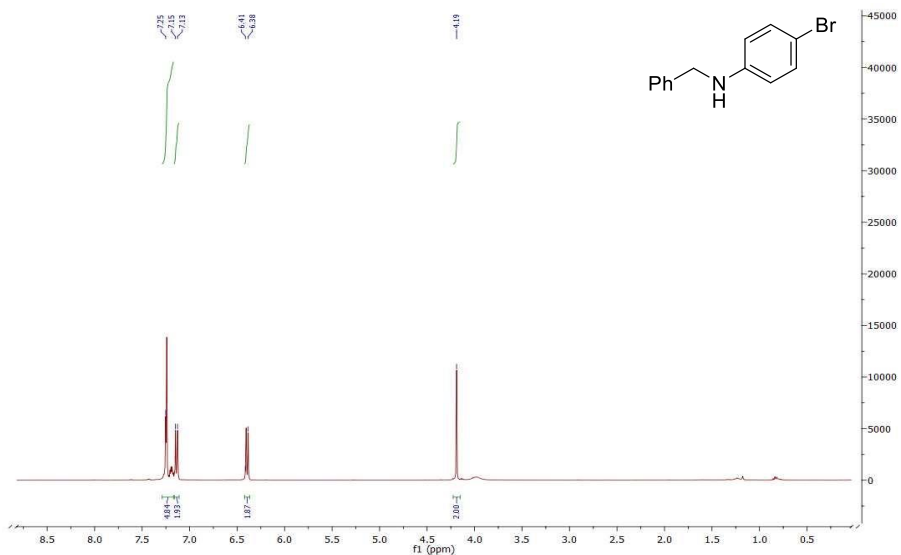


Figure 3.27 ¹H NMR (400 MHz) in CDCl₃ spectrum for N-benzyl-4-bromoaniline (table 2, entry 2)

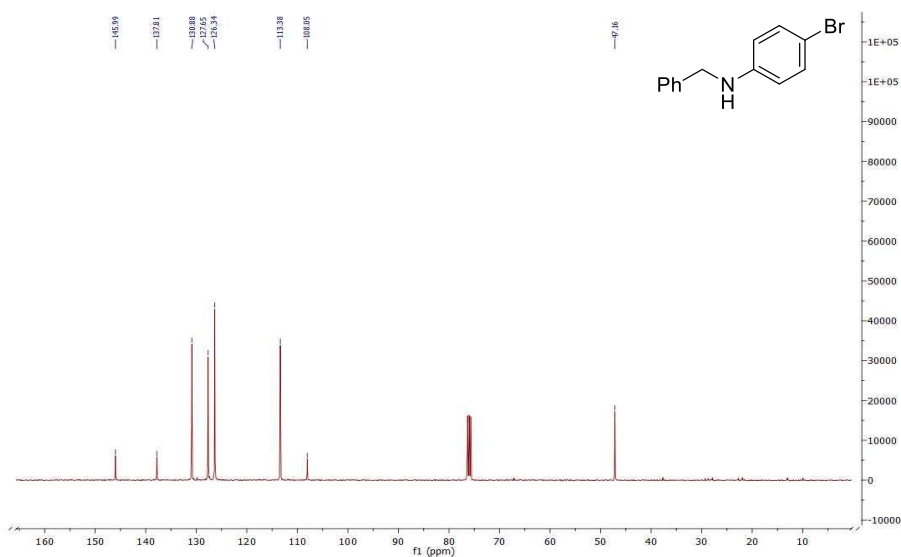


Figure 3.28 ¹³C NMR (400 MHz) in CDCl₃ spectrum for N-benzyl-4-bromoaniline (table 2, entry 2)

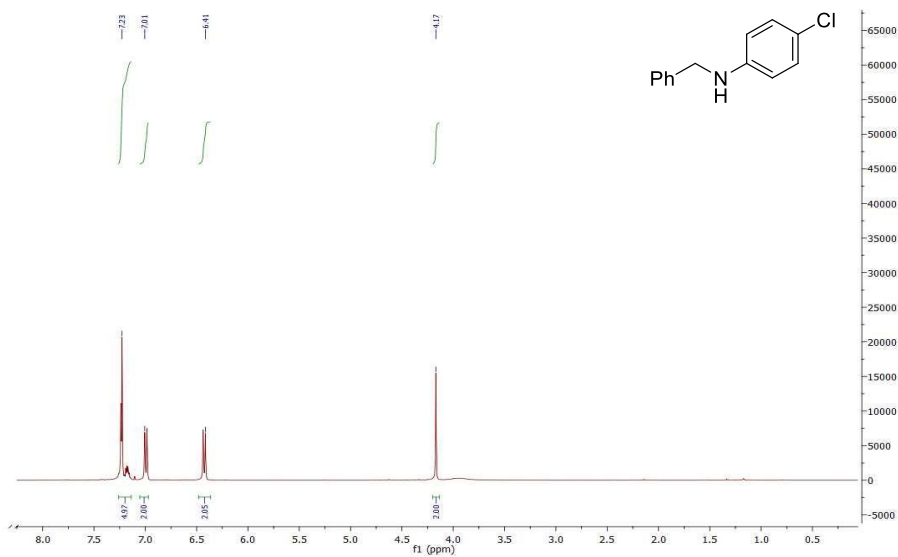


Figure 3.29 ^1H NMR (400 MHz) in CDCl_3 spectrum for N-benzyl-4-chloroaniline (table 2, entry 3)

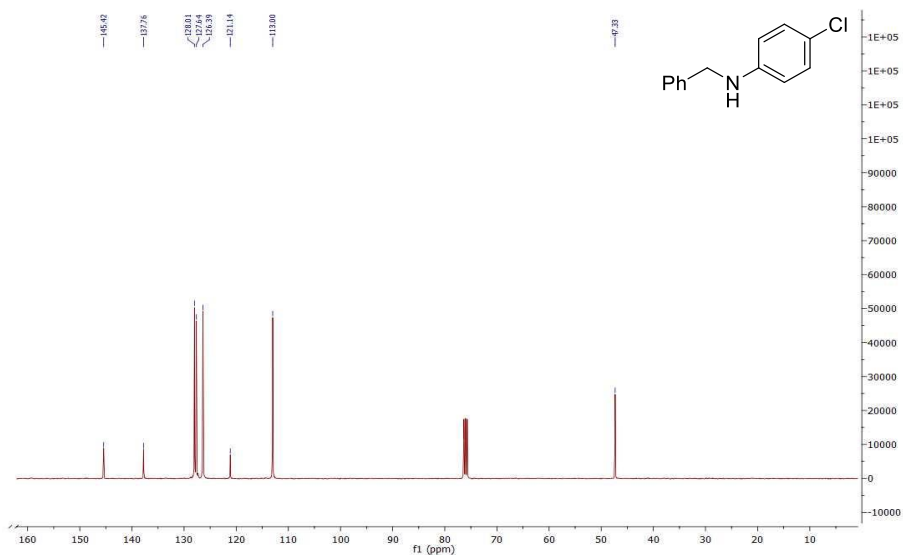


Figure 3.30 ^{13}C NMR (400 MHz) in CDCl_3 spectrum for N-benzyl-4-chloroaniline (table 2, entry 3)

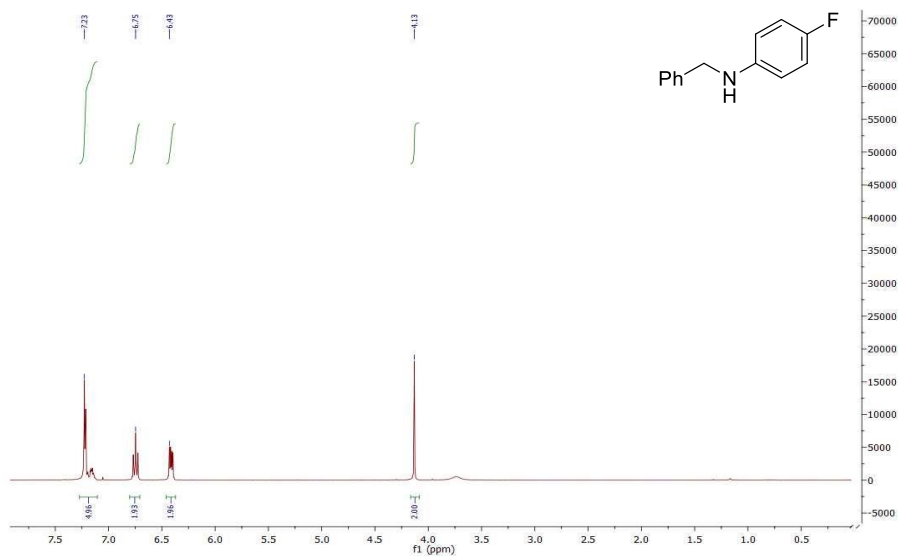


Figure 3.31 ¹H NMR (400 MHz) in CDCl₃ spectrum for N-benzyl-4-fluoroaniline (table 2, entry 4)

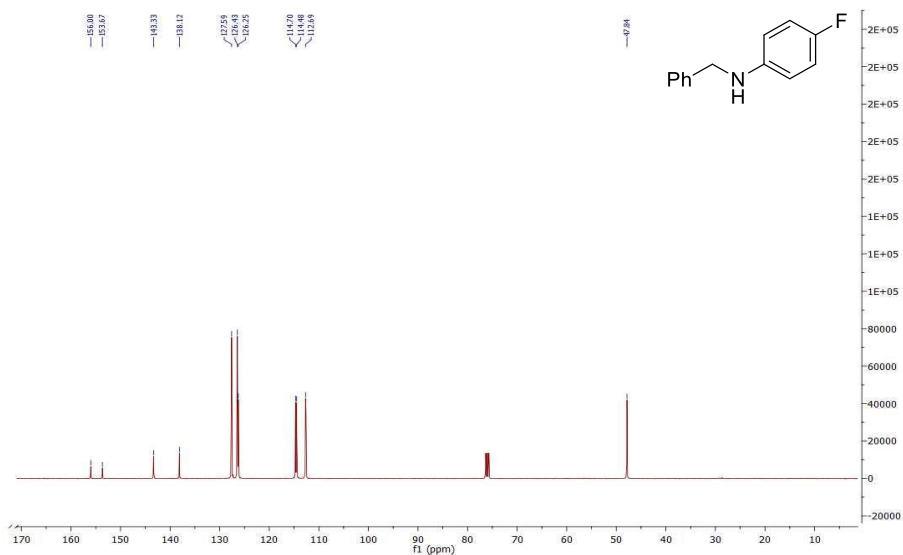


Figure 3.32 ¹³C NMR (400 MHz) in CDCl₃ spectrum for N-benzyl-4-fluoroaniline (table 2, entry 4)

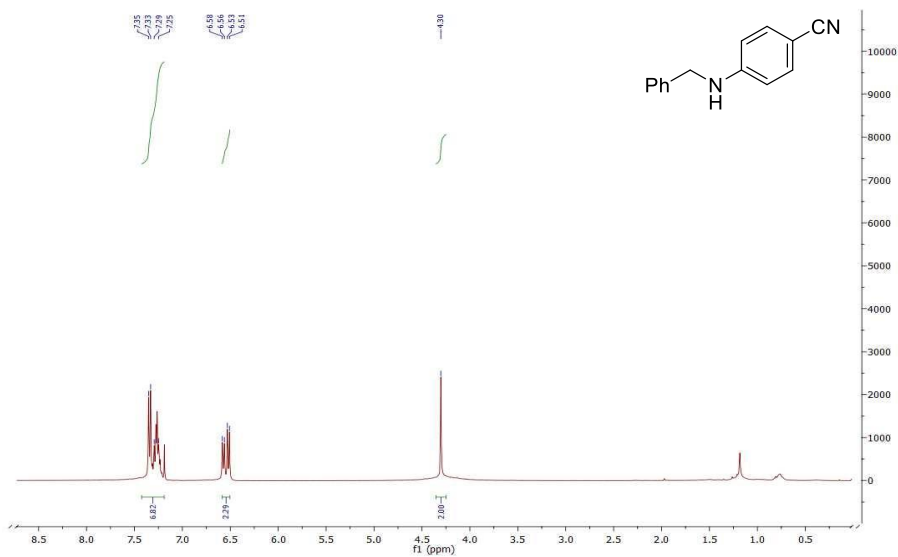


Figure 3.33 ^1H NMR (400 MHz) in CDCl_3 spectrum for 4-(benzylamino) benzonitrile (table 2, entry 5)

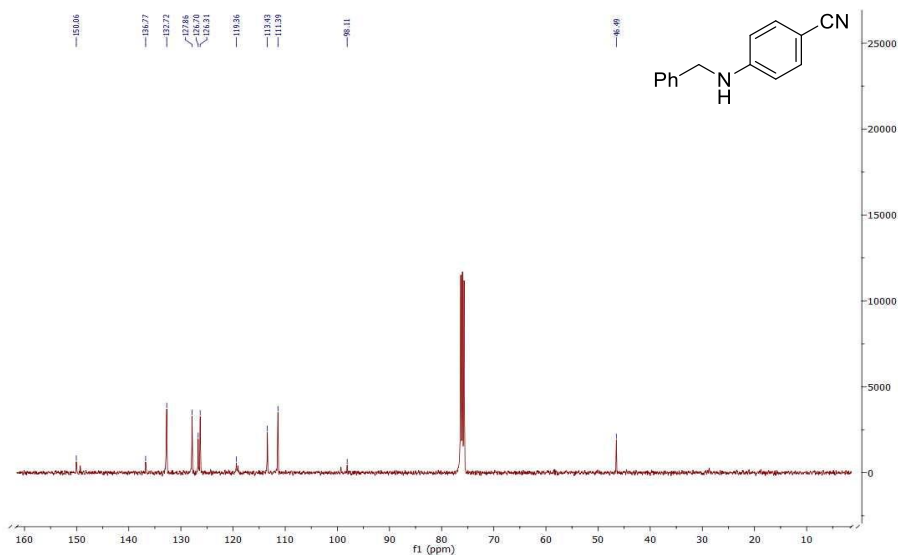


Figure 3.34 ^{13}C NMR (400 MHz) in CDCl_3 spectrum for 4-(benzylamino) benzonitrile (table 2, entry 5)

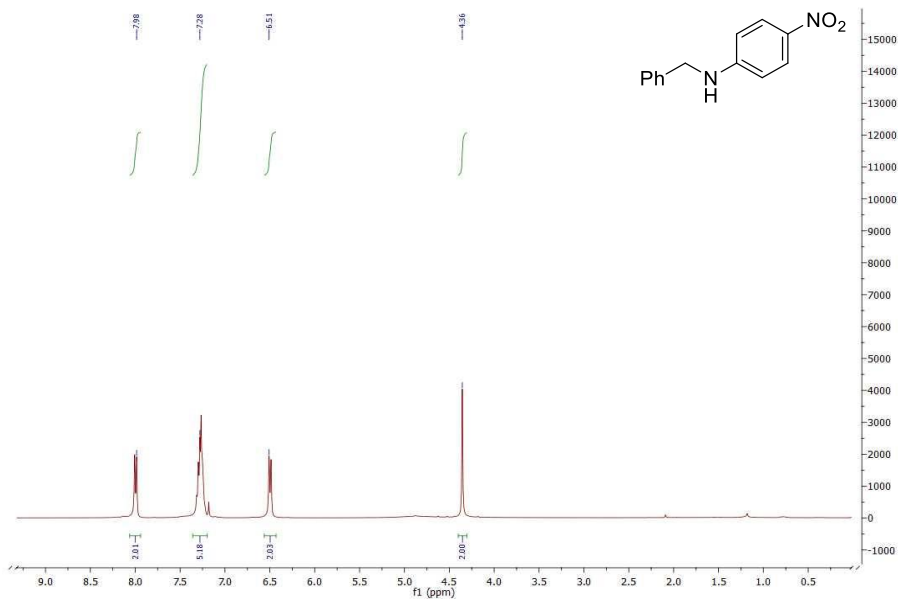


Figure 3.35 ¹H NMR (400 MHz) in CDCl₃ spectrum for N-benzyl-4-nitroaniline (table 2, entry 6)

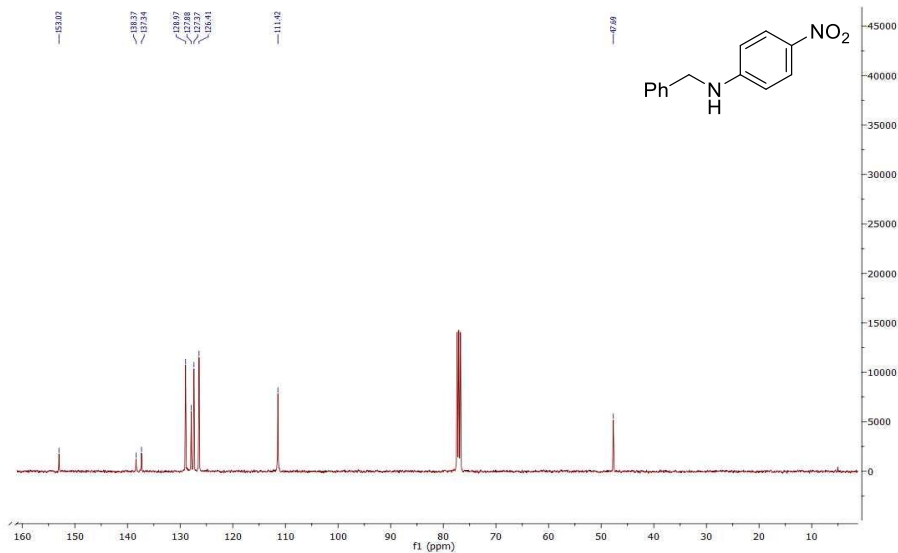


Figure 3.36 ¹³C NMR (400 MHz) in CDCl₃ spectrum for N-benzyl-4-nitroaniline (table 2, entry 6)

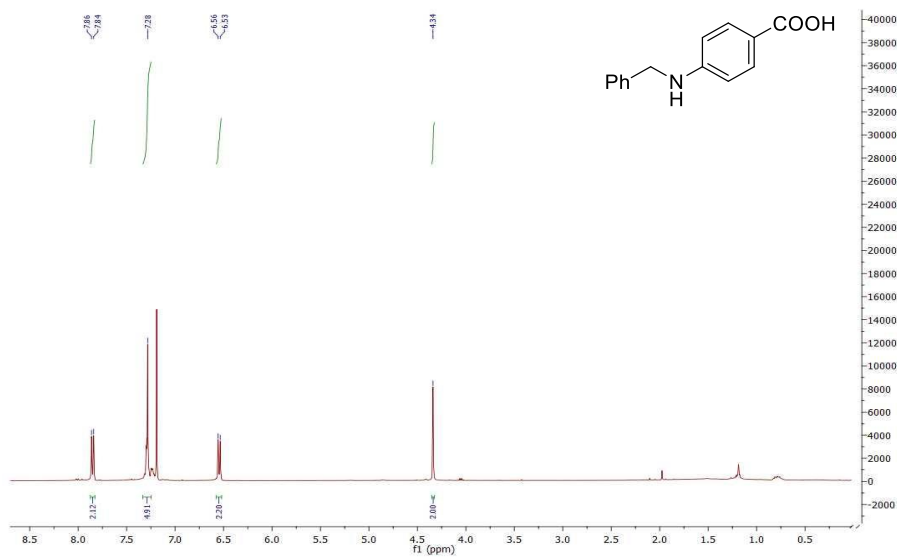


Figure 3.37 ¹H NMR (400 MHz) in CDCl₃ spectrum for 4-(benzylamino) benzoic acid (table 2, entry 7)

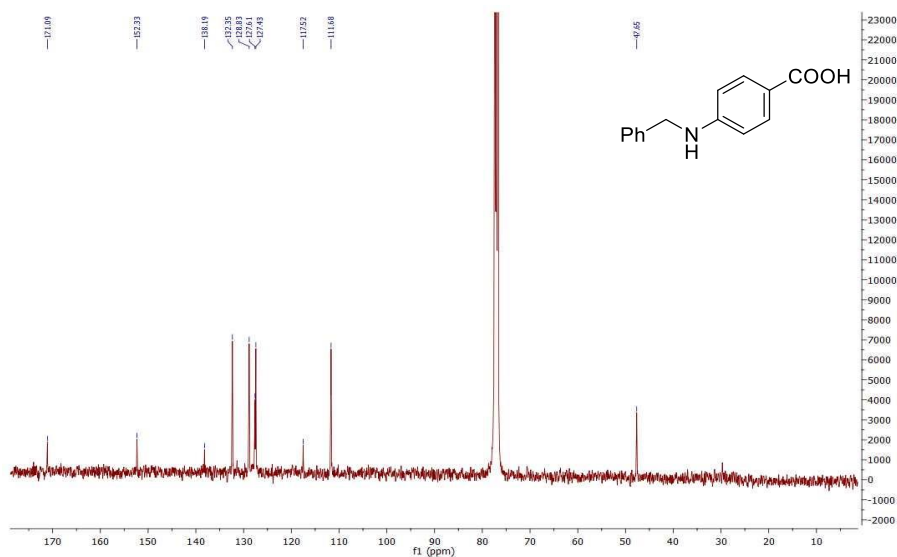


Figure 3.38 ¹³C NMR (400 MHz) in CDCl₃ spectrum for 4-(benzylamino) benzoic acid (table 2, entry 7)

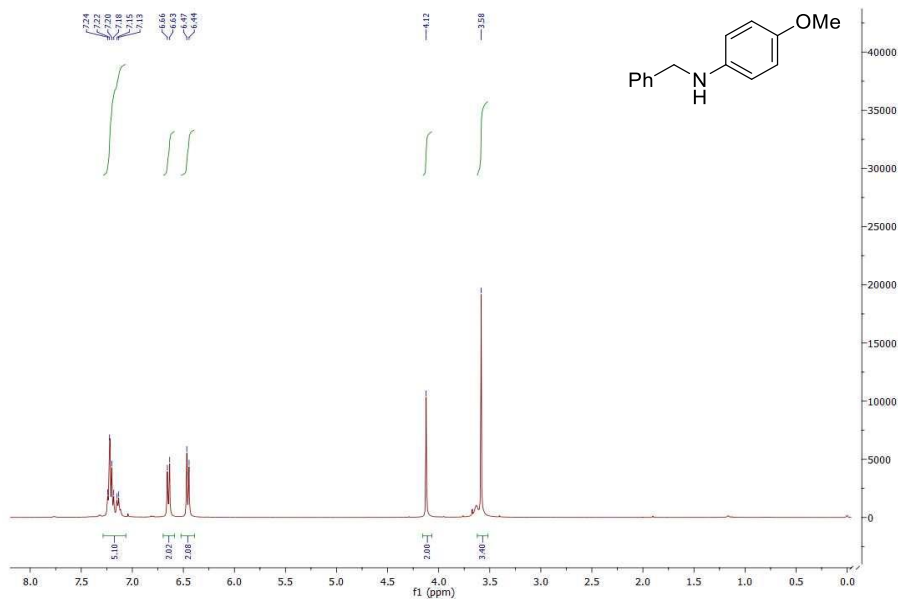


Figure 3.39 ¹H NMR (400 MHz) in CDCl₃ spectrum for N-benzyl-4-methoxyaniline (table 2, entry 8)

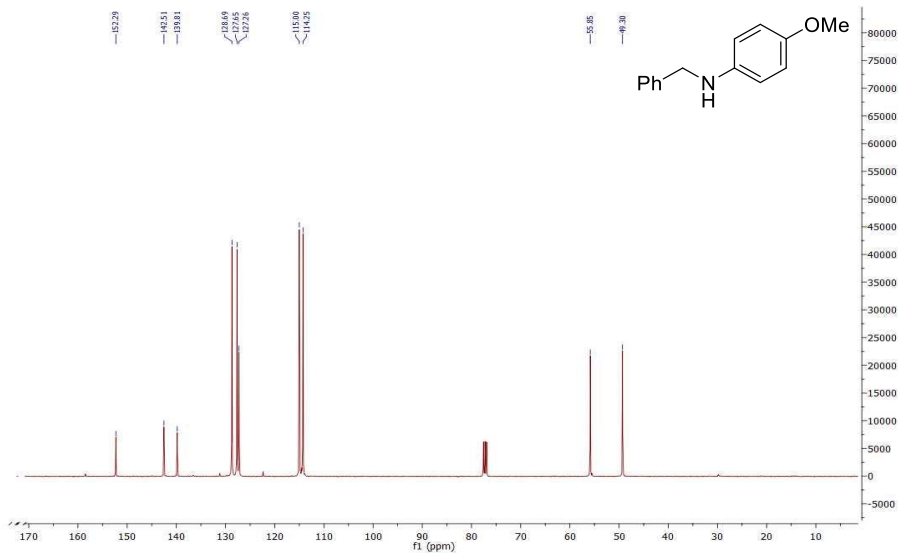


Figure 3.40 ¹³C NMR (400 MHz) in CDCl₃ spectrum for N-benzyl-4-methoxyaniline (table 2, entry 8)

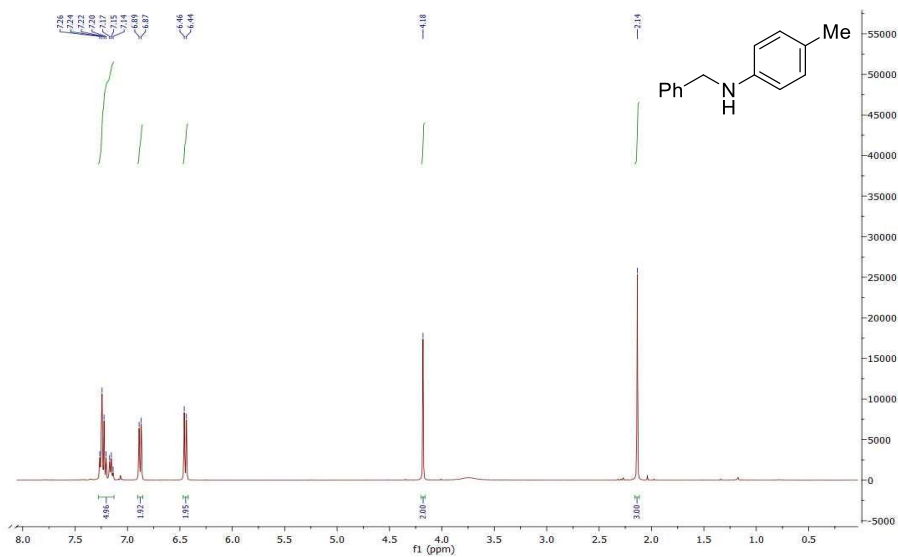


Figure 3.41 ^1H NMR (400 MHz) in CDCl_3 spectrum for Benzyl-4-tolyl-amine (table 2, entry 9)

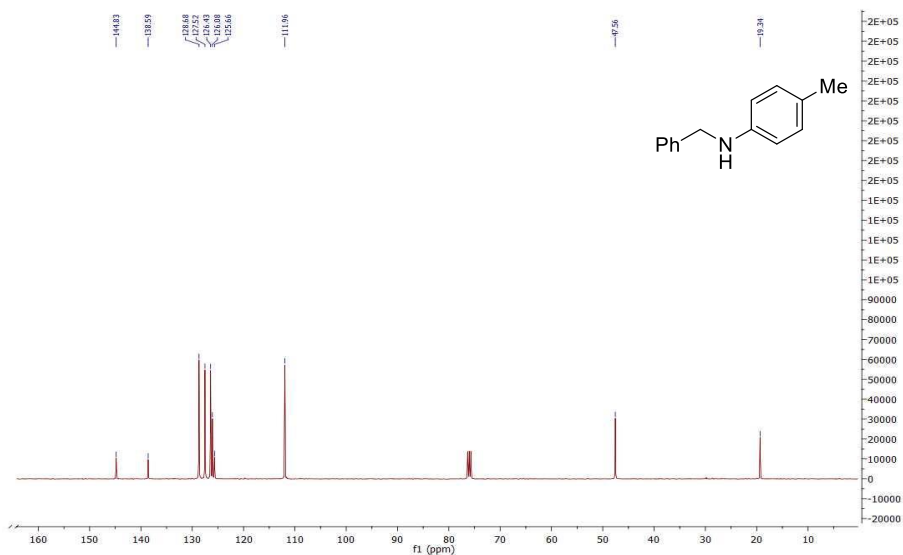


Figure 3.42 ^{13}C NMR (400 MHz) in CDCl_3 spectrum for Benzyl-4-tolyl-amine (table 2, entry 9)

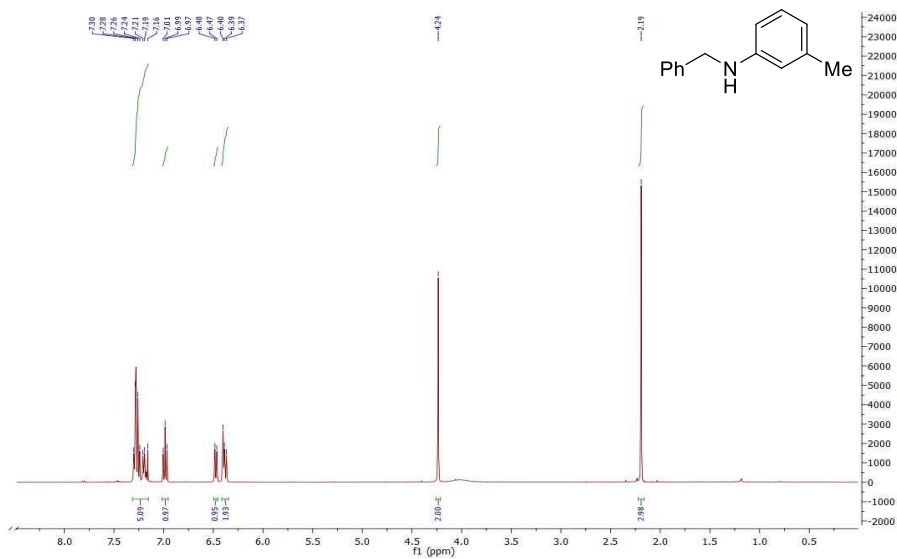


Figure 3.43 ¹H NMR (400 MHz) in CDCl₃ spectrum for Benzyl-3-tolyl-amine (table 2, entry 10)

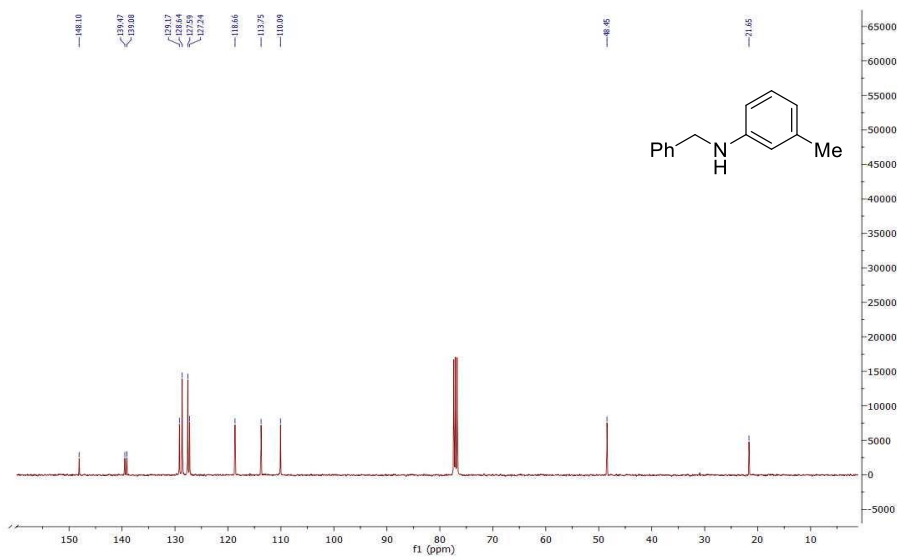


Figure 3.44 ¹³C NMR (400 MHz) in CDCl₃ spectrum for Benzyl-3-tolyl-amine (table 2, entry 10)

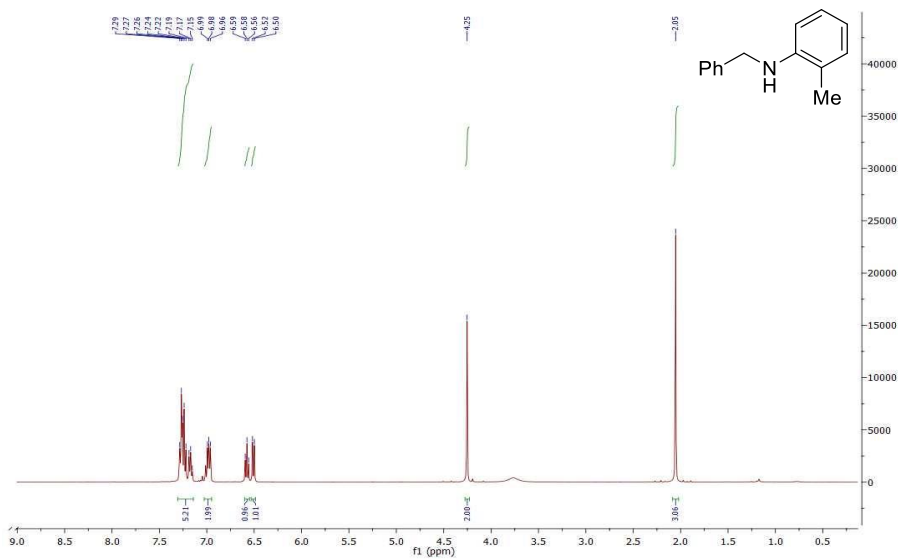


Figure 3.45 ^1H NMR (400 MHz) in CDCl_3 spectrum for Benzyl-2-tolyl-amine (table 2, entry 11)

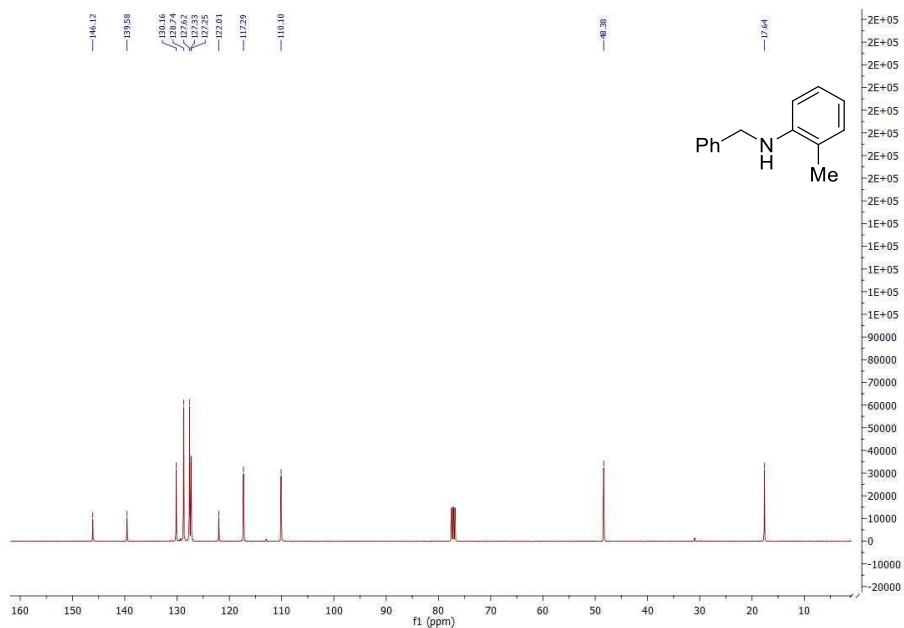


Figure 3.46 ^{13}C NMR (400 MHz) in CDCl_3 spectrum for Benzyl-2-tolyl-amine (table 2, entry 11)

3.7.6. NMR data for isolated products of table 3.3

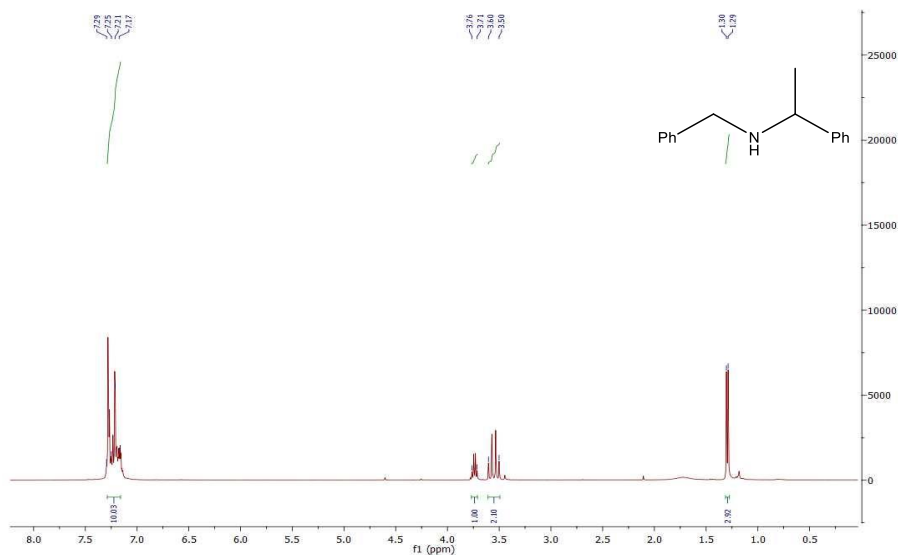


Figure 3.47 ¹H NMR (400 MHz) in CDCl₃ spectrum for N-(1-phenylethyl) aniline (table 3, entry 1)

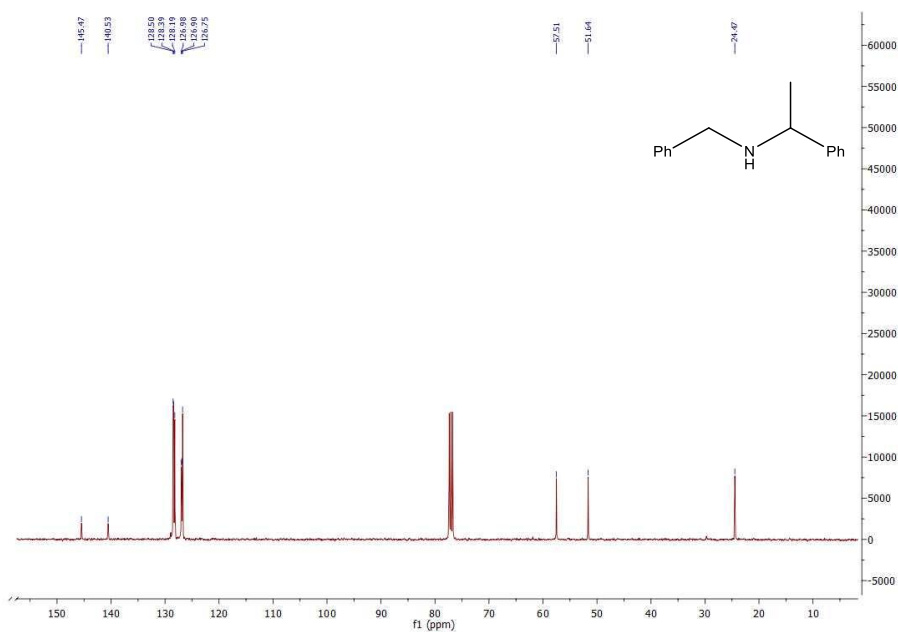


Figure 3.48 ¹³C NMR (400 MHz) in CDCl₃ spectrum for N-(1-phenylethyl) aniline (table 3, entry 1)

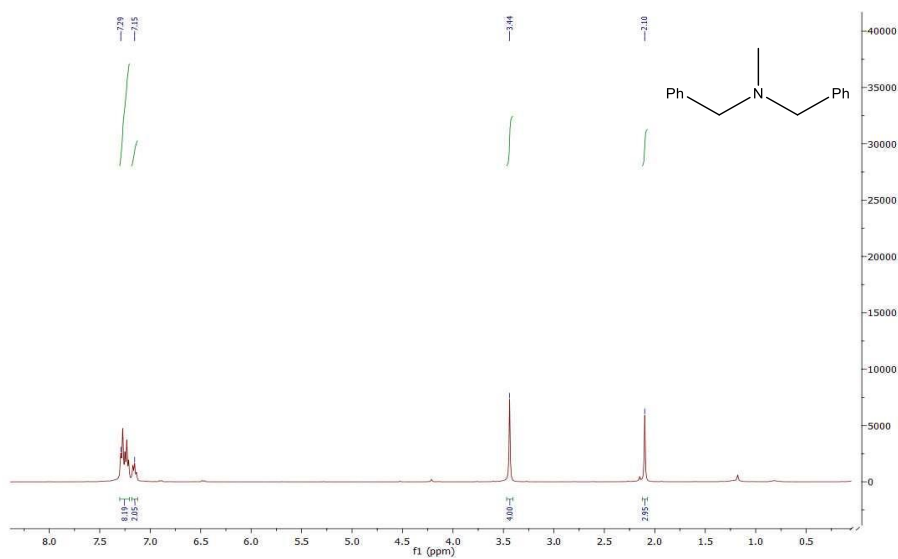


Figure 3.49 ^1H NMR (400 MHz) in CDCl_3 spectrum for N,N-dibenzylmethylamine (table 3, entry 2)

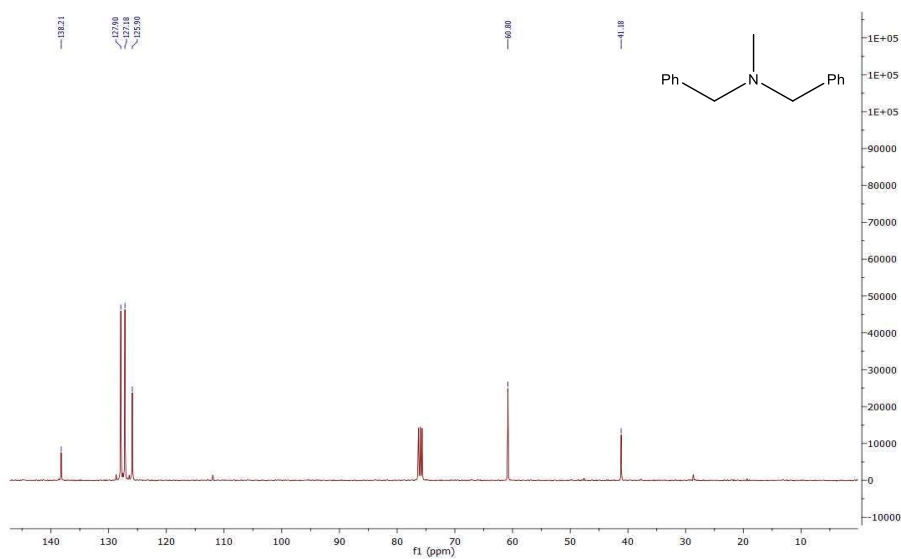


Figure 3.50 ^{13}C NMR (400 MHz) in CDCl_3 spectrum for N,N-dibenzylmethylamine (table 3, entry 2)

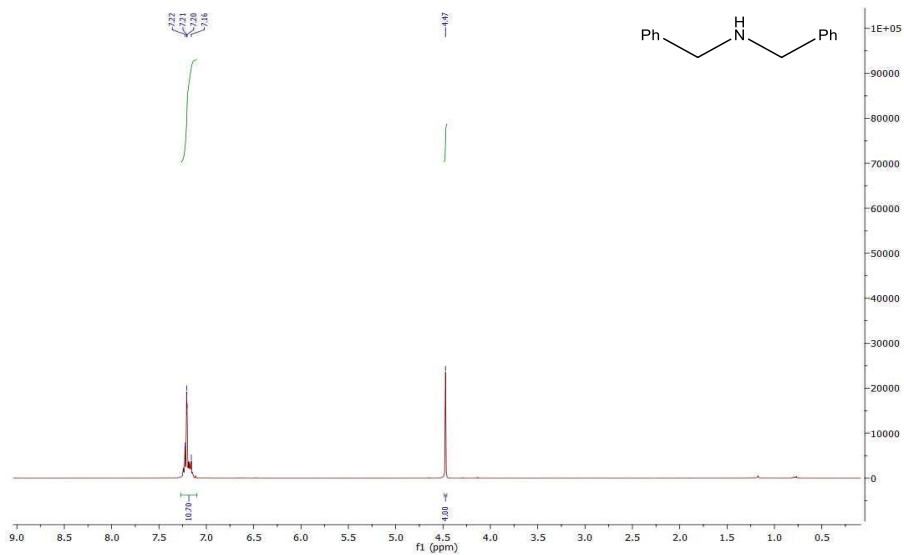


Figure 3.51 ¹H NMR (400 MHz) in CDCl₃ spectrum for Dibenzylamine (table 3, entry 3)

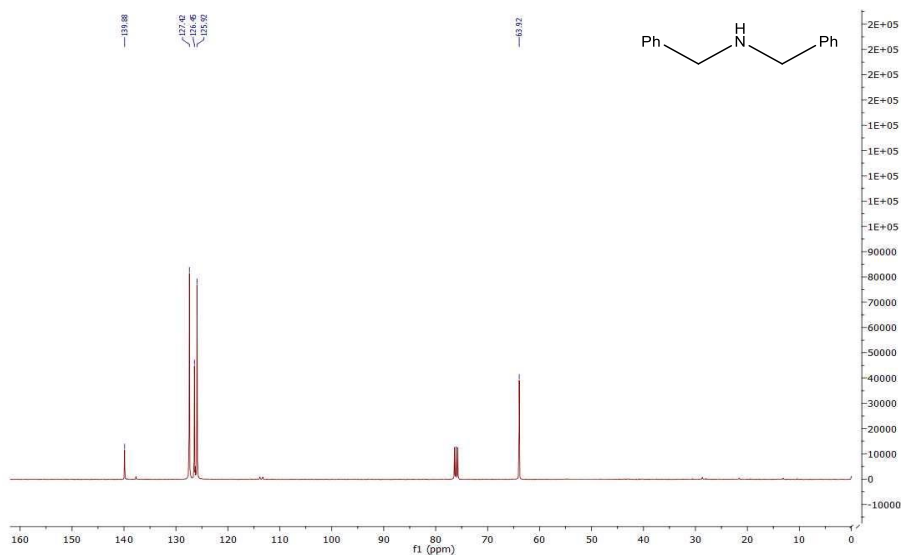


Figure 3.52 ¹³C NMR (400 MHz) in CDCl₃ spectrum for Dibenzylamine (table 3, entry 3)

3.7.7. NMR data for isolated products of table 3.4

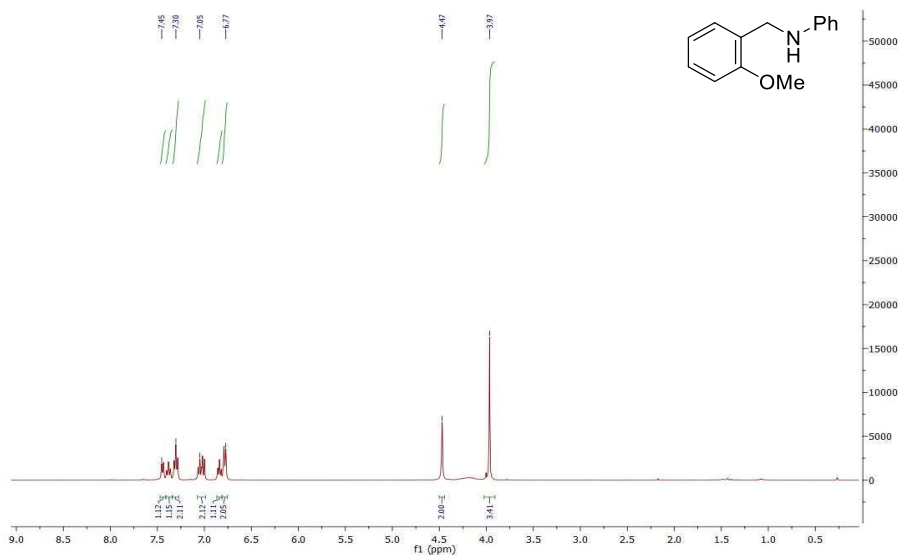


Figure 3.53 ^1H NMR (400 MHz) in CDCl_3 spectrum for N-(2-methoxybenzyl) aniline (table 4, entry 1)

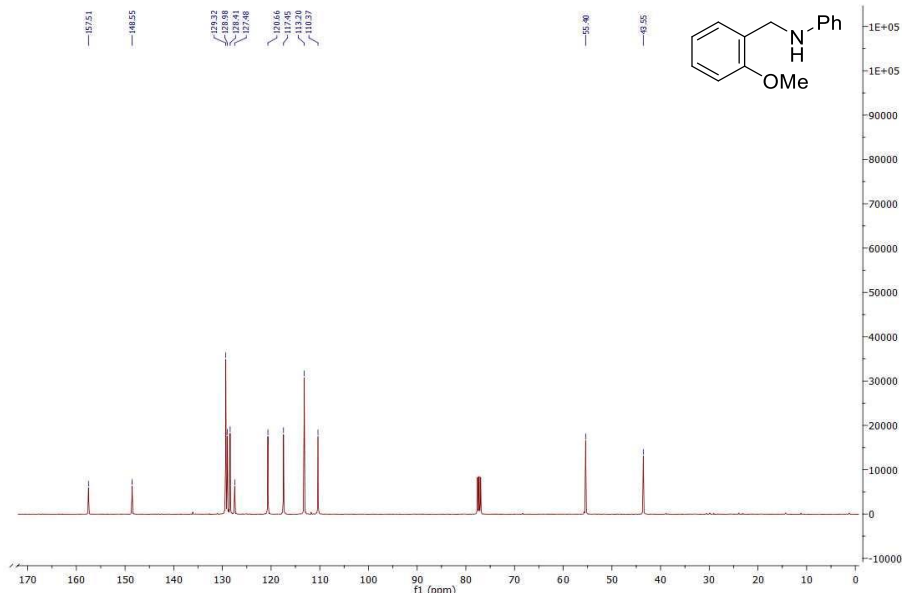


Figure 3.54 ^{13}C NMR (400 MHz) in CDCl_3 spectrum for N-(2-methoxybenzyl) aniline (table 4, entry 1)

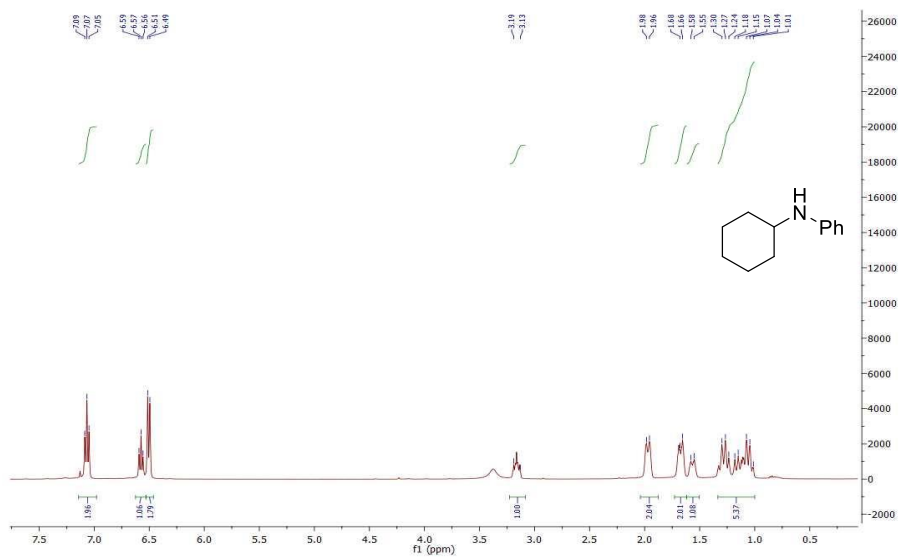


Figure 3.55 ¹H NMR (400 MHz) in CDCl₃ spectrum for N-cyclohexylaniline (table 4, entry 2)

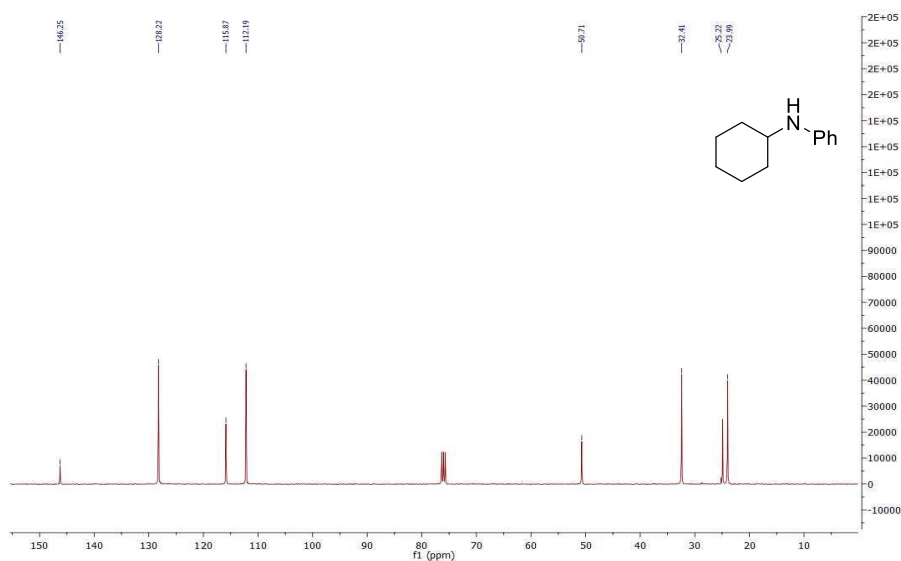


Figure 3.56 ¹³C NMR (400 MHz) in CDCl₃ spectrum for N-cyclohexylaniline (table 4, entry 2)

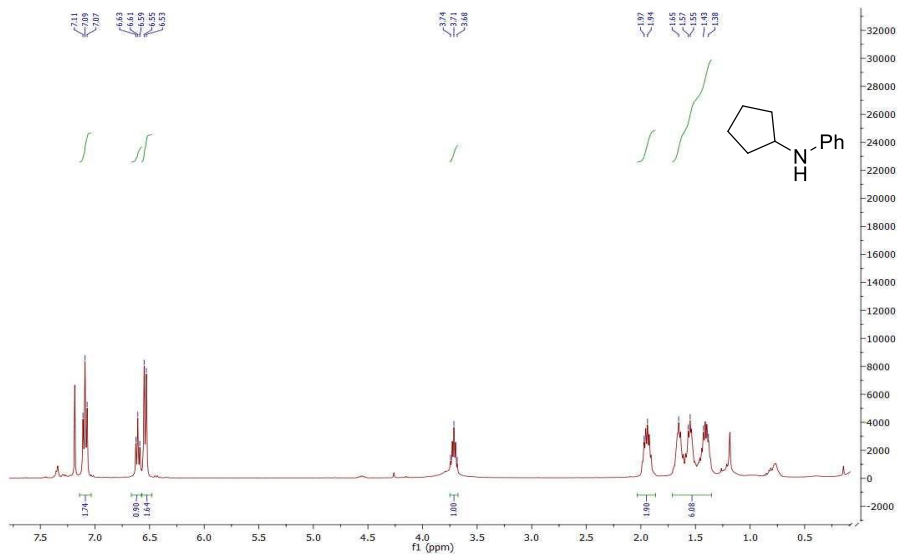


Figure 3.57 ^1H NMR (400 MHz) in CDCl_3 spectrum for N-cyclopentylaniline (table 4, entry 2)

Chapter 4

4. Half-sandwich iridium(III) complexes for the regeneration of NADH in the enzymatic reduction of MB9

Acknowledgements and contributions

Ana Fernandes performed all the experiments described in this chapter. Beatriz Royo and Lúgia O. Martins directed the research. M. C. Almeida is acknowledged for mass spectrometry (Research Facilities, ITQB-NOVA)).

4.1. Abstract

Several biotransformations of organic substrates by enzymes, for example azoreductases, that can be used in the treatment and valorization of azo dye rich wastewaters, are limited by the requirement of expensive exogenous cofactors, including NAD(P)H. Therefore, efficient methods capable to regenerate NAD(P)H from its reduced form, NA(P)D⁺, are highly sought in biocatalysis. This Chapter describes the development of a series of half-sandwich iridium(III) complexes that are active catalysts in the regeneration of NADH using formate anions as the source of hydrogen. Furthermore, it is demonstrated the combined action of iridium-based catalysts, involved in the NADH regeneration, with the enzymatic reduction of the model azo dye mordant black 9.

Half-sandwich iridium(III) complexes for the regeneration of
NADH in the enzymatic reduction of MB9 | 150

4.2. Introduction

The final chapter of this thesis describes the development of a catalytic system for *in-situ* regeneration of NADH under conditions that are compatible with the enzymatic reduction of the azo dye mordant black 9 (MB9). The combination of chemo and bio catalysis is very attractive from a synthetic and industrial point of view, since allows the production of valuable chemicals in an economical and eco-friendly manner ^[1,2].

To date, few examples are found in the literature describing the compatible use of enzymes and organometallic complexes. The vast majority of enzymes are not capable of maintaining an appropriate stability in the presence of organic solvents or at high temperatures and most organometallic complexes lose activity in aqueous media. Lipases and serine proteases are the only enzymes capable of maintaining activity in organic solvents and high temperatures ^[3]. These enzymes are mainly applied in dynamic kinetic resolution protocols where they have been successfully combined with palladium, rhodium and ruthenium based catalysts ^[4]. Due to the high activity and selectivity achieved with this approach, this methodology has been largely employed in the production of enantiomerically pure alcohols and amines on an industrial scale. In contrast, the development of cooperative chemo-enzymatic reactions in aqueous solutions is still in its infancy. The main reactions studied are metathesis or

hydrogenation reactions [2]. The noteworthy work of Hartwig and co-workers reported the tandem chemoenzymatic alkene metathesis with enzymatic epoxidation yielding aryl epoxides in aqueous solution [1]. This work highlighted the significant improvement that can be achieved through tandem chemoenzymatic reactions, obtaining moderated yields and excellent selectivities.

The aim of the present study is to develop an organometallic catalyst for NADH regeneration that can be used *in situ* with the enzymatic reduction of azo dyes mediated by PpAzoR. The azoreductase PpAzoR is an FMN-dependent enzyme with demonstrated high activity in the reduction of structurally diverse azo dyes that requires NAD(P)H as electron donor (Chapter 2) [5,6]. The use of protein engineering can enhance the compatibility of enzymes to harsh industrial methodologies. In this way, a more stable and active mutant of PpAzoR, 2A1-Y179H was obtained through directed evolution [7] and was utilized in this study.

In recent years, different methodologies have been described in the literature for the conversion of NAD⁺ into NADH, including enzymatic, photo- and electrochemical and homogeneous catalytic regeneration [8,9]. The use of the organometallic complexes in NADH regeneration is still scarcely explored. Most of the work found in the literature is based on half-sandwich complexes of rhodium, ruthenium, and iridium [10–15].

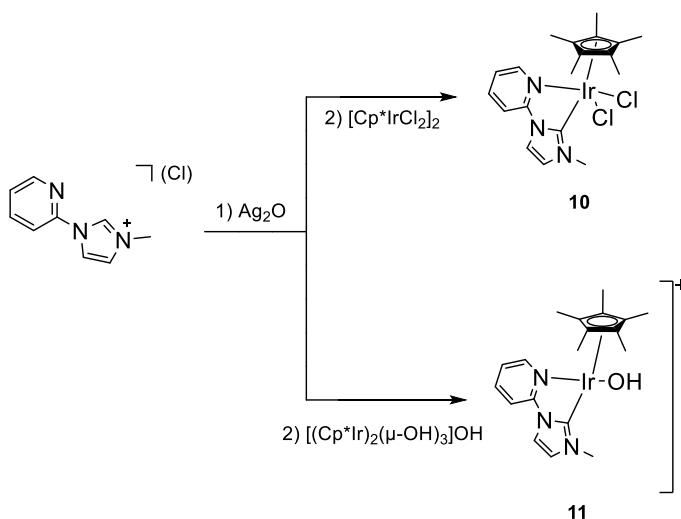
The rhodium catalysts, specifically $[\text{Cp}^*\text{Rh}(\text{bpy})(\text{H}_2\text{O})]^{2+}$, are highlighted due to their regioselectivity and versatility ^[16]. Furthermore, its compatibility with enzymatic reactions has been studied, which unfortunately revealed the mutual inactivation of the enzymatic and rhodium catalysts ^[17]. Although the majority of the studies for the regeneration of NADH ^[11,12,16–19] have been performed with rhodium, recent studies using iridium have demonstrated the potential of this metal in this type of reaction ^[14,15,18]. Interestingly, Macchioni and co-workers demonstrated the excellent performance of the iridium complex $[\text{Cp}^*\text{Ir}(\text{pica})\text{Cl}]$ (pica = picolinamidate) in the regeneration of NADH in aqueous solution ^[15]. They disclosed an improved iridium catalyst with a TOF (turnover frequency) three times higher than the fastest iridium catalyst reported in 2012 by Fukuzumi and co-workers ^[14]. Furthermore, they demonstrated the beneficial effect of NH-functionality on the intermolecular hydrogen bonding between the HCOO^- and the catalyst.

Based on these results, we decided to explore the development of half sandwich iridium(III) complexes bearing NHC and mixed NHC pyridine ligands prepared in this thesis and the iridium complex $[\text{Cp}^*\text{Ir}(2,2'\text{-bipyridyl})\text{OH}]^+$ ^[20], for the catalytic regeneration of NADH. The most efficient catalyst was further studied for the *in situ* regeneration of NADH coupled with the reduction of MB9 catalyzed by PpAzoR.

4.3. Results and Discussion

4.3.1. Synthesis and characterization

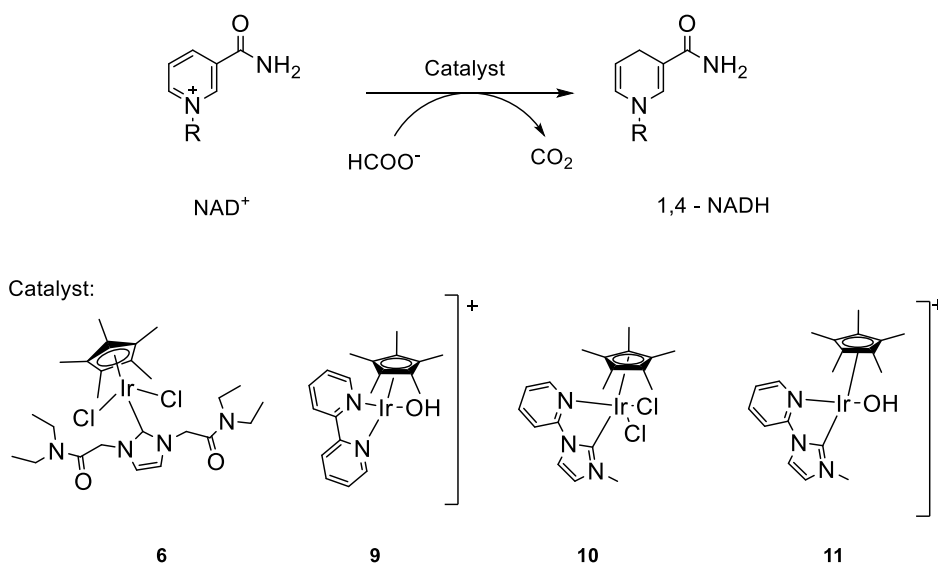
The NHC ligand precursors and the iridium(III) complexes **6** and **9** were synthesized following the procedures described in the literature [20–23]. The synthesis of the new iridium(III) complexes **10** and **11** is depicted in Scheme 4.1. All complexes were characterized by NMR spectroscopy and mass spectrometry (HRMS-ESI). The ^{13}C NMR spectra of **10** and **11** showed resonances at 165.5 and 167.9 ppm, respectively, attributed to the Ir-C_{carbene}, confirming the coordination of the NHC ligand to iridium.



Scheme 4.1 Synthesis of iridium(III) NHC complexes **10** and **11**.

4.3.2. Catalytic NADH regeneration

In previous work, we showed that complex **6** is an effective catalyst for hydrogen transfer reactions. In particular, we demonstrated its catalytic efficiency in the alkylation of amines with alcohols ^[23]. Based on these results, we become interested in exploring the activity of **6** and related bipyridine and mixed NHC-pyridine iridium complexes (**9-11**) in the reduction of NAD⁺ through transfer hydrogenation using formate as hydrogen donor (Scheme 4.2).



Scheme 4.2 Conversion of NAD⁺ to NADH catalyzed by complexes **6** and **9-11** in aqueous solution with sodium formate as hydrogen donor

The conversion of NAD⁺ to NADH was conducted at 45°C in D₂O and monitored by ¹H NMR, following both the formation of NADH and the consumption of NAD⁺. Complexes **6** and **10** were treated with 2 equivalents of AgBF₄ prior to use, generating complexes **6**⁺ and **10**⁺ *in*

situ. In a typical experiment, D₂O solutions of the appropriate complex **6**⁺, **9**, **10**⁺ or **11**, sodium formate and NAD⁺ were mixed in an NMR tube with a ratio of 1: 100: 5.5, complex: formate: NAD⁺. The initial pH of the reaction mixtures was between 6.8-7.2. The kinetic profile of the reactions showed no induction period for all iridium catalysts tested, indicating the rapid formation of the active species (Figure 4.1). Complexes **9** and **11** resulted to be the most active catalysts, achieving quantitative conversions in 4 and 6 h, respectively. When the catalytic reaction was performed using complexes **6**⁺ and **10**⁺, lower reaction rates were observed. Moreover, their kinetic profiles exhibited a plateau after an initial reaction period (at 54 % and 42 % conversions for **6**⁺ and **10**⁺, respectively) (Figure 4.1).

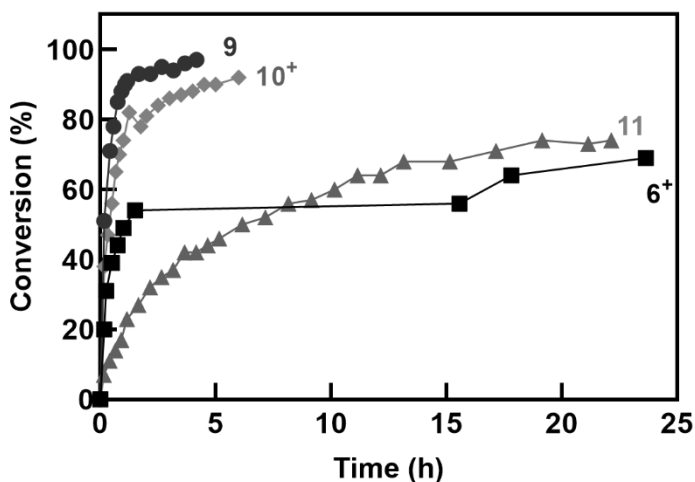


Figure 4.1 Kinetic profile of the conversion of NAD⁺ to NADH (2.5 mM) with formate (46 mM) as electron donor catalyzed by complex **6**⁺, **9-11** (0.46 mM).

Table 4.1 Conversion of NAD⁺ to NADH catalyzed by Ir-NHC complexes **6** and **9-11**.

Entry ^[a]	Catalyst	Loading (mol %)	Conversion (%) (time, h) ^[b]	TOF (h ⁻¹) ^[c]	Ir-H (ppm)
1	6 ⁺	16	69 (24)	3.1	-16.3
2	9	16	97 (4)	19.0	-11.2
3 ^[d]	9	16	78 (16)	2.7	-
4 ^[e]	9	8	78 (4)	6.2	-
5 ^[f]	9	1.6	12 (24)	-	-
6 ^[g]	9	0.4	0 (32)	-	-
7	10 ⁺	16	74 (22)	0.5	-14.6
8	11	16	92 (6)	8.8	-14.6

[a] Reaction conditions: catalyst (0.46 mM), sodium formate (46 mM) and NAD⁺ (2.5 mM) (molar ratio 1:100:5.5, catalyst: formate: NAD⁺), D₂O (0.6 μL), 45°C. [b] Conversion determined by ¹H NMR. [c] Calculated for 50 % of conversion. [d] Reaction with molar ratio of 1:25:5.5 [e] Reaction with molar ratio of 1:100:11 [f] Reaction with molar ratio of 1:100:62. [g] Reaction with molar ratio of 1:100:125.

The turnover frequencies for catalysts **6**⁺, **9-11** were determined at 50% conversion of NAD⁺ to NADH (Table 4.1). The turnover frequencies increased in the order **10**⁺ < **6**⁺ < **11** < **9**. The most active complex was [Cp*Ir(2,2'-bipyridyl)OH]⁺ (**9**) with a TOF value of 19.0 h⁻¹ producing exclusively 1,4-NADH. The isomer 1,6-NADH (enzymatically inactive)

is increasingly formed in the order $11 < 10^+ < 6^+$, in a 6, 16 and 23 % conversion respectively. These results clearly indicated a loss in activity when an NHC ligand is introduced into the coordination sphere of the metal.

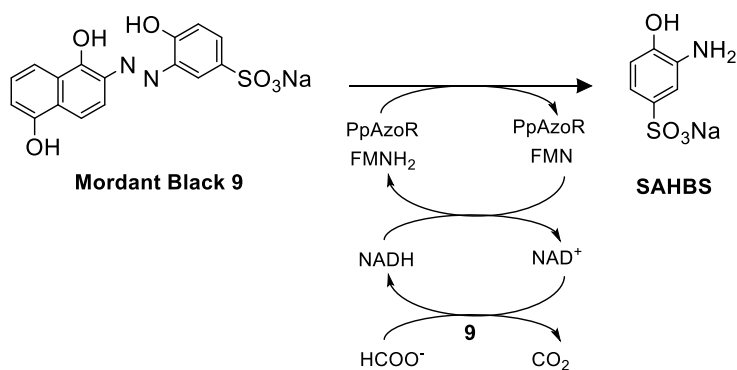
The acquisition of an NMR spectrum for each complex in the presence of equivalent amounts of formate confirmed the rapid appearance of an Ir-hydride species, formed by the hydrogen transfer from the formate molecule. The characteristic resonance of the Ir-H proton was observed in the ^1H NMR spectra at -11 to -17 ppm region (Table 4.1). The Ir-H bond is in a more shielded environment in the complexes, in the order $9 < 11 = 10^+ < 6^+$, reflecting the higher electron density on the metal center when NHC ligands are present. This is in accordance with their strong σ -donation properties.

After selecting the most efficient catalyst, complex **9**, different molar ratios to formate were tested in order to optimize the reaction conditions. When a ratio of 1:25 (complex: formate) was used, the TOF decreased almost 10-fold (Table 4.1, Entry 3), indicating a dependence for the hydride source. Soldevila-Barreda and co-workers ^[24] have demonstrated that NADH regeneration catalyzed by a Cp^*Rh complex was also dependent on the complex: formate ratio exhibiting a typical Michaelis-Menten behavior. In addition, when the catalyst loading was gradually decreased (from 16 to 0.4 mol %) a gradually decrease in

catalytic activity was observed (Table 4.1, Entry 4-6). Therefore, the optimized ratio 1: 100: 5.5 (complex: formate: NAD^+) was established.

4.3.3. Chemoenzymatic reduction of Mordant Black 9

As demonstrated in Chapter 2, mordant black 9 (MB9) is reduced by the action of PpAzoR in the presence of equimolar quantities of the co-factor NADH originating the aromatic amine SAHBS (Scheme 4.3). It was also expected the formation of a second aromatic amine (2-aminonaphthalene-1,5-diol), but it was not detected by NMR or HPLC. Probably, 2-aminonaphthalene-1,5-diol was initially formed, but it degraded due to its autoxidation forming oligomeric compounds upon exposure to oxygen ^[25,26].



Scheme 4.3 Organometallic NADH regeneration for the azo-reduction of azo dyes by PpAzoR.

The external addition of NADH to this reaction increases its costs, reducing the applicability of this methodology in an industrial context. So, we were interested in studying the viability of coupling the enzymatic reduction of MB9 with the catalytic regeneration of NADH mediated by an iridium complex. Therefore, the enzymatic reduction of MB9 was performed in the presence of complex **9** and sodium formate for the regeneration of the NADH (Scheme 4.3).

In the control reactions using equimolar quantities of commercial NADH, MB9 was reduced in 24 h yielding 80 % of SAHBS (as quantified by HPLC). When applying the iridium-based catalytic system for the regeneration of NADH, the reduction of MB9 takes 72 h yielding 59 % of SAHBS. The slower azo bond cleavage can be due to some loss in activity of the catalytic systems since mutual inactivation is a recurrent problem in the utilization in one-pot of organometallic and biocatalysts ^[2].

To understand better the observed loss of activity of PpAzoR, the stability of PpAzoR in the presence of complex **9** and sodium formate was studied. Purified enzyme preparations were incubated at 45°C in the presence of different concentrations of complex **9** and formate (molar ration 1:100, complex: formate). Aliquots were taken over time and the enzymatic activity was determined monitoring the consumption

of NADH at 340 nm on the standard reaction of AQS reduction. The half-life ($t_{1/2}$) of PpAzoR in the presence of complex **9** and formate was calculated (Table 4.2). It was observed that under the optimal conditions for the organometallic activity, the enzyme loses half of its activity in 0.7 h (Table 4.2, Entry 1). In order to maintain enzymatic activity for longer periods of time, concentrations lower than 0.02 mM of complex **9** and 2 mM of formate should be used (Table 4.2, Entry 5,6).

Table 4.2 PpAzoR half-life after incubation with catalyst **9** and sodium formate in 100 mM sodium phosphate pH 7 at 45°C.

Entry ^[a]	Catalyst (mM)	Formate (mM)	Half-life (h)
1	0.4	40	0.7
2	0.2	20	1
3	0.04	4	2
4	0.03	3	4
5	0.02	2	23
6	0.01	1	53
7	-	-	56

Considering the PpAzoR stability parameters in the presence of different concentrations of complex **9** and formate, assays were conducted using a lower amount of the organometallic regenerating system (0.04 and 0.02 mM of **9**). However, under these conditions, the enzymatic reduction of MB9 was not successful, since no decolorization was observed and no SAHBS detected. Despite these are preliminary studies, and further optimization of the system is needed, the results obtained are very promising and demonstrate the potential of this organometallic regenerating system for the development of reductive enzymes in industrial processes.

4.4. Conclusion

This work describes the catalytic activity of a series of half-sandwich iridium(III) complexes in the regeneration of NADH. The most active one, $[\text{Cp}^*\text{Ir}(\text{2,2}'\text{-bipyridyl})\text{OH}]^+$ (**9**) selectively produces 1,4-NADH with a TOF of 19.0 h^{-1} . The enzymatic reduction of MB9 by PpAzoR and the orthogonal regeneration of NADH by catalyst **9** was performed in one-pot producing 59% of SABHS in 72 h. Although with some loss in activity, it was demonstrated that PpAzoR and complex **9** can work in a cooperative manner under enzymatic conditions (0.1 mM sodium phosphate buffer pH 7).

4.5. Experimental Section

4.5.1. General Information

Compounds $[\text{Cp}^*\text{IrCl}_2]_2$ [27], $[(\text{Cp}^*\text{Ir})_2(\mu\text{-OH})_3]\text{OH}$ [28], **6** [23], **9** [20], and 1-(2-pyridyl)-2-methylimidazole [22], were synthesized according to literature procedures. All other reagents were purchased from commercial suppliers and used without further purification. ^1H and ^{13}C NMR spectra were recorded on a Bruker Avance III 400 MHz. Assignment of resonances was made from HMQC and HMBC experiments.

Preparation and characterization of 10. Silver oxide (0.12 g, 0.5 mmol) was added to a solution of 1-(2-pyridyl)-2-methylimidazole (0.2 g, 0.7 mmol) in dichloromethane (15 mL). The suspension was stirred at room temperature for 1 h in the dark. $[\text{Cp}^*\text{IrCl}_2]_2$ (0.28 g, 0.35 mmol) was added, and the reaction mixture was stirred at room temperature overnight. The suspension was filtered through Celite, and the solvent was evaporated. ^1H NMR (298 K, 400 MHz, CDCl_3): δ = 9.02 (s, 1H, NCHCHN), 8.93 (d, 1H, CHPy), 8.50 (d, 1H, CHPy), 8.15 (t, 1H, CHPy), 7.46 (s, 1H, NCHCHN), 7.43 (t, 1H, CHPy), 4.07 (s, 3H, NCH_3), 1.80 (s, 15H, CH_3Cp^*); ^{13}C NMR (298 K, 400 MHz, CDCl_3): δ = 165.5 (NHClr), 152.9 (NCNPy), 149.7 (CHPy), 142.7 (CHPy), 125.8 (NCHCHN), 124.0 (CHPy), 119.7 (NCHCHN), 114.7 (CHPy), 92.23

(ArCp*), 37.8 (NCH₃), 9.75 (CH₃Cp*); MS (ESI-TOF) in acetonitrile: m/z: calcd for [C₁₉H₂₄N₃ClIr]⁺: 522.13 [M]⁺; found: 522.12666.

Preparation and characterization of 11. Silver oxide (0.09 g, 0.38 mmol) was added to a solution of 1-(2-pyridyl)-2-methylimidazole (0.14 g, 0.5 mmol) in water (5 mL). The suspension was stirred at RT for 1 h in the dark. [(Cp*Ir)₂(μ-OH)₃]OH (0.25 mmol) was prepared in situ and added, and the reaction mixture was stirred at RT overnight. The suspension was filtered through Celite, and the solvent was evaporated. ¹H NMR (298 K, 800 MHz, D₂O): δ = 8.97 (d, 1H, CHPy), 8.09 (t, 1H, CHPy), 7.87 (d, 1H, NCHCHN), 7.82 (d, 1H, CHPy), 7.45 (t, 1H, CHPy), 7.38 (d, 1H, NCHCHN), 4.02 (s, 3H, NCH₃), 1.64 (s, 15H, CH₃Cp*); ¹³C NMR (298 K, 800 MHz, D₂O): δ = 167.9 (NHClr), 152.7 (NCNPy), 149.8 (CHPy), 142.0 (CHPy), 125.4 (NCHCHN), 123.8 (CHPy), 116.6 (NCHCHN), 111.7 (CHPy), 92.22 (ArCp*), 37.2 (NCH₃), 8.20 (CH₃Cp*); MS (ESI-TOF) in acetonitrile: m/z: calcd for [C₁₉H₂₄N₃Ir]⁺: 486.16 [M]⁺; found: 486.15024; [C₁₉H₂₅N₃OIr]⁺: 504.16 [M]⁺; found: 504.16056.

4.5.2. Catalytic NADH regeneration

Complexes **6**, **9-11** were dissolved in D₂O (1.4 mM). Complex **6** and **10** were first treated with 2 mol equiv. of silver tetrafluoroborate, the mixture was filtered through celite.

Solutions of sodium formate (100mM) and NAD⁺ (7.7 mM) were also prepared in D₂O. Aliquots of complex, formate and NAD⁺ were added to a 5 mm NMR tube, for a total reaction volume of 0.6 mL, different molar ratios were studied. ¹H NMR spectra were recorded at 45°C over time until completion of the reaction.

Molar ratios of substrate and product were determined by integration peaks for NAD⁺ (9.33 ppm) and 1,4-NADH (6.96 ppm). The turnover number (TON) was calculated for the end of each reaction as follows:

$$\text{TON} = \frac{\text{moles of 1,4 NADH}}{\text{moles of catalyst}}$$

4.5.3. Azoreductase (PpAzoR) stability assays

Purified enzyme preparations, complex **9** (0.01 - 0.46 mM) and sodium formate (1 - 46 mM) were incubated at 45 °C in sodium phosphate buffer (0.1mM, pH 7), and, over time, sample aliquots were withdrawn and tested for activity. Residual activities were determined at room temperature using AQS as the substrate in the presence of 0.25 mM 1,4-NADH in sodium phosphate buffer (0.1mM, pH7). The reactions were followed by monitoring the decrease in absorbance of 1,4-NADH at 340 nm ($\epsilon_{340} = 6,220 \text{ M}^{-1}\text{cm}^{-1}$) on a Synergy 2, Biotek microplate reader.

4.5.4. Chemoenzymatic reduction of Mordant Black 9

The enzymatic azo reduction of MB9 (2.5 mM) reactions were carried out in sodium phosphate buffer (0.1 mM, pH 7) at 45°C with 5 U mL⁻¹ of PpAzoR, in the presence of NAD⁺ (2.5 mM) and complex **9** (0.2 mM) and sodium formate (20 mM). The reactions without complex **9** and sodium formate were performed with 1,4-NADH (2.5 mM) instead of NAD⁺. The reactions were followed by UV-Vis at 550 nm (MB9 maximum wavelength). The final product was identified and quantified by HPLC on a Waters Alliance 2695 equipped with a Waters photodiode array detector. The separations were performed in a Purospher STAR RP-18e column (250 x 4 mm), 5 µm particle size (Merck, KGaA, Germany). The injection volume was 60 µl, the flow rate, 0.8 mL min⁻¹, at a column oven temperature of 40°C. The eluent A, was 0.1 M ammonium acetate pH 6.7, and the eluent B was a mixture of methanol:acetonitrile (70:30, v/v). The following gradient was used for products separation: 0-2 min - isocratic elution of 100% eluent A; 2-16 min - linear gradient from 100% to 60% of eluent A; 16-24 min - linear gradient from 60% to 45% of eluent A; 24-28 min - linear gradient from 45% to 20% of eluent A; 28-32 min - isocratic elution of 20% eluent A; 32-30 min - linear gradient from 20% to 100% of eluent A; 33-43 min - equilibrium to the initial conditions of the following injection.

4.6. References

- [1] C. A. Denard, H. Huang, M. J. Bartlett, L. Lu, Y. Tan, H. Zhao, J. F. Hartwig, *Angew. Chemie - Int. Ed.* **2014**, *53*, 465–469.
- [2] Y. Wang, H. Ren, H. Zhao, *Crit. Rev. Biochem. Mol. Biol.* **2018**, *53*, 115–129.
- [3] Y. Wang, H. Zhao, *Catalysts* **2016**, *6*, 194.
- [4] O. Verho, J. E. Bäckvall, *J. Am. Chem. Soc.* **2015**, *137*, 3996–4009.
- [5] S. Mendes, L. Pereira, C. Batista, L. O. Martins, *Appl. Microbiol. Biotechnol.* **2011**, *92*, 393–405.
- [6] S. Mendes, A. Farinha, C. G. Ramos, J. H. Leitão, C. A. Viegas, L. O. Martins, *Bioresour. Technol.* **2011**, *102*, 9852–9859.
- [7] V. Brissos, N. Gonçalves, E. P. Melo, L. O. Martins, *PLoS One* **2014**, *9*, e87209.
- [8] F. Hollmann, I. W. C. E. Arends, K. Buehler, *ChemCatChem* **2010**, *2*, 762–782.
- [9] X. Wang, T. Saba, H. H. P. Yiu, R. F. Howe, J. A. Anderson, J. Shi, *Chem* **2017**, *2*, 621–654.
- [10] J. Canivet, G. Süss-Fink, P. Štěpnička, *Eur. J. Inorg. Chem.* **2007**, 4736–4742.
- [11] J. J. Soldevila-Barreda, A. Habtemariam, I. Romero-Canelón,

- P. J. Sadler, *J. Inorg. Biochem.* **2015**, *153*, 322–333.
- [12] V. Ganesan, D. Sivanesan, S. Yoon, *Inorg. Chem.* **2017**, *56*, 1366–1374.
- [13] J. J. Soldevila-Barreda, P. C. A. Bruijninx, A. Habtemariam, G. J. Clarkson, R. J. Deeth, P. J. Sadler, *Organometallics* **2012**, *31*, 5958–5967.
- [14] Y. Maenaka, T. Suenobu, S. Fukuzumi, *J. Am. Chem. Soc.* **2012**, *134*, 367–374.
- [15] A. Bucci, S. Dunn, G. Bellachioma, M. Rodriguez, C. Zuccaccia, C. Nervi, A. Macchioni, *ACS Catal.* **2017**, DOI 10.1021/acscatal.7b02387.
- [16] F. Hollmann, B. Witholt, A. Schmid, *J. Mol. Catal. B Enzym.* **2002**, *19–20*, 167–176.
- [17] M. Poizat, I. W. C. E. Arends, F. Hollmann, *J. Mol. Catal. B Enzym.* **2010**, *63*, 149–156.
- [18] J. Canivet, G. Süss-Fink, P. Štěpnička, *Eur. J. Inorg. Chem.* **2007**, 4736–4742.
- [19] M. M. Grau, M. Poizat, I. W. C. E. Arends, F. Hollmann, *Appl. Organomet. Chem.* **2010**, *24*, 380–385.
- [20] U. Hintermair, S. M. Hashmi, M. Elimelech, R. H. Crabtree, *J. Am. Chem. Soc.* **2012**, *134*, 9785–9795.
- [21] M. Pellei, V. Gandin, M. Marinelli, C. Marzano, M. Yousufuddin, H. V. R. Dias, C. Santini, *Inorg. Chem.* **2012**, *51*, 9873–9882.

- [22] G. J. Barbante, P. S. Francis, C. F. Hogan, P. R. Kheradmand, D. J. D. Wilson, P. J. Barnard, *Inorg. Chem.* **2013**, *52*, 7448–7459.
- [23] A. Fernandes, B. Royo, *ChemCatChem* **2017**, *9*, 3912–3917.
- [24] J. J. Soldevila-Barreda, A. Habtemariam, I. Romero-Canelón, P. J. Sadler, *J. Inorg. Biochem.* **2015**, *153*, 322–333.
- [25] N. Dafale, S. Wate, S. Meshram, N. R. Neti, *Environ. Rev.* **2010**, *18*, 21–36.
- [26] M. Kudlich, M. J. Hetheridge, H. J. Knackmuss, A. Stolz, *Environ. Sci. Technol.* **1999**, *33*, 896–901.
- [27] R. G. Ball, W. A. G. Graham, J. K. Hoyano, A. D. McMaster, B. M. Mattson, D. M. Heinekey, B. M. Mattson, S. T. Michel, *Inorg. Chem.* **1990**, *29*, 2023–2025.
- [28] A. Nutton, P. M. Bailey, P. M. Maitlis, *J. Chem. Soc., Dalton Trans.* **1981**, *1*, 1997–2002.

Chapter 5

5. Conclusions and Final Remarks

Sustainable development is only accomplished when resources are used in a rate in which they can be replaced naturally and, most of all when waste generation is not faster than its remediation and conversion into new useful products or materials. This is the definition of green chemistry. To achieve these goals the development of methods that implement the circular economy concept is imperative. In this thesis, sustainable methodologies were developed allowing the reintroduction of waste in the product life cycle by its conversion into valuable end products.

The first methodology developed was the environmental-friendly enzymatic strategy for the valorization of azo dye-containing wastewaters. These azo dyes are xenobiotic molecules designed to resist decolorization and degradation representing a big environmental concern. It was demonstrated, with purified preparations of enzymes, that the azoreductase PpAzoR from *Pseudomonas putida* efficiently reduces five structurally different azo dyes into aromatic amines. And, in a sequential manner, CotA-laccase from *Bacillus subtilis* efficiently oxidizes these into phenoxazinones, phenazines, and naphthoquinones. To further increase the process sustainability free and immobilized whole-cells of recombinant *Escherichia coli* containing the overproduced enzymes were successfully used in a two-step conversion of the model azo dye mordant black 9 into sodium-2-amino-

3-oxo-3H-phenoxazine-8-sulfonate, with final product yields that goes up to 80%. The cell immobilization in sodium alginate allowed the biocatalyst recycling and resulted in less contaminated reaction mixtures improving downstream treatment. Furthermore, recycled immobilized cells co-producing both enzymes resulted in excellent phenoxazinone yields decreasing in twofold the costs associated with this methodology. In this way, a sustainable biocatalytic system for cleaning-up dye-containing wastewaters while producing valuable chemicals with a range of applications in the pharmaceutical and chemical industries was developed. The application of this promising biocatalytic system in an industrial setting can be further studied and optimized.

Then, bearing in mind the industrial relevance of aromatic amines, a different method for their valorization was studied. The *N*-alkylation of amines with alcohols catalyzed by organometallic complexes is a sustainable atom efficient process producing only water as by-product. The introduction of a sustainable source of aromatic amines, *i.e.* from azo dye degradation, and the use of water as solvent can further improve this process sustainability. Therefore, new water-soluble Cp*Ir(III)(NHC)Cl₂ complexes were synthesized, characterized, and their activity in the *N*-alkylation of amines with alcohols studied. It was disclosed the first iridium N-heterocyclic carbenes complexes that

catalyze the alkylation of amines with alcohols in water. From the four new catalysts, $\text{Cp}^*\text{Ir}(\text{NHC}^{\text{acetamide}})\text{Cl}_2$ (**6**) exhibited the best results without addition of base or other additives resulting in quantitative yields and a broad substrate scope for various alcohols and amines. The application of this catalyst was limited when aromatic amines substituted with sulfonate group were used as substrate. This high electron-withdrawing group in the *ortho* or *meta* position together with other functional groups on the aromatic ring impaired the catalytic activity of the iridium catalysts. Since aromatic amines highly substituted with sulfonated groups are the major compounds obtained from azo dye degradation, the application of this organometallic-based catalytic system together with the biocatalytic reduction of azo dyes was unsuccessful.

Finally, a method to improve the sustainability of enzymatic systems that require external addition of co-factor, such as NAD(P)H was studied. The advantages of combining bio- and chemo catalysts are well known. With this aim, a series of half-sandwich iridium(III) complexes were developed and their activity in the regeneration of NADH using formate anions as the source of hydrogen demonstrated. The most active one, $[\text{Cp}^*\text{Ir}(2,2'\text{-bipyridyl})\text{OH}]^+$ (**9**) selectively produces 1,4-NADH with a TOF of 19.0 h^{-1} . Furthermore, the enzymatic reduction of MB9 by PpAzoR and the orthogonal regeneration of NADH

by catalyst **9** was performed in one-pot producing 59% of SABHS in 72 h. Although with some loss in activity, it was demonstrated that PpAzoR and complex **9** can work in a cooperative manner under enzymatic conditions (0.1 mM sodium phosphate buffer pH 7).

The work developed in this thesis highlights the potential of multi-catalytic systems in the development of sustainable methodologies. The use of multi-enzymatic systems was already known to allow the attainment of interesting molecules and herein we further demonstrate this through the production of important molecules such aromatic amines, phenazines, phenoxazinones, and quinones. On the other hand, it is widely known that the cooperative use of bio- and chemo catalysts is hampered by incompatibilities in reactional conditions that mostly lead to mutual inactivation. Nonetheless, in this thesis, we were able to demonstrate the potentiality that lies in the combined use of iridium(III) catalysts with azoreductases, like PpAzoR.

ITQB-UNL | Av. da República, 2780-157 Oeiras, Portugal
Tel (+351) 214 469 100 | Fax (+351) 214 411 277

www.itqb.unl.pt